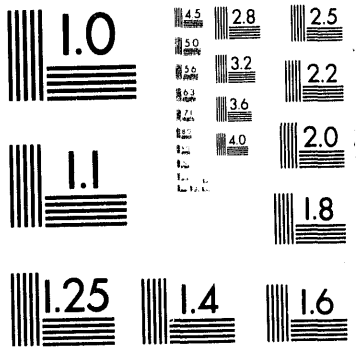
1.0
1.1
1.25
1.4
1.6
1.8
2.0
2.2
2.5
2.8
3.2
3.6
4.0
4.5
5.0
5.6
6.3
7.1

1 of 2

DOE/MC/24193-3491
(DE94000024)
Distribution Category UC-103

Metal Wastage Design Guidelines for Bubbling Fluidized-Bed Combustors

Final Report

R.W. Lyczkowski
W.F. Podolski
J.X. Bouillard
S.M. Folga

Work Performed Under Contract No.: DE-AC21-89MC24193

For
U.S. Department of Energy
Office of Fossil Energy
Morgantown Energy Technology Center
P.O. Box 880
Morgantown, West Virginia 26507-0880

By
Argonne National Laboratory
Energy Systems Division
9700 South Cass Avenue
Argonne, Illinois 60439

November 1992

Contents

Contents (cont'd)

Contents (cont'd)

Tables

Tables (cont'd)

Figures

Figures (cont'd)

Figures (cont'd)

Figures (cont'd)

Figures (cont'd)

Acknowledgments

The support of the Cooperative R&D Venture Participants listed on the cover page is gratefully acknowledged. All of the Steering Committee participants contributed materially to the genesis of this document through discussions at Steering Committee Meetings.

We wish to especially thank Gary Nelkin of U.S. Department of Energy Morgantown Energy Technology Center and Jeffery Stallings and John Wheeldon of Electric Power Research Institute for written comments on earlier drafts of this document and for the valuable advice and constructive criticisms they offered.

Nomenclature

c	Compaction modulus
d_p	Particle diameter, m
G	Solids elastic modulus, Pa
g	Acceleration due to gravity, m/s^2
n	Number of phases
t	Time, s
U_{mf}	Minimum fluidizing velocity, m/s

Greek Letters

ε	Gas volume fraction
ε_s	Solids volume fraction = 1 - ε
ε^*	Compaction gas volume fraction
ρ	Density, kg/m^3
ρ_s, ρ_g	Solids and gas phase densities, respectively, kg/m^3
μ_k	Microscopic viscosity, Pa·s (1 Pa·s = 10 poise)

Subscripts

i, k	Phase i, k
s	Solids phase
g	Gas phase

Metal Wastage Design Guidelines for Bubbling Fluidized-Bed Combustors

by

Robert W. Lyczkowski, Walter F. Podolski,
Jacques X. Bouillard, and Stephen M. Folga

Abstract

These metal wastage design guidelines identify relationships between metal wastage and (1) design parameters (such as tube size, tube spacing and pitch, tube bundle and fluidized-bed height to distributor, and heat exchanger tube material properties) and (2) operating parameters (such as fluidizing velocity, particle size, particle hardness, and angularity). The guidelines are of both a quantitative and qualitative nature. Simplified mechanistic models are described, which account for the essential hydrodynamics and metal wastage processes occurring in bubbling fluidized beds. The empirical correlational approach complements the use of these models in the development of these design guidelines. Data used for model and guideline validation are summarized and referenced. Sample calculations and recommended design procedures are included. The influences of dependent variables on metal wastage, such as solids velocity, bubble size, and in-bed pressure fluctuations, are discussed.

1 Introduction

"To know what we do not know is the beginning of wisdom."
Maha Sthavira Sangharakshita

Fluidized-bed combustion (FBC) is an established means of burning high-sulfur coal and various other difficult-to-burn feedstocks in an efficient, cost-effective, and environmentally acceptable manner, notwithstanding the wear or wastage of in-bed components and enclosure walls observed in many units. Erosion wear received little attention in very early investigations of FBC, because fluidizing velocities were typically between 1 and 2 m/s, which, it turns out, are too low to produce significant wear. Consequently, early materials testing concentrated on understanding corrosion and corrosion/erosion processes that could result in heat exchanger and gas turbine component failures.[1.1, 1.2] Results of these and other studies led to the belief that, with selection of alloys appropriate for their intended service and with careful design and operation of FBC systems, the corrosion problem was manageable. Subsequent experience has shown this belief to be generally true.

Nevertheless, metal wastage of in-bed components caused by means primarily other than corrosion has been reported in a large number of units in commercial service.[1.2-1.5] "Metal Wastage" is intended to refer to the wearing away of heat exchanger tubes by whatever erosion and/or abrasion wear mechanisms are operating. The experience with metal wastage is widespread but unfortunately quite varied, and the evidence with respect to a cause is frequently inconsistent. Bubbling beds have experienced wear on in-bed and convection pass tubes and on membrane water walls near the upper level of the fluidized bed. Circulating fluidized beds (CFBs) have experienced wear just above the interface between the water-walls and the refractory lining protecting the lower portion of the combustor. In addition, some CFBs have experienced wear on

heat exchanger surfaces hung in the gas flow path high in the combustor and on refractory-lined components, such as cyclones in the solids recirculation loop.

Useful service life, in some cases, has been reduced to one year or less; the maximum acceptable wear rate for steel boiler tubes in a coal-fired utility plant is usually taken to be 50 nm/h (0.05 mm/1000 h, 0.002 in/1000 h). The complexity of the problem is such that consistent cause-and-effect relationships among the parameters influencing metal wear have not been established. Presently, it is not possible to fully explain why some FBC units, or regions of a specific bed, undergo rapid wear and others do not.

The interactions among design parameters, such as tube size and spacing, and operating parameters, such as degree of fluidization, and the propensity for wear (by whatever mechanisms are causing mechanical wear) determine the rate of metal wastage. Mechanical processes leading to tube wear are the focus of this work. The hydrodynamics controlling solids and gas motion around in-bed components is considered the main component influencing wear. Hence, detailed knowledge of solids circulation and bubble motion is essential to understanding metal wear in FBC units. Bubbling FBCs are considered, although the methodologies and modeling techniques that are used apply equally well to circulating FBCs.

Corrosion can be thought of as altering the surface of the tubes, making them more prone to wear. Tightly adherent deposits on tubes, however, can confer some protection from wear.

An eight-member cooperative R&D venture was formed in 1986 to investigate metal wastage in FBCs. The eight parties were DOE's Morgantown Energy Technology Center (METC), Argonne National Laboratory (ANL), Electric Power Research Institute (EPRI), Tennessee Valley Authority (TVA), State of Illinois Center for Research on Sulfur in Coal (CRSC), ASEA Babcock (ASEA-B), ABB Combustion Engineering Systems (ABB/CE), and Foster Wheeler Development Corporation (FWDC). The British Coal Corporation (BCC) and CISE Technologie Innovative joined in 1991 and 1992, respectively.

The objectives of the R&D effort are to (1) develop and validate computer models for the prediction of hydrodynamics and erosion in FBCs, (2) develop guidelines for the design and operation of FBC units with minimum metal wastage rates, and (3) demonstrate the feasibility of a continuous erosion monitor[1.6] for use in pilot plant and full-scale FBC units. Figure 1.1 summarizes the modeling and supporting activities performed during the course of the R&D Cooperative Venture.

Two-dimensional[1.7,1.8] and three-dimensional[1.9] computer models have been developed that are capable of calculating detailed hydrodynamics of the solids and bubble motion and the erosion of tubes resulting from the impaction and abrasion of particles. The hydrodynamic calculations provide inputs to the EROSION/MOD1[1.10] computer program, such as the solids kinetic energy and direction of motion, to calculate rates from the various erosion models contained therein.

ANL's contributions to the development of the metal wastage guidelines are to (1) provide physical insights for correlation development, (2) develop a database of experimental findings, (3) provide critical evaluations of correlations, and (4) develop designer-friendly procedures using simplified and realistic models and correlations.

This document distills the details of the modeling effort down to simplified mechanistic models leading to the development of guidelines for the design, operation, and scaleup of FBC's having minimum erosion. These simplified models capture the essence of the detailed computer models and, as such, represent easy-to-use tools that designers may apply to understand the

influence of various operating and design parameters on erosion. Complementing these models is the correlative approach, which is also described.

This document is presented in a tabular loose-leaf form in order to facilitate subsequent revisions and additions. It is intended to be a living document capable of easy revision into a customized set of design guidelines and procedures reflecting data and experience bases particular to an individual user or organization.

In Sec. 2, the methodologies used in developing the guidelines are outlined. Section 2 also contains sufficient background information to provide the reader a broader perspective on the activities of the joint venture.

Section 3 sketches the development of the simplified models and describes the key inputs and outputs.

Section 4 describes the relationships of fluidizing velocity, particle size, particle angularity, particle hardness, and bed/tube temperature to metal wastage. Sample problems are presented that show the reader how to use the simple models to understand the interactions between the important variables affecting metal wastage and how to translate the model predictions into design guidelines. Each subsection is intended to be independent of the others; however, frequent cross-references between sections are made. The user should be able to extract the needed information without reading the entire document. A discussion of the pertinent data used to validate the models preceeds each subsection, and the sensitivity of the model to changes in the specific parameter is described. Each subsection also includes discussion of the model's range of applicability and provides caveats and warnings to the user about parameters not covered by the guidelines.

Section 5, which is similar to Sec. 4, discusses the following design parameters: distance of tube/tube bundle to the air distributor, tube material hardness, tube-bundle arrangement, tube pitch spacing, tube inclination, and protective devices.

A discussion of scaling that relates small and/or cold experiments to data from larger/hot units is presented in Section 6. Also, relationships between dependent variables (such as porosity, bubble size, and particle velocity) and metal wastage are presented.

Section 7 describes the parameters that have uncertain effects on metal wastage. These parameters include tube vibration, particle collisional frequency, bubble coalescence, and pressure fluctuations.

Finally, Sec. 8 provides conclusions and offers recommendations for further development of the design guidelines.

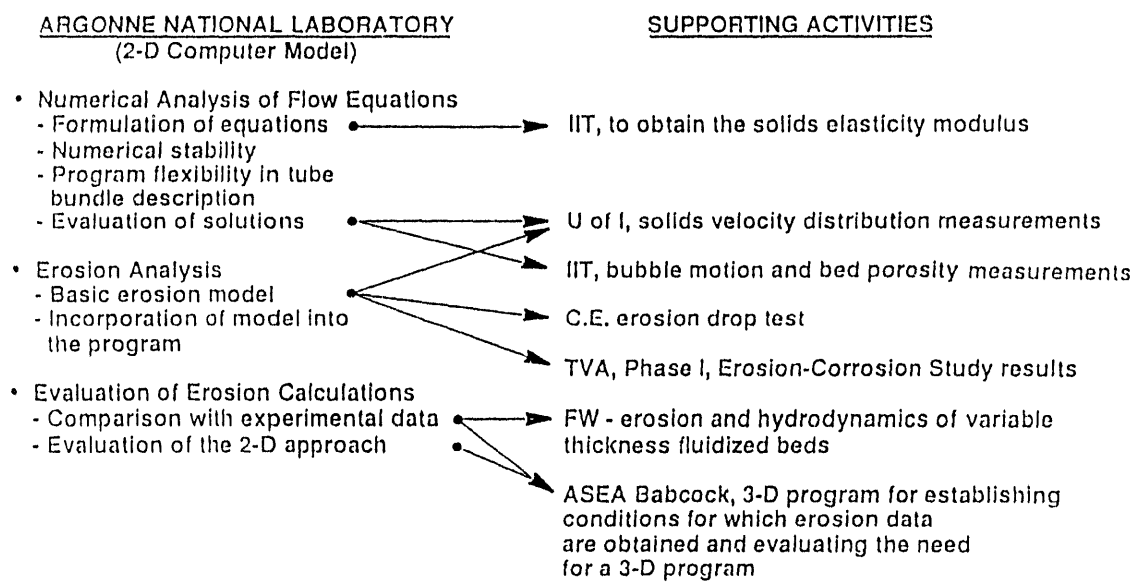

FIGURE 1.1 Erosion of FBC Heat Transfer Tubes —Summary of Modeling and Supporting Activities

References

1.1 National Coal Board, *Materials Problems in Fluidized-Bed Combustion Systems*, Electric Power Research Institute Report No. CS-1449, Palo Alto, CA (May 1980).

1.2 Minchener, A.J., E.A. Rogers, and R.D. LaNauze, *Materials Problems in Fluidized-Bed Combustion Systems*, Electric Power Research Institute Report No. CS-1475, Palo Alto, CA (August 1980).

1.3 Stringer, J., *Current Information on Metal Wastage in Fluidized Bed Combustors*, Proceedings of the 9th International Conference on Fluidized Bed Combustion, J.P. Mustonen, ed., Vol. 2, pp. 685-696, American Society of Mechanical Engineers, New York (1987).

1.4 Stringer, J., and I.G. Wright, *Erosion/Corrosion in FBC Boilers*, Workshop Proceedings, Wastage of In-Bed Surfaces in Fluidized-Bed Combustors, held at Argonne National Laboratory Nov. 2-6, 1987, Vol. I, Paper 1.1, Electric Power Research Institute (1988).

1.5 Stringer, J., J.W. Stallings, and J.M. Wheeldon, *Wastage in Bubbling Fluidized-Bed Combustors: An Update*, Proceedings of the 10th International Conference on Fluidized Bed Combustion, A.M. Manaker, ed., Vol. 2, pp. 857-862, American Institute of Mechanical Engineers, New York (1989).

1.6 Reimann, K.J., *Development of a High Temperature Erosion Monitor for FBC Heat Exchanger Tubes*, Argonne National Laboratory Report ANL/FE-89-4, Argonne, IL (May 1990).

1.7 Lyczkowski, R.W., J.X. Bouillard, and S.M. Folga, *Users Manual for FLUFIX/MOD2: A Computer Program for Fluid-Solids Hydrodynamics*, Argonne National Laboratory Report, Argonne, IL (April 1992).

1.8 Lyczkowski, R.W., J.X. Bouillard, D. Gidaspow, and G.F. Berry, *Computer Modeling of Erosion in Fluidized Beds*, Argonne National Laboratory Report ANL/ESD/TM-1, Argonne, IL, July 1986 (January 1990).

1.9 Burge, S.W., *FORCE2: A Multidimensional Flow Program for Gas-Solids Flow, Theory Guide and User's Guide*, Babcock & Wilcox, Alliance, OH (May, 1991).

1.10 Lyczkowski, R.W., J.X. Bouillard, S.M. Folga, and S.-L. Chang, *User's Manual for EROSION/MOD1: A Computer Program for Fluid-Solids Erosion*, Argonne National Laboratory Report, Argonne, IL (September 1992).

2 Approach

"Imagination is more important than knowledge."
Albert Einstein

The methodologies used to develop metal wastage guidelines and procedures are described in this section.

Parameters that are known to have or that are suspected of having an influence on metal wastage in FBCs are grouped into (1) those that are related to the design of the unit and (2) those that are related to the operation of the unit. Examples of the first group of parameters include tube size, tube spacing and pitch, tube bundle and fluidized bed height, distributor type, and heat exchanger tube material properties. Examples of the second group of parameters include fluidizing velocity, particle size and distribution, and particle hardness and angularity.

Each of the above parameters can be controlled by FBC designers and, therefore, can be considered independent. Another set of parameters, including solids velocity and flow patterns, bubble frequency, size and flow patterns, and pressure fluctuation frequency, is determined by the first set and, therefore, can be considered dependent. The interaction between the independent and dependent variables is shown in Table 2.1. A change in any one of the independent variables will likely result in changes in all of the dependent variables and perhaps in the amount of metal wastage as well.

The approach taken has been to closely couple hydrodynamic and erosion modeling efforts at ANL with experimental activities at other participating organizations in order to provide hydrodynamic and erosion data that can be used to validate the models.

This approach adopted by ANL to develop metal wastage guidelines and scaleup procedures can be summarized as follows:

1. Apply hydrodynamic and erosion codes to generic and specific FBC geometries.
2. Simplify the models to their essential components and place them in dimensionless form.
3. Define input parameters for simplified models and correlations.
4. Develop procedures and recommendations for model calculations.
5. Develop calculation procedures to relate simplified models for any geometry.
6. Validate guidelines, procedures, and scaling.

Argonne National Laboratory has developed a computer code named "FLUFIX/MOD2"[2.1] to predict hydrodynamics in fluidized-bed combustors. This code is based on a hydrodynamic model of fluidization and can be used to predict frequency of bubble formation, bubble size and growth, bubble frequency and rise-velocity, solids volume fraction, and gas and solids velocities. The results of the hydrodynamic model are used as inputs to ANL's "EROSION" computer program, which contains various erosion models,[2.2,2.3] including the monolayer energy dissipation (MED) erosion model developed by ANL in this project.[2.4,2.5]

Babcock & Wilcox (B&W), with ASEA-B funding, developed the FORCE2[2.6] computer code, which is a three-dimensional transient and steady-state version of FLUFIX/MOD2.[2.1] ANL has implemented the FORCE2 computer program on its CRAY X-MP/18 vector supercomputer and has performed quality assurance and validation using some of the experimental results. Good agreement of the computed overall solids flow patterns, major porosity and pressure

frequencies, bubble sizes and frequencies, and time-averaged porosity profiles with experimental data has been achieved.[2.2-2.5,2.7-2.10]

Advanced graphics have been implemented that serve to speed up the validation process and to render the computer simulations more comprehensible to the users of the FLUFIX, FORCE2, and EROSION computer programs.

In part of the experimental work, data on erosion rates at particle sizes, velocities, and loadings typically found in FBCs were obtained in the Ash Erosion Test Facility at ABB/CE.[2.11] In these experiments, sand and/or crushed quartz was dropped through a vertical tube onto a heated carbon steel target in order to determine the erosion rate as a function of particle size, loading, and impact velocity.

Other experiments sponsored by the consortium provided hydrodynamic and erosion data from several fluidized beds. Experiments at the Illinois Institute of Technology (IIT) measured fluctuating and time-averaged porosities in a thin, "two-dimensional," fluidized bed containing single obstacles of various shapes.[2.12] A Computer Aided Particle Tracking Facility (CAPTF) was employed at the University of Illinois at Urbana-Champaign (UI-UC) to track the movement of a radioactive tracer particle in two- and three-dimensional fluidized beds containing single obstacles that were round, square, or rectangular in cross section.[2.11] Other experiments employed small arrays of round tubes immersed in the fluidized bed. In addition, pressure fluctuations were measured at numerous locations in both two- and three-dimensional beds. Erosion of tubes in the three-dimensional experiment was also measured. The particle motion data were processed to provide direction and speed distribution information.

Experiments in a variable-dimension (dimensions varied between experiments), large-scale cold model fluidized bed at FWDC provided information on the significance of erosion data from experiments in small-scale fluidized beds.[2.11] Metal wastage of tubes in small arrays were measured and compared with calculated erosion rates. The simulation of the most recent experiments at FWDC are a basis from which the sensitivity of metal wastage to changes in various parameters are assessed in Sec. 5.1.

A comparison of model predictions with other data reported in the literature has resulted in order of magnitude and better agreement with wastage rates and correct prediction of observed trends.[2.2-2.5,2.13] The comparison of model predictions with data involves the simulation of each experiment to obtain detailed hydrodynamic and erosion predictions. Each simulation requires extensive computer time and subsequent analysis of the detailed computations in order to present results that can be directly compared with data. This type of analysis was necessary in order to validate the models and to develop confidence in their predictive capability and to provide insights used to simplify the models for design applications.

A simplified, yet mechanistic, means of developing design guidelines is necessary to provide design engineers with easy-to-use procedures and to avoid the necessity of detailed computation for each design variation. Therefore, the detailed hydrodynamic and erosion models were distilled down to contain the essential parameters in dimensionless form. When results obtained using the simplified models were compared with the detailed model calculations, agreement was close. Thus, the simplified models can, with a small amount of hand calculation, capture the essence of the detailed models and provide the means for developing design guidelines.

The dimensionless erosion rates calculated using the simplified models can then be translated into erosion rates by using appropriate constants as shown in Sec. 3.

Because all of the parameters listed in Table 2.1 are not explicitly contained in the simplified model, a primarily empirical approach is taken in Sec. 5 to understand the influence of the design parameters on erosion. The empirical approach can, in principle, be validated by performing sensitivity studies using the detailed models. The simplified models can then be extended to incorporate the results of these sensitivity studies.

The subsections in Secs. 4 and 5 are written as if the parameters are independent of each other, and the reader can refer to a specific subsection when seeking information on the influence of that parameter on erosion. Where there is significant interdependence between variables, the reader is cautioned to not neglect the effect of the other variables on erosion. Studies by Foster Wheeler Power Products[2.14] indicate no single parameter is solely responsible for metal wastage, but rather the wastage in a particular location is related to a combination of the main parameters. Some parameters, principally fluidizing velocity, are more important than others. No simple remedy exists, and only by careful consideration of all the parameters, in the correct combination, can acceptable solutions be offered.

The discussions in each subsection describe the data that were used to validate the guidelines and the limitations on the range of applicability. The final validation of the models and the guidelines developed from them will be achieved when they are compared with field data. In order to accomplish the final validation, some details of the hydrodynamics, as well as erosion, must be determined from units in the field.

Finally, parameters that have uncertain effects on metal wastage and the remaining information gaps are identified in Sec. 7.

References

2.1 Lyczkowski, R.W., J.X. Bouillard, and S.M. Folga, *Users Manual for FLUFIX/MOD2: A Computer Program for Fluid-Solids Hydrodynamics,* Argonne National Laboratory Report, Argonne, IL (April 1992).

2.2 Lyczkowski, R.W., J.X. Bouillard, D. Gidaspow and G.F. Berry, *Computer Modeling of Erosion in Fluidized Beds,* Argonne National Laboratory Report ANL/ESD/TM-1, Argonne, IL July, 1986. (January 1990).

2.3 Lyczkowski, R.W., S. Folga, S.L. Chang, J.X. Bouillard, C.S. Wang, G.F. Berry, and D. Gidaspow, *State-of-the-Art Computation of Dynamics and Erosion in Fluidized Bed Tube Banks,* Proceedings of the 10th (1989) International Conference on Fluidized Bed Combustion, A.M. Manaker, ed., Vol. 1, pp. 465-478, American Society of Mechanical Engineers, New York (1989).

2.4 Lyczkowski, R.W., and J.X. Bouillard, *State-of-the-Art Review and Status of Erosion Modeling in Fluid/Solids Systems,* Proceedings Corrosion-Erosion-Wear of Materials at Elevated Temperatures, Berkeley, CA, January 31-February 2, 1990, A.V. Levy, ed., pp. 27-1 to 27-66, National Association of Corrosion Engineers, Houston, TX (June 1991).

2.5 Bouillard, J.X., R.W. Lyczkowski, S. Folga, D. Gidsapow, and G.F. Berry, *Hydrodynamics of Erosion of Heat Exchanger Tubes in Fluidized-Bed Combustors,* Canadian Journal of Chemical Engineering, *67*:218-229 (April 1989).

2.6 Burge, S.W., *FORCE2: A Multidimensional Program for Gas-Solids Flow, Theory Guide and User's Guide,* Babcock & Wilcox, Alliance, OH (May 1991).

2.7 Lyczkowski, R.W., J.X. Bouillard, D. Gidaspow, and G.F. Berry, *Hydrodynamics of Fluidization: Time-Averaged and Instantaneous Porosity Distributions in a Fluidized-Bed with an Immersed Obstacle,* Argonne National Laboratory Report ANL/ESD/TM-4, Argonne, IL, September 1986 (February 1990).

2.8 Bouillard, J.X., R.W. Lyczkowski, and D. Gidaspow, *Porosity Distributions in a Fluidized Bed with an Immersed Obstacle,* AIChE Journal, *45*(6):908-922 (June 1989).

2.9 Lyczkowski, R.W., I.K. Gamwo, F. Dobran, Y.H. Ai, B.T. Chao, and M.M. Chen, *Comparison of Experimental and Computed Solids Motion and Bed Dynamics for Fluidized Beds Containing Obstacles,* Proceedings of the 11th (1991) International Conference on Fluidized Bed Combustion, E.J. Anthony, ed., Vol. 1, pp. 325-333, American Society of Mechanical Engineers, New York (1991).

2.10 Bouillard, J.X., D. Gidaspow, and R.W. Lyczkowski, *Hydrodynamics of Fluidization: Fast Bubble Simulation in a Two-Dimensional Fluidized Bed,* Powder Technology *66*:107-118 (1991).

2.11 Podolski, W.F., R.W. Lyczkowski, E. Montrone, J. Drennen, Y.H. Ai, and B.T. Chao, *A Study of Parameters Influencing Metal Wastage in Fluidized Bed Combustors,* Proceedings of the 11th (1991) International Conference on Fluidized Bed Combustion, E.J. Anthony, ed., Vol. 2, pp. 609-618, American Society of Mechanical Engineers (1991).

2.12 Gamwo, I.K., *Multi-Dimensional Hydrodynamic and Erosion Modeling of Fluidized Beds*, Ph.D. Dissertation, Illinois Institute of Technology (May 1992).

2.13 Bouillard, J.X., and R.W. Lyczkowski, *On the Erosion of Heat Exchanger Tube Banks in Fluidized-Bed Combustors*, Powder Technology, *68*:37-51 (1991).

2.14 Ellis, F., and C. Armitage, *Combating Metal Wastage in Fluidized Bed Combustors*, 1988 Seminar on Fluidized Bed Combustion Technology for Utility Applications, Volume I: Atmospheric Fluidized Bed Combustion, Electric Power Research Institute, Palo Alto, CA (May 1988).

TABLE 2.1 FBC Metal Wastage Dependencies

Independent Variables	Dependent Variables	
<u>Design Parameters</u> Tube size Tube spacing/pitch Tube shape/flow disruptors Tube bundle/bed height Tube inclination Height from distributor Type of distributor <u>Operating Parameters</u> Particle size/size distribution Particle shape/angularity particle hardness/density Fluidizing velocity Bed/tube temperature Chemical environment	→	Solids velocity Bubble frequency Bubble size Bubble velocity Pressure fluctuations → Metal wastage

3 Description of Simplified Models

**"As far as the laws of mathematics refer to reality,
they are not certain; as far as they are certain,
they do not refer to reality."
Albert Einstein**

This section describes the simplified monolayer energy dissipation (MED) erosion model and a suggested empirical complementary approach that relies upon data correlations. Also included is a brief description of the input parameters required for each approach.

There have been several attempts to develop simplified models of fluidized bed hydrodynamics and erosion.[3.1-3.5] Soo's[3.3] and Wood and Woodford's[3.4] were discussed by Lyczkowski et al.[3.6]; Staub's[3.2] was discussed by Wood and Woodford[3.4] and Parkinson et al.[3.7]

Energy-dissipation erosion models, which relate the particles' energy dissipation rate adjacent to the eroding surfaces to erosion, were derived and used by Bouillard et al.[3.8, 3.9] and Lyczkowski et al.[3.10, 3.11] In these models, the authors initially used the empiricism that 10% of the dissipated energy in a monolayer of particles next to the surfaces causes erosion. Later, they showed this factor is accounted for by the coefficient of restitution.[3.9]

Other fluidized-bed erosion models have recently appeared in the literature. Yates[3.12] derived a simple erosion model that showed the erosion rate to be proportional to the fourth power of the bubble diameter. Levy and Stallings[3.12] developed an erosion model by considering the impact of bubble wakes on the tube resulting from the coalescence of bubble pairs. They found very strong effects of the bed geometry and bubbling conditions on the computed erosion rates. Gansley and O'Brien[3.14] have used Finnie's single-particle-impact erosion model in conjunction with Davison's bubble model to calculate erosion in FBCs. However, the bubble size, bubble rise velocity, and bubble frequency have to be assumed in the calculations.

Bouillard and Lyczkowski developed a simplified mechanistic erosion model from the monolayer energy dissipation (MED) erosion model.[3.8] A modification of that model is utilized herein to assist in developing metal wastage design guidelines and procedures.

3.1 Simplified MED Erosion Model

The erosion rate from the simplified quasi one-dimensional MED model, $\dot{E}_{EDCF}$,[3.8] may be written in the form, modified for hydrodynamic model B:[3.8]

$$\dot{E}_{EDCF} = \dot{E}_o \frac{(1-\varepsilon)(\varepsilon - \varepsilon_{gd})}{\varepsilon^2} + K\frac{(\varepsilon - \varepsilon_{gd})}{\varepsilon^2}(U - \varepsilon V_s) \tag{3.1}$$

where the erosion rate group, $\dot{E}_o$, is given by

$$\dot{E}_o = (1 - e^2)\frac{75\mu_g g x_d}{(\phi_s d_p E_{sp})} \tag{3.2}$$

and

$$K = (1 - e^2)\frac{0.875 g x_d \rho_g}{E_{sp}} \quad . \tag{3.3}$$

The units of $\dot{E}_o$ are in terms of a velocity; e.g., mm/1000 h and K is dimensionless.

In Eqs. 3.1-3.3, above,

μ_g = gas viscosity, Pa·s;
g = acceleration due to gravity, m/s^2;
x_d = characteristic distance, m;
d_p = particle diameter, m;
E_{sp} = an erodent (target) material property related to hardness, Pa;
e = coefficient of restitution, ratio of rebound and approach particle velocities;
ε = porosity (fluid volume fraction);
ε_{gd} = porosity in the densest region of the bed;
ϕ_s = partical sphericity;
U = superficial gas fluidizing velocity, m/s; and
V_s = solids velocity, m/s.

Experimental evidence[3.15] strongly supports the additional approximation that the solids velocity, V_S, in the vicinity of tubes is close to the superficial gas velocity, U. With the approximation $V_S = U$, Eq. 3.1 may be written in the strikingly simple dimensionless form as

$$\frac{\dot{E}_{EDCF}}{\dot{E}_o} = f(\varepsilon)(1 + 0.01167 Re) \tag{3.4}$$

where the Reynolds number, Re, is defined in the usual way as $Re=(\phi_s d_p)\rho_g U/\mu_g$
and

$$f(\varepsilon) = \frac{(1 - \varepsilon)(\varepsilon - \varepsilon_{gd})}{\varepsilon^2} \quad . \tag{3.5}$$

Note that the erosion rate group $\dot{E}_o$ has the dimension of velocity and acts as a natural scaling parameter for metal wastage. The additional scaling parameters are the Reynolds number and the porosity dependence through $f(\varepsilon)$. Equation 3.4 clearly shows that metal wastage measurements performed in laboratory experiments will scale to field units if the average bed porosity, Reynolds number, and erosion rate group given by Eq. 3.2 are the same for both units. These are the first mechanistic erosion scaling equations known to these authors.

Not all design parameters are contained explicitly in Eq. 3.4. They are, however, contained implicitly in the porosity dependence, $f(\varepsilon)$. For example, different tube spacing would cause a different porosity for the same fluidizing velocity. Therefore, x_d can be taken to be the tube spacing to explicitly account for this effect.

3.2 Correlative Erosion Model

Complementing the simplified mechanistic approach is the correlative approach where laboratory data are curve fit to various empirical or semi-empirical expressions. Section 4 discusses several correlations developed mainly by changing one operating parameter at a time, keeping all others constant. Section 5 also contains data that be correlated. Once the individual correlations are established, a master calculation can be developed of the form:

$$\frac{\dot{E}}{\dot{E}_o} = \frac{C_1 U^a d_p^b (C_2 - \phi_s) \dot{M}_s^c E_p^d (H_v/H_h)^e \ldots}{E_t} \tag{3.6}$$

where the new variables are the solids mass flux, $\dot{M}_s$, the particle hardness, E_p, target material property related to hardness, E_t, and the vertical and horizontal center-to-center spacing (pitch) of the tubes, H_v and H_h, respectively. Other features (such as tube inclination, square versus staggered pitch) can be added as the correlations of the raw data are developed. Such an approach has been adopted by Zhu et al.,[3.16] utilizing tube data for metal wastage. A further discussion of such models is described in Sec. 6.

3.3 Utilization of Erosion Models

Both the simplified mechanistic model given by Eq. 3.4 and the master correlation given by Eq. 3.6 can be used to renormalize erosion data and to extrapolate it. In the first case, erosion data taken under different conditions can be renormalized to the same conditions and compared for consistency. In the second case, erosion data taken under one set of conditions can be extrapolated to different conditions and used to develop trends without the need of many experiments. The assumption is, of course, that the equations are valid in the range of interest.

Both approaches require input parameters that must either be measured or estimated. In the case of Eq. 3.1, these include the sphericity, restitution coefficient, bed porosity, and the appropriate target material property related to hardness. The physical constants can be obtained from the ideal gas laws and other correlations.

Several caveats must be kept in mind in applying these two approaches:

1. Only mono-sized particles are considered having a mean diameter for the size range used. The effect of the addition of small amounts of very large particles that may increase erosion rates cannot be accounted for yet.

2. Sphericity may not truly represent angularity effects. The hypothesis that it can should be tested for particles of different shapes. Nevertheless, sphericity is used as a first approximation to characterize particle angularity in this study.

3. The reader/user must keep in mind that the input parameters are not truly independent. For example, when the particle size changes, the minimum fluidizing velocity, U_{mf}, changes and, thus, the quantities (U/U_{mf}) or $(U-U_{mf})$ would change.

4. No chemical effects have been considered.

5. Only a limited number of model calculations have been used to check the validity of the simplified mechanistic model, the correlation, and the empirical

effects since the detailed computations are time-consuming and expensive. An analytical sensitivity study using the FWDC experiment described in Sec. 5 is under way.

References

3.1 Martin, H., *Fluid-Bed Heat Exchangers – A New Model for Particle Convective Energy Transfer,* Report No. 80-HT-60, ASME/AICLE National Heat-Transfer Conference, Orlando, Florida, July 27-30 (1980).

3.2 Staub, F.W., *Solids Circulation in Turbulent Fluidized Beds and Heat Transfer to Immersed Tube Banks,* ASME Journal of Heat Transfer, *101*(3):301 (August 1979).

3.3 Soo, S.L., *A Note on Moving Dust Particles,* Powder Technology, *17*:259-263 (1977).

3.4 Wood, R.T., and D.A. Woodford, *Tube Erosion in Fluidized Beds,* General Electric Co. Report 11/ET-FUC79, U.S. Energy Research and Development Administration Report 81-12 (December 1980).

3.5 Gansley, R.R., and T.J. O'Brien, *A Model for Bubble-Induced Erosion in Fluidized-Bed Combustors and Comparison with Experiment,* Wear, *137*:107-127 (1990).

3.6 Lyczkowski, R.W., J.X. Bouillard, D. Gidaspow, and G.F. Berry, *Computer Modeling of Erosion in Fluidized Beds,* Argonne National Laboratory Report ANL/ESD/TM-1, Argonne, IL, July 1986 (January 1990).

3.7 Parkinson, M.J., A.W. Jury, B.A. Napier, T.J. Kempton, and J.C. Holder, *Cold Model Erosion Studies in Support of Pressurized Fluidized Bed Combustion,* Electric Power Research Institute Draft Final Report for Project 1337-2 (April 1986).

3.8 Bouillard, J.X., R.W. Lyczkowski, S. Folga, D. Gidaspow, and G.F. Berry, *Hydrodynamics of Erosion of Heat Exchanger Tubes in Fluidized-Bed Combustors,* Canadian Journal of Chemical Engineering, *67*:218-229 (April 1989).

3.9 Bouillard, J.X., and R.W. Lyczkowski, *On the Erosion of Heat Exchanger Tube Banks in Fluidized-Bed Combustors,* Powder Technology, *68*:37-51 (1991).

3.10 Lyczkowski, R.W., S. Folga, S.L. Chang, J.X. Bouillard, C.S. Wang, G.F. Berry, and D. Gidaspow, *State-of-the-Art Computation of Dynamics and Erosion in Fluidized Bed Tube Banks,* Proceedings of the 10th (1989) International Conference on Fluidized Bed Combustion, A.M. Manaker, ed., Vol. 1, pp. 465-478, American Society of Mechanical Engineers, New York (1989).

3.11 Lyczkowski, R.W., and J.X. Bouillard, *State-of-the-Art Review and Status of Erosion Modeling in Fluid/Solids Systems,* Proceedings Corrosion-Erosion-Wear of Materials at Elevated Temperatures, Berkeley, CA, January 31-February 2, 1990, A.V. Levy, ed., pp. 27-1 to 27-66, National Association of Corrosion Engineers, Houston, TX (June 1991).

3.12 Yates, J.G., *On the Erosion of Metal Tubes in Fluidized Beds,* Chem. Eng. Sci., *42*:379-380 (1987).

3.13 Levy, E.K., and J.W. Stallings, *Tube Erosion in Bubbling Fluidized Beds,* 11th Conference on Fluidized Bed Combustion, E.J. Anthony, ed., Vol. 3, pp. 1139-1144, American Society of Mechanical Engineers, NY (1991).

3.14 Gansley, R.R., and T.J. O'Brien, *A Model for Bubble Induced Erosion of Fluidized-Bed Heat Transfer Tubes*, Wear, *137*:107-127 (1990).

3.15 Zhu, Jingxu, *Tube Erosion in Fluidized Beds*, Ph.D Thesis, Department of Chemical Engineering, The University of British Columbia (May 1988).

3.16 Zhu, J., C.J. Liu, J.R. Grace, and J.A. Lund, *Tube Wear in Gas Fluidized Beds - II. Low-Velocity Impact Erosion and Semi-Empirical Model for Bubbling and Slugging Fluidized Beds*, Chem. Eng. Sci., *46*(4):1151-1156 (1991).

4 Operating Parameters

Operating parameters (such as fluidizing velocity, particle size and size distribution, particle shape, and particle hardness) have been studied extensively in order to determine their effect on in-bed tube wear. In this section, information that is available in the literature on the effect of each parameter on erosion is compared with model predictions in order to determine the accuracy of prediction, particularly the prediction of the correct trends. The sensitivity of the model to changes in each parameter is assessed by predicting erosion at the limits of the range of realistic values of the specific parameter and, where possible, comparing predictions with data. The envelope within which bubbling beds operate is described below. A similar discussion concerning the mechanical design envelope for bubbling beds is found in the beginning of Sec. 5.

Three types of bubbling beds define the operating envelope for the sensitivity studies; namely, "conventional" AFBCs, such as the 20 MWe and 160 MWe units at TVA; a pressurized FBC, such as the Tidd demonstration plant; and the external bubbling bed heat exchanger in some circulating fluidized beds (CFB).

Velocity Range

The low-end of the velocity range is typified by the external CFB heat exchanger. The cold model experiment at FWDC simulating such a design specifies a velocity of 0.6 ft/s in one half of the fluidized bed. The high-end of the velocity range, around 8 ft/s, is defined by "conventional" AFBCs, such as at TVA.

Particle Diameter Range

The low end of particle size range is defined by the CFB external heat exchanger – 150-200 mm. The high end is defined by the 3200-μm (1/8-in.) feed size typical of AFBC and PFBC bubbling beds.

Particle Shape Range

Particle shape is frequently discussed as a significant parameter in tube wear. It is conjectured that angular or sharp particles cause more wear than rounded particles. In this work, the particle shape is defined by the parameter sphericity as first defined by Wadell (see Sec. 4.3), which ranges from a value of 1 for spherical particles to approximately 0.8 for particles typically found in fluidized beds.

Particle Hardness Range

The particle hardness ranges from relatively soft limestone to the harder alumino-silicates, quartz, and pyrite found in coal ash. The hardness of the limestones used by Air Products in the Stockton CFB unit was determined to be about 160 HV (kg/mm^2), while the silicon-rich particles had hardness numbers up to 2040 HV.[4.1]

Primary Experiment Sources of Erosion Data

Five significant literature sources are referred to frequently in Secs. 4 and 5. of this document. The first two describe a very comprehensive experimental study of metal wastage by Zhu et al. in a cold, three-dimensional fluidized bed having a rectangular cross section of 203 × 216 mm.[4.2,4.3] Figure 4.1, reproduced from Ref. 4.2, uses a multi-axis representation

to succinctly and graphically summarize the parameters that were varied in these erosion studies. In addition to experiments in a fluidized bed, drop-tube erosion experiments were also performed. The third literature source is a reanalysis of some of the Parkinson et al.[4.4] data by Wheeldon.[4.5] The fourth and fifth literature sources are that of Nieh et al.[4.6] and Lee,[4.7] which describe a systematic study of the effect of tube bundle height and configuration (triangular versus in-line) on erosion and that attempt to correlate erosion rates with particle impaction frequency.

In the early sections of this document, the discussions are probably longer than desired by the reader; however, they provide background for subsequent sections that refer to the same experiments.

References

4.1 Slusser, J., *Aggressive and Non-Aggressive Bed Materials Comparison of Individual Particle Properties*, Proceedings: Workshop on Wear Potential of FBC Bed Material, in Fluidized Bed Combustors, pp. 141-158, Electric Power Research Institute Report No. TR-100056 (November 1991), Palo Alto, CA.

4.2 Zhu, J.. *Tube Erosion in Fluidized Beds*, Ph.D. Thesis, Department of Chemical Engineering, The University of British Columbia (May 1988).

4.3 Zhu, J., J.R. Grace, and C.J. Lim, *Tube Wear in Gas Fluidized Beds—I. Experimental Findings*, Chemical Engineering Science, *45*(4):1003-1015 (1990).

4.4 Parkinson, M.J., A.W. Jury, B.A. Napier, T.J. Kempton, and J.C. Holder, *Cold Model Erosion Studies in Support of Pressurized Fluidized Bed Combustion*, Electric Power Research Institute Draft Final Report for Project 1337–2 (April 1986).

4.5 Wheeldon, J.M., *A Re-Evaluation of Tube Wastage Data Collected from a Bubbling Fluidised Bed Cold Model*, Proceedings: Corrosion-Erosion-Wear of Materials at Elevated Temperatures, Berkeley, Calif., Jan. 31-Feb. 2, 1990, A.V. Levy, ed., pp. 41-1 to 41-13, National Association of Corrosion Engineers, Houston, Texas (June 1991).

4.6 Nieh, S., S.Y. Lin, S.W. Lee, and T.T. Fu, *Measurements of In-Bed Tube Bundle Erosion and Particle-Tube Frequency in a Gas Fluidized Bed*, Particulate Science and Technology, 6, pp. 269-282 (1988).

4.7 Lee, S.W., *Analysis and Modeling of In-Bed Tube Erosion in a Gaseous Fluidized Bed*, Doctoral Dissertation, The Catholic University of America, Washington, D.C. (Feb. 1989).

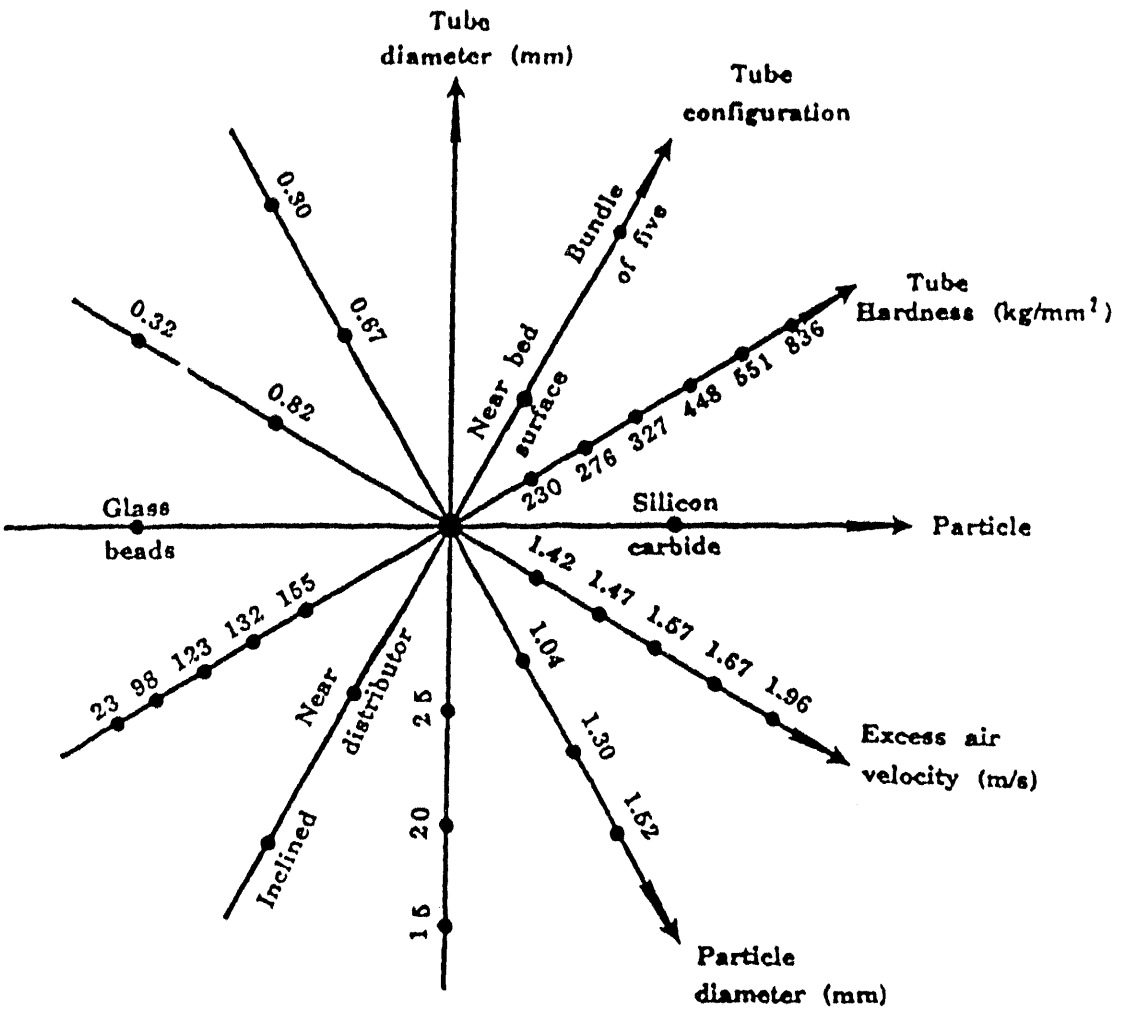

Center point:
32 mm single tube, 308 mm above the distributor, Tube hardness 98 -- 276 kg/mm², 1.0 mm silica sand and excess air velocity of 1.31 m/s

FIGURE 4.1 Multi-Axes Design of Zhu's Room Temperature Three-Dimensional Bed Experiments[4.2]

4.1 Fluidizing Velocity

4.1.1 Discussion

Because the gas fluidizing velocity is under direct control of the experimenter or field operator and is the easiest operating parameter to change, its effect on erosion has been studied far more than any other. Varying any other parameter, especially the design parameters, such as bed geometry, requires dismantling, modifying, and reassembling the fluidized bed. Furthermore, the fluidizing velocity appears to be the variable with the greatest effect on erosion.

The dependency of metal wastage on fluidizing velocity can be expressed in several ways. One could plot the local erosion at a point, the average erosion for a single tube, or the average erosion for an entire tube bundle versus the fluidizing velocity, U, the ratio of the fluidizing velocity to the minimum fluidization velocity, U/U_{mf}, the difference between the two, $(U-U_{mf})$, or a derived parameter (such as the bed porosity). Additional expressions include U/U_T, where U_T is the terminal velocity, or the fluidization index given by

$$FI = \ln(U/U_{mf})/\ln(U_T/U_{mf}), \qquad (4.1.1)$$

which varies from 0 for a bed at minimum fluidization to 1.0 for complete particle entrainment when $U = U_T$.

4.1.1.1 Parkinson et al. Experiments

Parkinson et al.[4.1.1,4.1.2] studied erosion in a cold, scaled atmospheric fluidized bed. The bed for Tasks I and III of their study was 0.3×0.3 m in cross section and contained 17 PVC tubes (33 mm o.d.) in the IEA Grimethorpe tube bank "C1" configuration, with a vertical pitch of 80 mm (2.4 tube diameters) and a horizontal pitch of 89 mm (2.7 tube diameters) by eight rows high. The air distributor had 16 standpipes on a 75-mm^2 pitch. Each standpipe had 20 round holes, 10 of which were 3.2 mm in diameter and 10 of which were 4 mm in diameter for a total open area of 2.06 cm^2. Fluidizing velocities ranged from 0.3 to 4.8 m/s for bed material consisting of 0.4-mm- to 1.3-mm-diameter silica sand. The run durations were 48 h for the 0.7-, 1.0-, and 1.3-mm-diameter particles and 200 h for the 0.4-mm-diameter particles. The ratio, U/U_{mf}, varied from 2.6 to 10.1, and the excess gas velocity, $U-U_{mf}$, varied from 0.18 to 4.29 m/s.

The Parkinson et al.[4.1.2] average mass loss data are shown in Figs. 4.1.1 through 4.1.4 plotted versus U, U/U_{mf}, $U-U_{mf}$, and porosity, ε, respectively. Note that 1 g of loss per tube for the 0.7-, 1.0-, and 1.3-mm-diameter particles corresponds to approximately 0.56 mm/1000 h and 0.13 mm/1000 h for the 0.4-mm-diameter particles, respectively. The 0.4-mm-particle data were not included in Ref. 4.1.1. We have drawn dashed lines through the data in Fig. 4.1.3 for the four different particle sizes. The particle size dependency will be discussed in Sec. 4.2.

The total mass loss data of Parkinson et al.[4.1.2] are shown to the left of Fig. 4.1.4 plotted versus the bed porosity (not reported for the 0.4-mm-diameter particles). Although the data are scattered, smooth dashed curves have been drawn through the data for each particle size. These smooth curves more clearly show that maxima in the erosion rates exist and that they occur at porosities around 0.6. The solid curve is a normalized modification of a relationship developed

by General Electric. This normalization and derivation of the relationship is described by Parkinson et al.[4.1.2]

The erosion rates predicted from the EROSION computer program for 0.5-mm-diameter particles using the full MED erosion model are shown to the right of Fig. 4.1.4 for aluminum tube material. Details of the calculations are presented in Refs. 4.1.3 and 4.1.4. The dashed curve is a plot of the predicted erosion rates versus time-averaged bed porosities estimated from predicted expanded bed heights. The solid curve used the time-averaged porosities in the vicinity of the tubes. These computations also suggest that a maximum exists in the erosion rates around a porosity of 0.6; however, further calculations need to be performed.

The simplified MED erosion model predicts a maximum erosion rate to exist at

$$\varepsilon = \frac{2\varepsilon_{gd}}{(1 + \varepsilon_{gd})} . \tag{4.1.2}$$

With $\varepsilon_{gd} = \varepsilon_{mf} = 0.4$, the maximum erosion rate occurs at $\varepsilon = 0.57$. The erosion rates predicted by the full MED erosion model shown to the right of Fig. 4.1.4 are in reasonable agreement with the rates if one multiplies the erosion rate by a factor of 6, which is roughly the ratio of the hardness of aluminum to PVC.[4.1.3] An erosion rate of 0.5 mm/1000 h predicted near the probable maximum for aluminum corresponds to approximately 3.0 mm/1000 h for PVC tube material, while the data lie in the range of 2.52 to 2.8 mm/1000 h.

The maximum erosion rates measured anywhere by Parkinson et al.[4.1.1] are compared with the predictions in Figs. 4.1.5 and 4.1.6. As can be seen in the figures, this time a maximum does not occur, at least over the range of fluidizing velocities covered. Logically, there should be a maximum in the erosion rate because the bed is becoming dilute. As the bed empties itself of material at very high U/U_{mf}, the erosion rate should approach zero, since the solids loading also approaches zero, as reinformed by Eq. (3.5) $(\varepsilon \rightarrow 1)$ for this simplified MED erosion model. A slightly more general version of the simplified MED erosion model given by Eq. 3.1 does a reasonable job of correlating the data as indicated by the solid lines marked "theory."[4.1.3]

Figure 4.1.7 shows a plot of the predicted erosion rates for three different erosion models[4.1.4] as a function of U/U_{mf}. At higher fluidizing velocities, the rate levels off. The shape of the curve is remarkably similar to the Parkinson et al.[4.1.2] data shown in Fig. 4.1.2 for 0.4-mm- to 1.0-mm-diameter particles. For more details of the calculations, refer to Lyczkowski et al.[4.14]

Wood and Woodford[4.1.5] did not observe a fluidizing velocity dependence because they estimated that they were well into what is loosely termed the "turbulent" fluidization regime. Most of their data were in a range of porosities $(0.9 > \varepsilon > 0.7)$ where the erosion rate is a maximum (as shown in Fig. 4.1.6) and not changing rapidly.

Parkinson et al.[4.1.1,4.1.2] developed empirical expressions to describe their data. The first one relates the average weight loss, ΔW, to the fluidizing velocity, U, as:

$$\Delta W = 1.29\ U - 0.91 \tag{4.1.3}$$

where

ΔW = mass loss, g, and
U = fluidizing velocity, m/s.

This curve is shown in Fig. 4.1.1 compared with the data. The data for the 0.7-mm particles indicate a decrease in erosion rate with increasing fluidizing velocity, U, above 2 m/s and departs from the curve fit. A threshold velocity of about 0.7 m/s is suggested. The minimum fluidizing velocities vary from 0.13 to 0.73 m/s.

The average mass loss data were correlated with U/U_{mf} and particle diameter as:

$$\Delta W = 0.66\ (d_p)^{1.5}(U/U_{mf} - 1.3) \qquad (4.1.4)$$

where

ΔW = mass loss, g;
d_p = particle diameter, mm;
U = fluidizing velocity, m/s; and
U_{mf} = minimum fluidization velocity, m/s.

See Sec. 4.2.1 for an expanded discussion and Figure 4.2.4.

The total mass loss was correlated with the excess fluidizing velocity, $(U-U_{mf})$, as:

$$\Delta W = 1.38\ (U-U_{mf}) - 0.35 \qquad (4.1.5)$$

where

ΔW = mass loss, g;
U = fluidization velocity, m/s; and
U_{mf} = minimum fluidization velocity, m/s.

This curve is plotted in Fig. 4.1.3 and compared with the data. Clearly, this curve only approximately fits the 1.0- to 1.3-mm-diameter particle data.

Wheeldon[4.1.6] reanalyzed some of the Parkinson et al.[4.1.2] PVC tube erosion data with a different approach using local metal thickness losses. The data were correlated using the excess fluidizing velocity $(U-U_{mf})$. The data are shown in Figs. 4.1.8 and 4.1.9 for tube 2 at three different locations: 180, 90/270, and 145/215° as measured clockwise from the top center of the tube. The 0° location showed no clear trend. The time interval for the measurements was 48 h (100 microns/48 h = 2.1 mm/1000 h).

The curve fits developed to correlate the metal thickness loss, dL, are:

180° location

$$dL = 35.2\ (U-U_{mf})^2 \qquad (4.1.6)$$

90/270° locations

$$dL = 17.0\ (U-U_{mf}) \qquad (4.1.7)$$

145/215° locations

$$dL = 60.0\ (U\text{-}U_{mf})^{1.5} \qquad (4.1.8)$$

In Eqs. 4.1.6 through 4.1.8,

dL = material loss, microns;
U = fluidization velocity, m/s; and
U_{mf} = minimum fluidization velocity, m/s.

The curve fits given by Eqs. 4.1.6-4.1.8 are plotted in Fig. 4.1.8 and at the top of Fig. 4.1.9, together with the data.

The dependency of the PVC thickness loss, dL, at the 145/215° locations on the 1.5 power of the excess velocity suggested that the wastage might be due to a combined erosive (square) and abrasive (linear) mechanism. The data were refit as:

$$dL = 24.0\ (U\text{-}U_{mf})^2 + 36.1\ (U\text{-}U_{mf}). \qquad (4.1.9)$$

The units are the same as those for Eqs. 4.1.6-4.1.8. The curve fit given by Eq. 4.1.9 is as good as Eq. 4.1.8, as shown in the bottom and top of Fig. 4.1.9, respectively.

All of the curve fits given by Eqs. 4.1.3 through 4.1.9 appear to disregard clear experimental indications of maxima and leveling off of the erosion rates, as shown in Figs. 4.1.2, 4.1.3, 4.1.4 (left), 4.1.9, and 4.1.10, and as predicted by the simplified MED erosion model. These trends are indicated by the dashed lines roughly drawn through the data in Figures 4.1.3, 4.1.4 (left), 4.1.9, and 4.1.10.

4.1.1.2 Lee's Experiment

Lee[4.1.7] studied the effect of fluidizing velocity and distance to the distributor in a cold model consisting of a single 17-mm-diameter wax cylinder mounted in the center of a 21 × 21-cm (cross section) fluidized bed containing 0.55-mm glass beads. The tube was placed at 3 and 5 cm (1.76 and 2.94 tube diameters) above the perforated plate distributor with 1,025 orifice holes, each with a diameter of 0.8 mm in a triangular pattern. The minimum fluidization velocity was determined to be 19 cm/s. The slumped bed height was fixed at 12.5 cm. The length of each test run was four hours. Results of specific weight loss are plotted versus the excess air velocity (U-U_{mf}) in Figure 4.1.8. Note that significant erosion occurred above a fluidizing velocity, U, of 26 cm/s. The threshold velocity of 26 cm/s was found to be close to the bubbling velocity (slightly above the minimum fluidization velocity) of the test particles.

Lee curve fit his data to an expression of the form

$$\frac{\Delta W}{A} - \left(\frac{\Delta W}{A}\right)_2 = C(U\text{-}U_{mf})^m \qquad (4.1.10)$$

where

$\frac{\Delta W}{A}$ and $\left(\frac{\Delta W}{A}\right)_o$ = specific weight loss above and at U = 26 cm/s, respectively, mg/cm^2;

U = fluidizing velocity, cm/s; and

U_{mf} = minimum fluidization velocity, cm/s.

The curve fits to Eq. 4.1.10 are compared with data in Figure 4.1.10. An erosion rate can be obtained by dividing $\frac{\Delta W}{A}$ over the four-hour test run by the target density of 0.91 g/cm^3 (1 mg/cm^2 = 2.74 mm/1000 h). Comparison with the Parkinson et al. PVC data at comparable fluidizing velocity and particle diameter from Figure 4.1.3 suggests that wax erodes about 20 times faster than PVC. Lee claimed that his results were reproducible and consistent within an accuracy of 15%. Similar results were found at circumferential locations around the tube, with the maximum erosion occurring at the bottom section, but no curve fits were given. The effect of height above the distributor will be discussed in Sec. 5.1.1.

4.1.1.3 Zhu et al. Experiment

Zhu et al.[4.1.8,4.1.9] conducted erosion experiments in a cold fluidized bed having a cross section of 203 × 216 mm. A single 32-mm tube was located 308 mm above a perforated plate consisting of 182 3-mm holes spaced 15 mm apart. Using 1.0-mm-particle-diameter silica sand, the superficial velocity, U, was varied from 0.88 to 2.51 m/s. The minimum fluidization velocity, U_{mf}, was 0.55 m/s. Therefore, the excess velocity ($U-U_{mf}$) varied from 0.33 to 1.96 m/s and U/U_{mf} varied from 1.6 to 4.6.

The results are shown in Fig. 4.1.11. Clearly, the erosion rate for each of the materials increases with fluidization velocity. The superficial velocity, U, was converted to a slug or void rise velocity, U_S, using standard formulae.[4.1.8,4.1.9] The data are replotted in Fig. 4.1.12. The slug and superficial velocities are nearly identical.

The erosion data shown in Fig. 4.1.12 were curve fit using the expression:

$$\dot{E} = C\,(U_S)^n \qquad (4.1.11)$$

where

$\dot{E}$ = erosion rate, μm/100 h, and
U_S = slug or void velocity, m/s.

Table 4.1.1 lists the constants, n and c, determined from least squares fits for the various materials, along with the correlation coefficients for Eq. 4.1.11. The curve fits are plotted in Fig. 4.1.12. The average value of the slug velocity exponent, n, was found to be 2.1, close to that obtained for their drop-tube erosion data.[4.1.8]

4.1.2 Recommended Design Guidelines and Procedures

A design guideline of a qualitative nature generally known in the fluidization community is to keep the fluidizing velocity below 2 m/s.[4.1.10] Figure 4.1.13 shows, for the seven shallow tube banks studied by Ellis and Armitage,[4.1.10] how the maximum wear rate reduced to acceptable levels at fluidizing velocities below 2.0 m/s. In cold model tests[4.1.11], increasing the fluidizing velocity from 1.5 m/s to 2.5 m/s caused a three-fold increase in tube wear. The data of

Parkinson et al.[4.1.2] corroborated this finding. Figure 4.1.6 shows that reducing the bed porosity from 0.75 (U~3 m/s, U/U_{mf}~4) to 0.50 (U~1 m/s, U/U_{mf}~2) reduces the maximum metal wastage by almost an order of magnitude. However, Fig 4.1.4 (left) shows that the bed-average erosion rate goes through a maximum (~3 mm/1000 h) upon decreasing the bed porosity from 0.75 to 0.55, changing by a factor of 5 on either side of the maximum.

At values of U/U_{mf} less than 2, an erosion threshold may exist. Figure 4.1.10 shows that erosion ceases at about $U/U_{mf} = 1.5$ ($U_{mf} = 19$ cm/s) where the erosion decreases over an order of magnitude to essentially zero. Dorr Oliver, as reported by Stringer,[4.1.12] defines 1.8 m/s as the critical fluidizing velocity below which there is essentially no metal wastage. The data of Parkinson et al. shown in Fig. 4.1.1 suggest a value of 0.8 m/s (U/U_{mf} ~ 1.5 in Fig. 4.1.2).

Brains and Michner[4.1.13] recommended that good operating practice should be observed. In particular, the fluidizing velocity should be kept below 2.5 m/s and preferably below 2 m/s. The fluidizing velocity is the single most important parameter in its effect on wear rates.

The in-kind data reports received from the British Coal Corporation Coal Research Establishment addressing the dependence of erosion rates upon fluidization velocity corroborated previous findings. When the fluidizing velocity, U, was reduced from 0.8 to 0.6 m/s and the mean particle size of the bed material, d_p, from 0.75 to 0.4 mm, a large reduction (~60%) in the tube loss was recorded.[4.1.14] For these conditions the highest tube loss was about the same as that measured for the tubes in the lowest rows of the 'D' bank when U was 0.8 m/s and $d_p = 0.75$ mm. It was felt that further tests were needed to ascertain whether the large decrease in tube wear is caused principally by the reduction in fluidizing velocity or in mean particle size. Localized wastage of tubes should also be studied in greater detail.

These tests were performed later for Test Series 1, and it was found that for a fixed bed material and particle size, the measured tube wastage rates were directly proportional to $(U-U_{mf})$.[4.1.15] Still later tests[4.1.16] for test series A2 gave further confirmation that tube wear for a given mean particle size of bed material is directly proportional to $(U-U_{mf})$.

Design guideline procedures are now given in the form of step-by-step examples.

Example 1: Assessment of Erosion Rates Based Upon Computed Bed Hydrodynamics

Equation 3.4 may be used to quickly assess the effect of fluidizing velocity on the metal wastage for a given particle size. In this first example, we will use "experimental" data obtained from the CRE few tube simulations using the FLUFIX computer program.[4.1.3] The "data" used will be the expanded bed height, a parameter fairly easy to measure in the field from wall static pressure probes.

Column 3 in Table 4.1.2 lists the time-averaged expanded fluidized bed height as a function of U/U_{mf} and U.

Step 1: Compute Minimum Fluidization Porosity

Measure or estimate the porosity at minimum fluidization, ε_{mf}. Lacking any data, the following expression may be used to estimate ε_{mf}:[4.1.17]

$$\varepsilon_{mf} = \left(14\ \phi_s\right)^{-1/3} \tag{4.1.12}$$

where ϕ_s is the sphericity (see Sec. 4.3). Using a sphericity of 1.0, Eq. 4.1.2 yields $\varepsilon_{mf} = 0.41$.

Step 2: Compute the Average Bed Porosity

Obtain the fluidized bed porosity as a function of expanded bed height, H, from the following solids overall mass conservation equation:

$$\varepsilon = 1 - H_{mf}\,\varepsilon_{smf}/H \tag{4.1.13}$$

where ε_{smf} is the solids porosity at minimum fluidization and H_{mf} is bed height at minimum fluidization.

Step 3: Evaluate Eq. 3.4 with the following parameters: 25°C, 1.01 k Pa

μ_g = 1.82×10^{-5} Pa·s;
ρ_g = 1.83 kg/m^3;
E_{sp} = 294 MPa;
d_p = 0.05 cm;
x_d = 55 mm;
e^2 = 0.9; and
ε_{gl} = 0.4.

E_{sp} corresponds to the hardness of pure aluminum (30 kgf/mm^2), x_d is the minimum horizontal spacing between tubes (89 mm - 33.7 mm = 55.3 mm) for Grimethorpe tube bank "C1"[4.1.2], and e^2 is the square of coefficient of restitution.[4.1.3] The results of the calculations are listed in Table 4.1.2 and are plotted in Fig. 4.1.14, where they are compared with the full MED erosion model results. As can be seen, the agreement is excellent. Also shown is the sensitivity of the results to a three-fold increase in the apparent hardness of aluminum due to surface oxidation. Also plotted are roughly renormalized erosion data for aluminum and aluminum alloy (90 kgf/mm^2). In spite of the diverse sources of the data, the agreement with the simplified MED erosion model is remarkable. The simplified MED erosion model takes a few minutes to compute on a pocket calculator instead of a month on a mainframe computer using the FLUFIX and EROSION computer programs.

Example 2 Extrapolation of Erosion Rates from Experimental Data

The erosion rate dependency on U/U_{mf} may be determined another way – by renormalizing the simplified MED erosion model to calculate $\dot{E}_o$ from an experimental erosion rate. In this example, the experimental erosion rate at U/U_{mf} = 1.12 is 0.18 mm/1000 h as shown in Fig. 4.1.15. The values of $\dot{E}_{EDCF}$ for values of U/U_{mf} greater than 1.12 are determined from Table 4.1.2 by ratioing the experimental value of $\dot{E}_o$ (0.18/0.075 mm/1000 h) by the calculated values of $\dot{E}_{EDCF}/\dot{E}_o$. For example, the erosion rate at U/U_{mf} = 1.7 is $0.18 \times (0.203/0.075)$ =

0.48 mm/1000 h; similarly, those at U/U_{mf} = 2.3 and 2.7 are 0.65 and 0.71 mm/1000 h, respectively. The results are plotted in Fig 4.1.15.

An alternative is to renormalize at the maximum erosion rate so that $\dot{E}/\dot{E}_{max} = 1$. Then all of the other values are obtained by ratios.

Example 3: Estimate Bed Expansion Given Fluidizing Velocity and Bubble Diameter

In this example, the bed expansion is determined from the two-phase theory of fluidization[4.1.18] via

$$\frac{H-H_{mf}}{H_{mf}} = \frac{U-U_{mf}}{U_b} \tag{4.1.14}$$

where U_b, the bubble rise velocity, is given by a correlation. For example, $U_b \sim 0.71\,(d_e g)^{1/2}$[4.1.18] where d_e is the equivalent sphere bubble diameter (see Sec. 6, Eq. 6.3). One can also use the Babu et al. correlation.[4.1.19] A particularly easy way to obtain the bed expansion is from Ho and Park's menu driven floppy disk program called FBCAD, which contains these formulas, as well as others.[4.1.20]

Example 4: Estimate Tube Lifetime

Estimate the lifetime of a 32-mm carbon steel tube (CS1020) subjected to a fluidizing velocity of 2 m/s for 1000-μm sand particles using Eq. 4.1.11 and Table 4.1.1, of Zhu, et al. Zhu's curve fit given by Eq. 4.1.11 with the values given in Table 4.1.1 is somewhat simpler to use than the simplified MED erosion model. It can also be used to renormalize data and predict the trends.

$$\begin{aligned}\dot{E} &= 0.59(2)^{2.14} = 2.6\ \mu m/100\ h \\ &= 0.026\ mm/1000\ h \\ &= 0.23\ mm/yr\end{aligned}$$

Assuming a 50% safety factor, for a 4.5-mm tube Parkinson et al.[4.1.2] wall thickness, the tube life would be

$$\frac{4.5 \times 0.5}{0.23} = 9.78\ yr.$$

This may represent the upper bound since Zhu et al.[4.1.8,4.1.9] found a 60% reduction in erosion for a tube array versus a single tube and Lee[4.1.6] found an order of magnitude decrease.

The maximum wear for PVC tubes in the Grimethorpe "C1" tube bank cold model experiment may be used to compare with the above estimate, assuming that PVC is approximately 140 times more erosion prone than carbon steel. Use Fig. 4.1.5 with $U/U_{mf} = 2/0.56 = 3.57$ to obtain $\dot{E}$ = 3 mm/1000 h for PVC tubes. Then the erosion rate for carbon steel tubes is given by $\dot{E} = 3/140 = 0.021$ mm/1000 h or about the same estimated lifetime.

Example 5: Rework Example 4 Using the Simplified MED Erosion Model

If we assume the 32-mm carbon steel tubes (CS 1020) are in a bundle of vertical pitch of about 4-tube diameters (13 cm), one can estimate the erosion rate $\dot{E}$ from the simplified MED erosion model using Eqs. 3.2, 3.4, and 3.5. $\dot{E}_o$ is given by

$$\dot{E}_o = (1 - e^2) \times \frac{7.5\, \mu_g\, g x_d}{(\phi_s d_p)\, E_{sp}}$$

or, with $\phi_s = 1$,

$$\dot{E}_o = \frac{0.1 \times 75 \times 1.8\ 10^{-5} \times 9.8 \times 0.13}{10^{-3} \times (40 \times 10^6)} = 4.3 \times 10^{-9}\ \text{m/s}$$

for plastic tubes of 40 MPa hardness, or

$$\dot{E}_o = 15.5\ \text{mm/1000 h.}$$

The erosion rate is given by Eq. 3.4, or

$$\dot{E} = \dot{E}_o\, f(\varepsilon)\, (1 + 0.0116\, Re)$$

where

$$f(\varepsilon) = \frac{(1 - \varepsilon)(\varepsilon - \varepsilon_{gd})}{\varepsilon^2}\ .$$

Let us estimate the bed porosity from the bed expansion. The Babu et al. expression for the bed expansion is given by[4.1.19]

$$\frac{H}{H_{mf}} = 1 + \frac{1.95\, (U - U_{mf})^{0.74}\, d_p\, \rho_p^{0.38}}{U_{mf}^{0.937}\ \ \rho_g^{0.123}}\ \text{(cgs units)}$$

where U_{mf} can be estimated from Figure B.1 (about 70 cm/s). The bed expansion becomes

$$\frac{H}{H_{mf}} = 1 + \frac{1.95\, (200 - 70)^{0.74}\, 0.1\, (2.4)^{0.38}}{(70)^{0.94}\ \ (1.2 \times 10^{-3})^{0.123}} = 1.42\ .$$

The bed porosity is given by Eq. 4.1.13, that is

$$\varepsilon = 1 - \frac{1}{1.42}\, 0.6 = 0.58.$$

The function $f(\varepsilon)$ Eq. 3.5 yields

$$f(0.58) = \frac{(1 - 0.58)(0.58 - 0.4)}{0.58^2} = 0.22.$$

The Reynolds number is given by $Re = \frac{\phi_s \rho_g d_p U}{\mu_g}$, which yields

$$Re = \frac{1.2 \times 10^{-3} \times 2}{1.8 \times 10^{-5}} = 133 .$$

The estimated erosion rate for plastic tubes finally is

$$\dot{E} = 15.5 \times 0.22 \times (1 + 0.0116 \times 133) = 8.7 \text{ mm/1000 h},$$

and the erosion rate for carbon steel tubes = $1/140 \times 8.7$ mm/1000 h = 0.06 mm/1000 h. Note that Eqs. 3.2, 3.4, and 3.5 tend to overpredict erosion rates when compared with those plotted in Figures 4.1.5 and 4.1.6 (8.7 vs. ~ 4 mm/1000 h). The reason for this phenomenon is that the curves generated by Bouillard et al. used a drag function β, which is about ε times greater than that assumed in Eqs. 3.2, 3.4, and 3.5 (~0.5-0.6). When rescaled, the erosion rate, $\dot{E}$, becomes $\dot{E} = 8.7 \times 0.58 = 5$ mm/1000 h for PVC tubes and $\dot{E} = 5/140 = 0.036$ mm/1000 h for carbon steel, or 0.31 mm/yr. These erosion rates are of the same order as those recorded at Grimethorpe. An estimated lifetime (assuming 50% safety factor for the tubes) would be about 7.2 years.

References

4.1.1 Parkinson, M.J., B.A. Napier, A.W. Jury, and T.J. Kempton, *Cold Model Studies of PFBC Tube Erosion*, Proceedings of the 8th International Conference on Fluidized-Bed Combustion, Vol. II, pp. 730-738, National Technical Information Service, DOE/METC-85/6021, Springfield, Va. (1985).

4.1.2 Parkinson, M.J., A.W. Jury, B.A. Napier, T.J. Kempton, and J.C. Holder, *Cold Model Erosion Studies in Support of Pressurized Fluidized Bed Combustion*, Electric Power Research Institute Draft Final Report for Project 1337–2 (April 1986).

4.1.3 Bouillard, J.X., and R.W. Lyczkowski, *On the Erosion of Heat Exchanger Tube Banks in Fluidized Bed Combustors*, Powder Technology, *68*:37-51 (1991).

4.1.4 Lyczkowski, R.W., J.X. Bouillard, S.L. Chang, and G.F. Berry, *Modeling of Hydrodynamics and Erosion in Bubbling and Circulating Fluidized Beds*, in Proceedings: Workshop on Materials Issues in Circulating Fluidized-Bed Combustors, pp. 5-1 to 5-42. Electric Power Research Institute Report GS-6746 (Feb. 1990).

4.1.5 Wood, R.T., and Woodford, *Tube Erosion in Fluidized-Beds*, ERDA Report 81-12 911/ET-FUC/79), prepared for New York State Energy Research and Development Authority by General Electric Co., Schenectady, N.Y. (Dec. 1980).

4.1.6 Wheeldon, J.M., *A Re-evaluation of Tube Wastage Data Collected from a Bubbling Fluidised Bed Cold Model*, Proceedings Corrosion-Erosion-Wear of Materials at Elevated Temperatures, Berkeley, Calif., Jan. 31-Feb. 2, 1990, A.V. Levy, ed., pp. 41-1 to 41-13, National Association of Corrosion Engineers, Houston, Texas (1991).

4.1.7 Lee, S.W., *Analysis and Modeling of In-Bed Tube Erosion in a Gaseous Fluidized Bed*, Doctoral Dissertation, The Catholic University of America, Washington, D.C. (Feb. 1989).

4.1.8 Zhu, Jingxu, *Tube Erosion in Fluidized Beds*, Ph.D. Thesis, Department of Chemical Engineering, The University of British Columbia (May 1988).

4.1.9 Zhu, J., J.R. Grace, and C.J. Lim, *Tube Wear in Gas Fluidized Beds—I. Experimental Findings*, Chemical Engineering Science, *45*(4):1003-1015 (1990).

4.1.10 Ellis, F., and C. Armitage, *Combating Metal Wastage in Fluidized Bed Combustors*, 1988 Seminar on Fluidized Bed Combustion Technology for Utility Applications, Volume I: Atmospheric Fluidized Bed Combustion, Electric Power Research Institute (May 1988).

4.1.11 Brain, S.A., and E.A. Rogers, *Experience of Erosion of Metal Surfaces in U.K. Fluid Bed Boilers*, Int. Specialist Meeting on Solid Fuel Utilisation, Comb. Inst. Lisbon (July 1987).

4.1.12 Stringer, J., *Current Information on Metal Wastage in Fluidized Bed Combustors*, Proceedings of the 9th International Conference on Fluidized Bed Combustion, J.P. Mustonen, ed., Vol. 2, pp. 685-6967, American Society of Mechanical Engineers, New York (1987).

4.1.13 Brain, S.A. and A. Michner, *Minimization of Wastage in Bubbling Atmospheric Fluidized Bed Boilers,* Proceedings on Corrosion-Erosion-Wear of Materials at Elevated Temperatures, Berkeley, CA, Jan 31-Feb. 2, 1990, A.V. Levy, ed., pp. 40.1 to 40.16, National Association of Corrosion Engineers, Houston, TX (1991).

4.1.14 British Coal Corporation, Coal Research Establishment, *Cold Model Studies of Tube Wear in Support of PFBC, (December 1985-February 1986),* PFBC/MOA/P9, Stoke Orchard, Cheltenham, U.K. (April 9, 1987).

4.1.15 Parkinson, M.J., A.W. Jury, B.A. Napier, N.C. Moon, and C.M. Barrety, *Cold Model Studies on the Effect of Fluidizing Velocity and Mean Particle Size on Tube Wear, Test Series I,* PFBC/MOA/P15, British Coal Corporation, Coal Research Establishment, Stoke Orchard, Cheltenham, U.K. (June 12, 1987).

4.1.16 British Coal Corporation, Coal Research Establishment, *Cold Model Studies on the Effect of Fluidizing Velocity and Mean Particle Size on PFBC Tube Wear, Test Series A2,* PFBC/MOA/P28, Stoke Orchard, Cheheltenham, U.K. (April 21, 1988).

4.1.17 Wen, C.Y., and Y.H. Yu, *A Generalized Method for Predicting the Minimum Fluidizations Velocity,* AIChE Journal, *12*:610 (1966).

4.1.18 Howard, J.R., *Fluidization Technology,* Adam, Hulger, Bristol, and New York (1989).

4.1.19 Babu, S.P., B. Shah, and A. Talwalkar, *Fluidization Correlations for Coal Gasificvation Materials - Minimum Fluidization Velocity and Fluidized Bed Expansion Ratio,* in Fluidization: Application to Coal Conversion Processes, AIChE Symposium Series, 74(176):176, American Institute of Chemical Engineers, New York (1978).

4.1.20 Ho, T.-C., and S.-C. Park, *FBCAD Fluidized Bed Computer Aided Design,* Version 1.0. Available from T.-C. Ho, Department of Chemical Engineering, Lamar University, Beaumont, TX 77710 (December 1988).

TABLE 4.1.1 Constants from Least Squares Curve Fitting of Eq. 4.1.11[4.1.8]

Material	C	n	Correlation Coefficient
Brass	2.96	2.23	0.98
Copper	1.94	2.04	0.99
Al2011	3.02	2.22	0.97
SS304	0.31	1.83	9.95
CS1020	0.59	2.14	0.91
Mean value		2.1	
Standard deviation		0.17	

Conditions:

Sample size: 26 data points for every material
Particles: 1.0-mm silica sand
Particle sphericity: 0.89

The units of $C = (\text{mm}/100\ \text{h})/[(\text{m/s})^n]$

TABLE 4.1.2 Metal Wastage Predictions from Simplified MED Erosion Model

(Example 1)

U/U_{mf}	U, cm/s	H, cm	e	f(e)	Re	$\frac{\dot{E}_{EDCF}}{\dot{E}_o}$
1.0	0.209	44.2	0.40	0	10.5	0
1.12	0.234	46	0.42	0.066	11.7	0.075
1.7	0.355	50	0.47	0.168	17.8	0.203
2.3	0.481	55	0.52	0.213	24.2	0.273
2.7	0.564	59	0.55	0.223	28.4	0.296

$\dot{E}_o$ = 1.8 mm/1000 h.

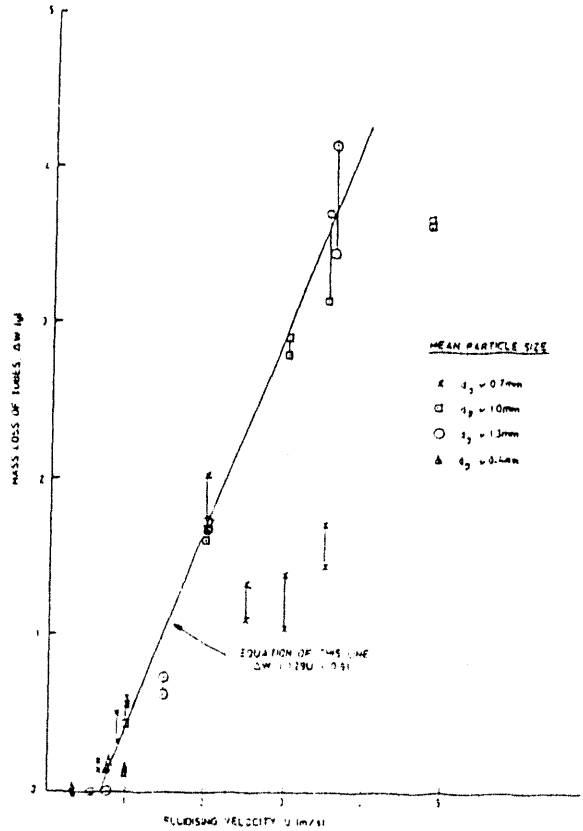

FIGURE 4.1.1 Average Mass Loss per PVC Tube vs. Fluidizing Velocity, U(4.1.2)

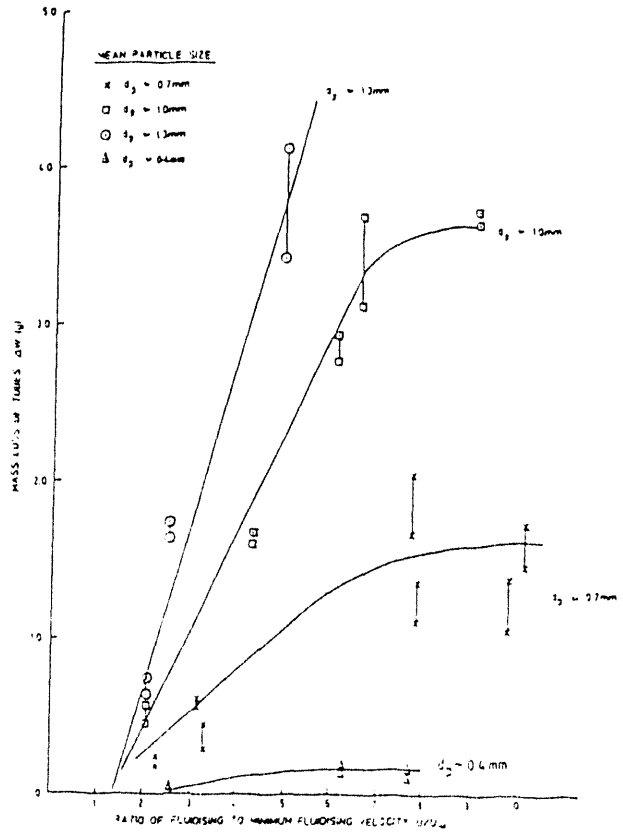

FIGURE 4.1.2 Average Mass Loss per PVC Tube vs. (U/U_{mf})(4.1.2)

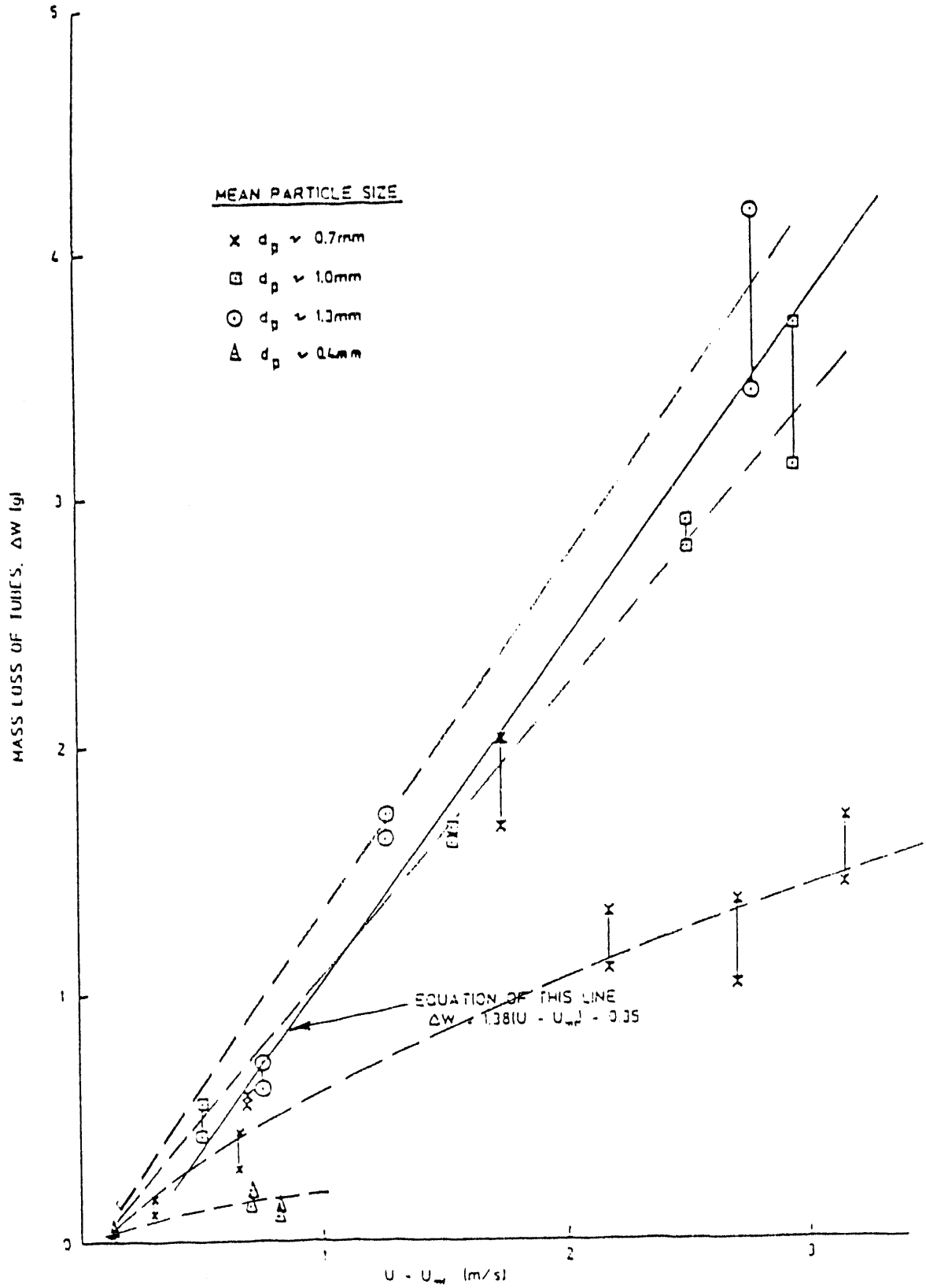

FIGURE 4.1.3 Average Mass Loss per PVC Tube versus $(U-U_{mf})$[4.1.2]

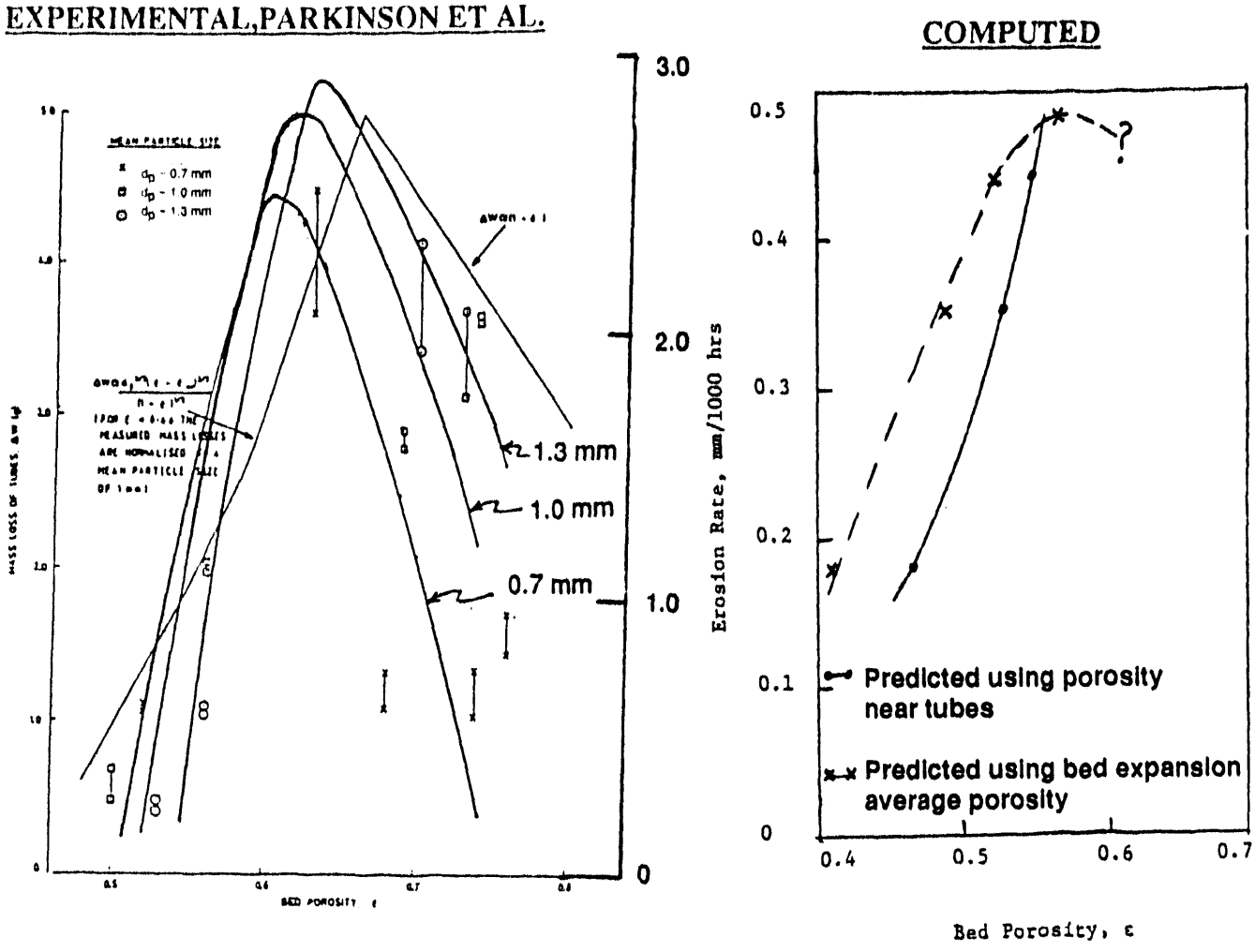

FIGURE 4.1.4 Comparison of Experimental (left)[4.1.7] and Computed (right) Erosion Rates as a Function of Bed Porosity

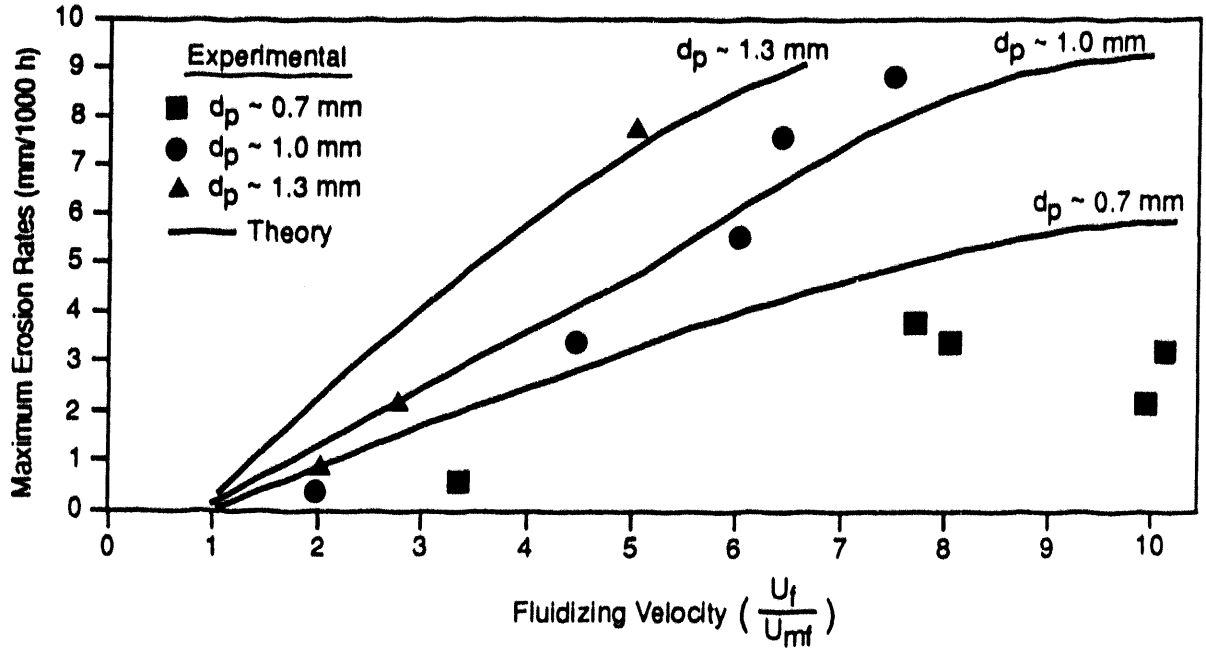

FIGURE 4.1.5 Predicted Maximum Rates versus U/U_{mf} for Several Particle Sizes Experimental Data from Parkinson et al.[4.1.1]

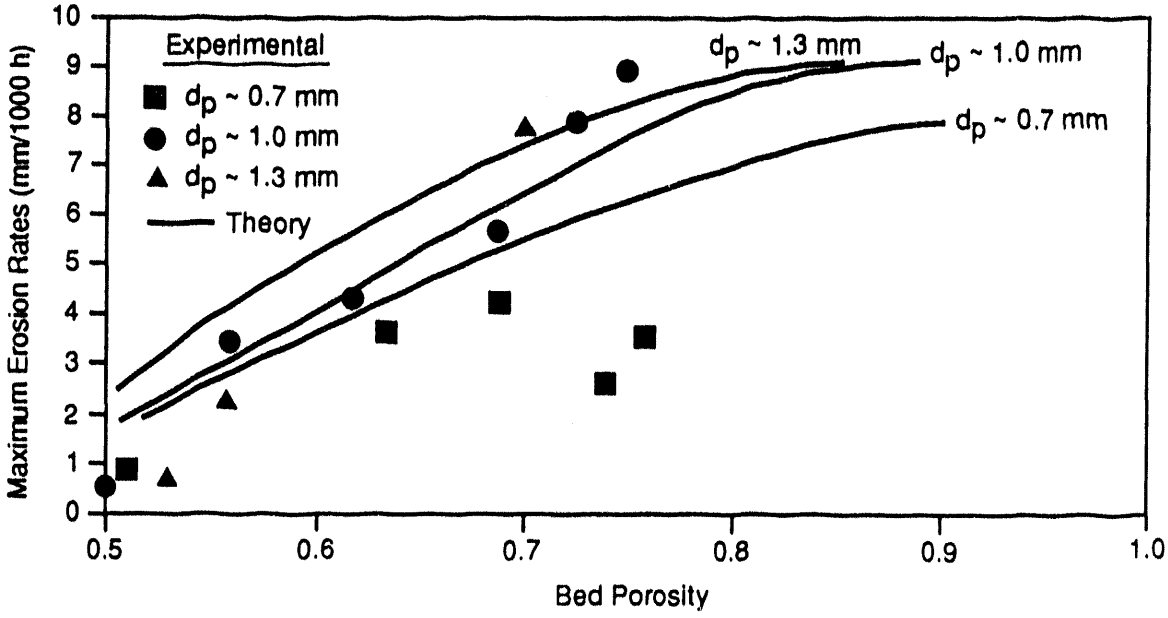

FIGURE 4.1.6 Predicted Maximum Erosion Rates versus Bed Porosity for Several Particle Sizes Experimental Data from Parkinson et al.[4.1.1]

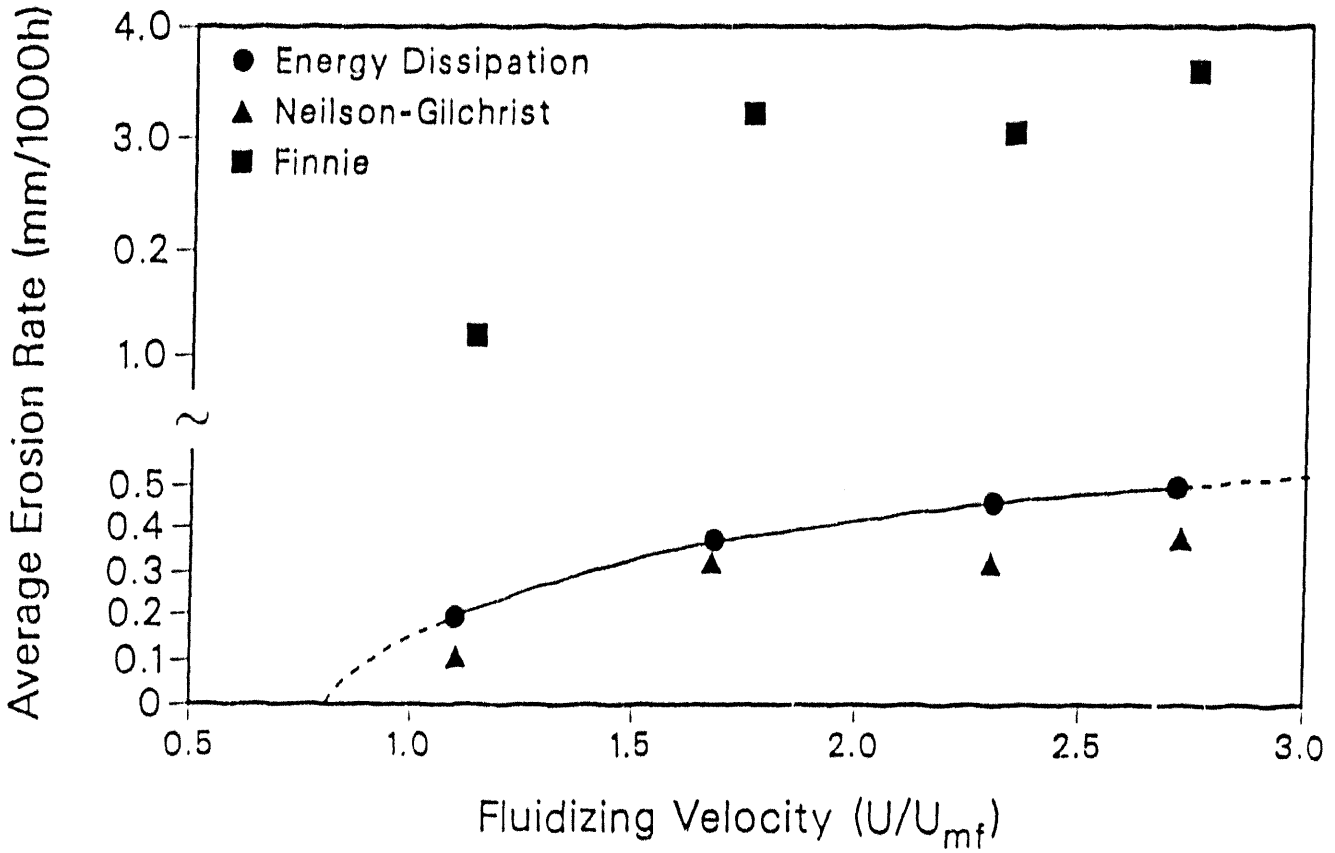

FIGURE 4.1.7 Comparison of Time-Averaged Transient Erosion Rates for Aluminum (Three Tubes) for the Monolayer Energy Dissipation Erosion Model and the Neilson-Gilchrist and Finnie Erosion Models for 0.55-mmDiameter Glass Beads[4.1.4]

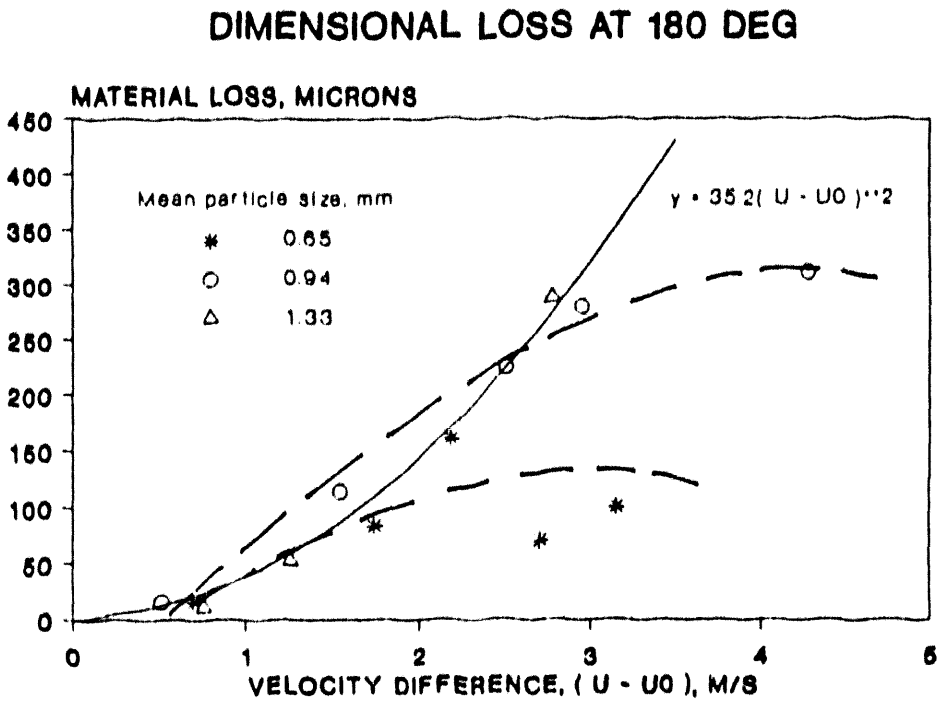

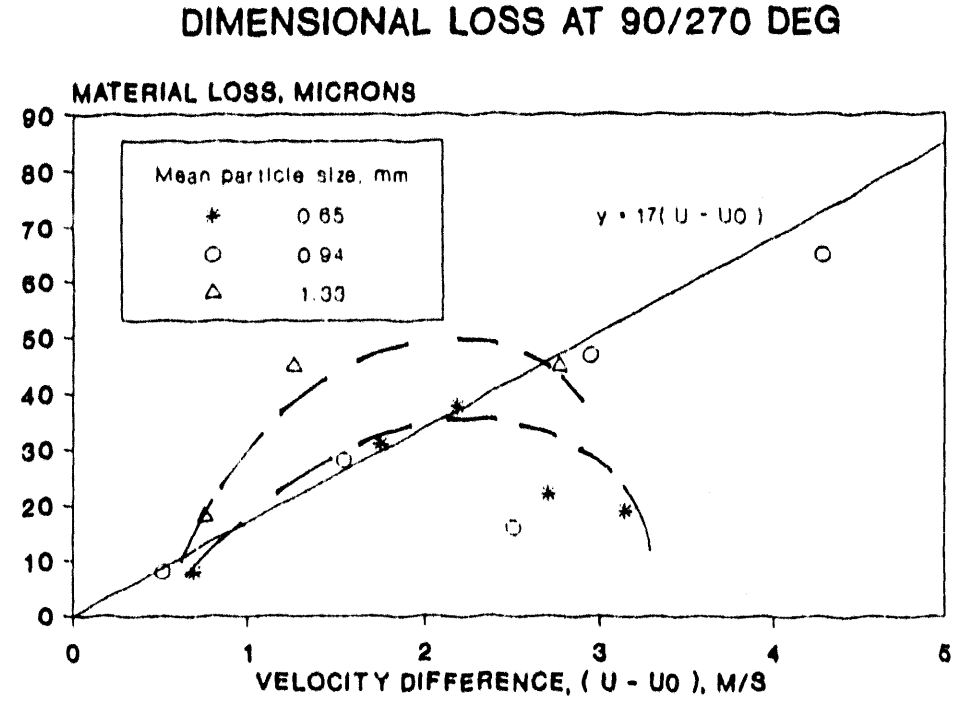

FIGURE 4.1.8 CRE 0.3-m × 0.3-m Cold Bed Material Dimensional Loss for Tube 2 at the 180 and 90/270° Locations[4.1.7]

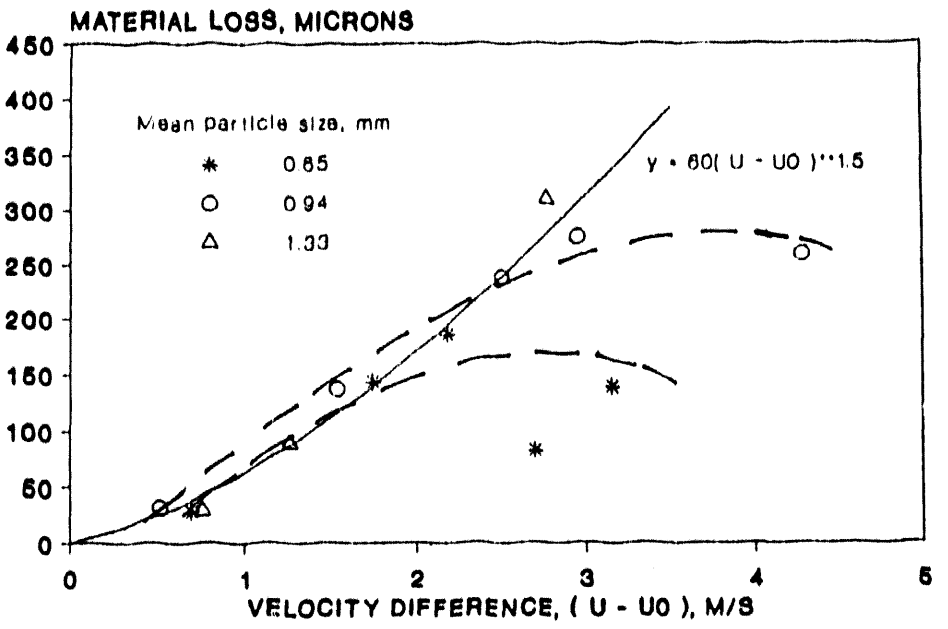

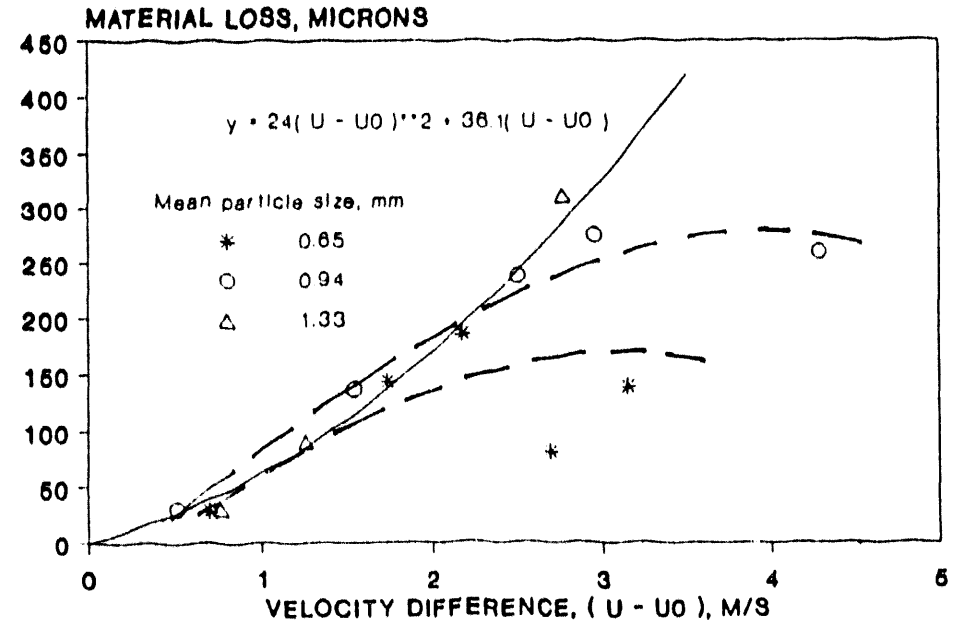

FIGURE 4.1.9 CRE 0.3-m × 0.3-m Cold Bed Material Dimensional Loss for Tube 2 at the 145/215° Location[4.1.7]

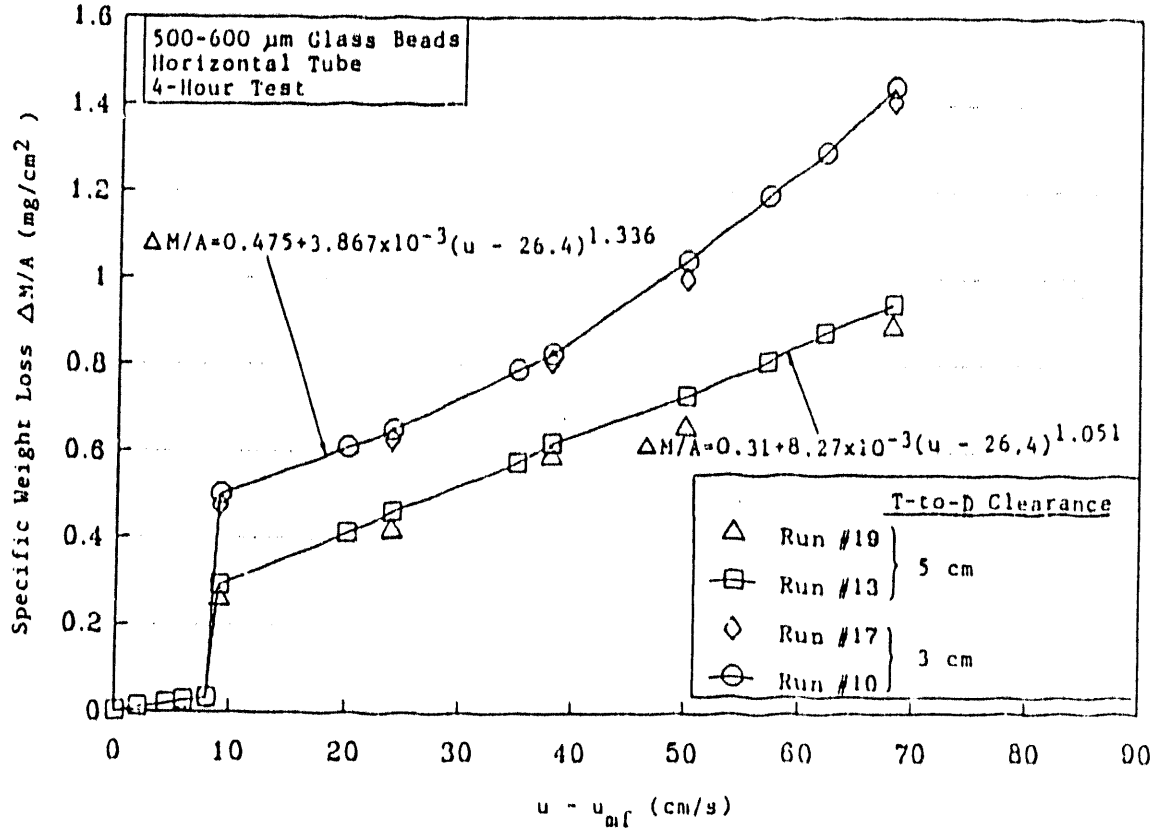

FIGURE 4.1.10 Effect of Superficial Fluidizing Velocity on In-Bed Tube Erosion for a Single 17-mm-Diameter Wax Tube[4.1.7]

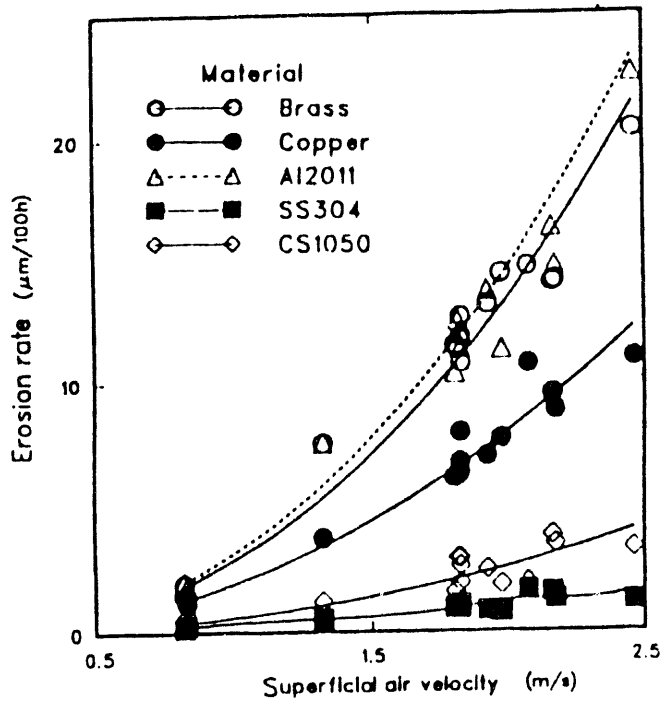

FIGURE 4.1.11 Erosion Rate versus Superficial Air Velocity for Single 32-mm-o.d. Tube Exposed to 1.0-mm Silica Sand of Shape Parameter 0.89[4.1.8,4.1.9]

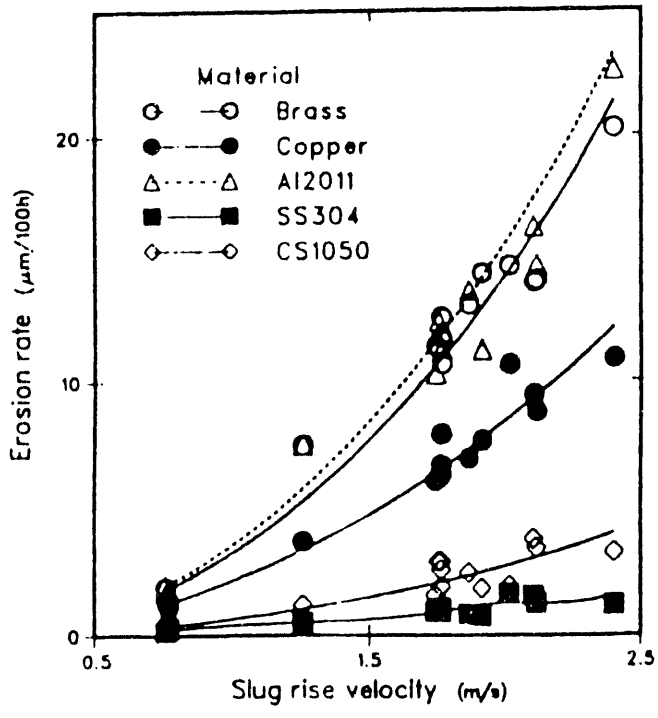

FIGURE 4.1.12 Erosion Rate versus Calculated Slug Rise Velocity for Single 32-mm-o.d. Tube Exposed to 1.0mm Silica Sand of Shape Parameter 0.89[4.1.8, 4.1.9]

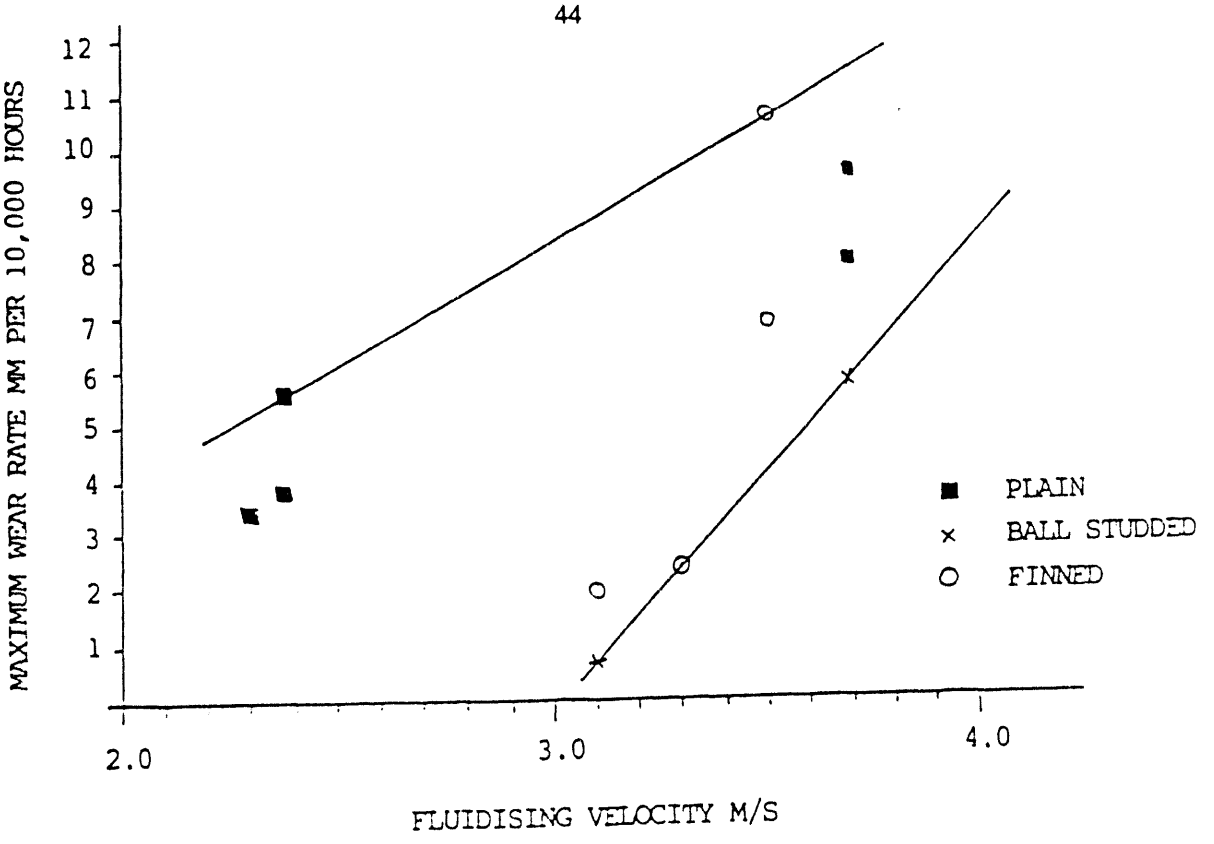

FIGURE 4.1.13 Maximum Wear Rate vs. Fluidization Velocity[4.1.10]

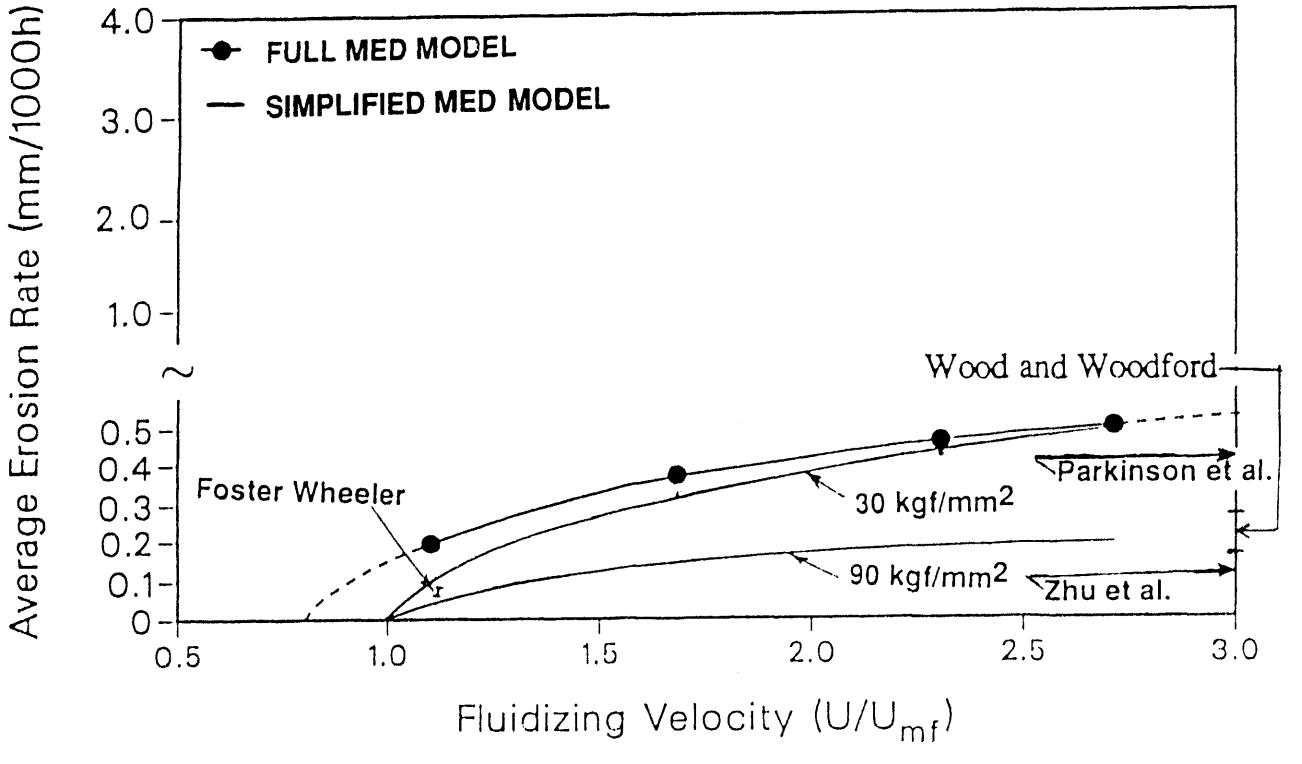

FIGURE 4.1.14 Comparison of Simplified and Full MED Erosion Models for Aluminum

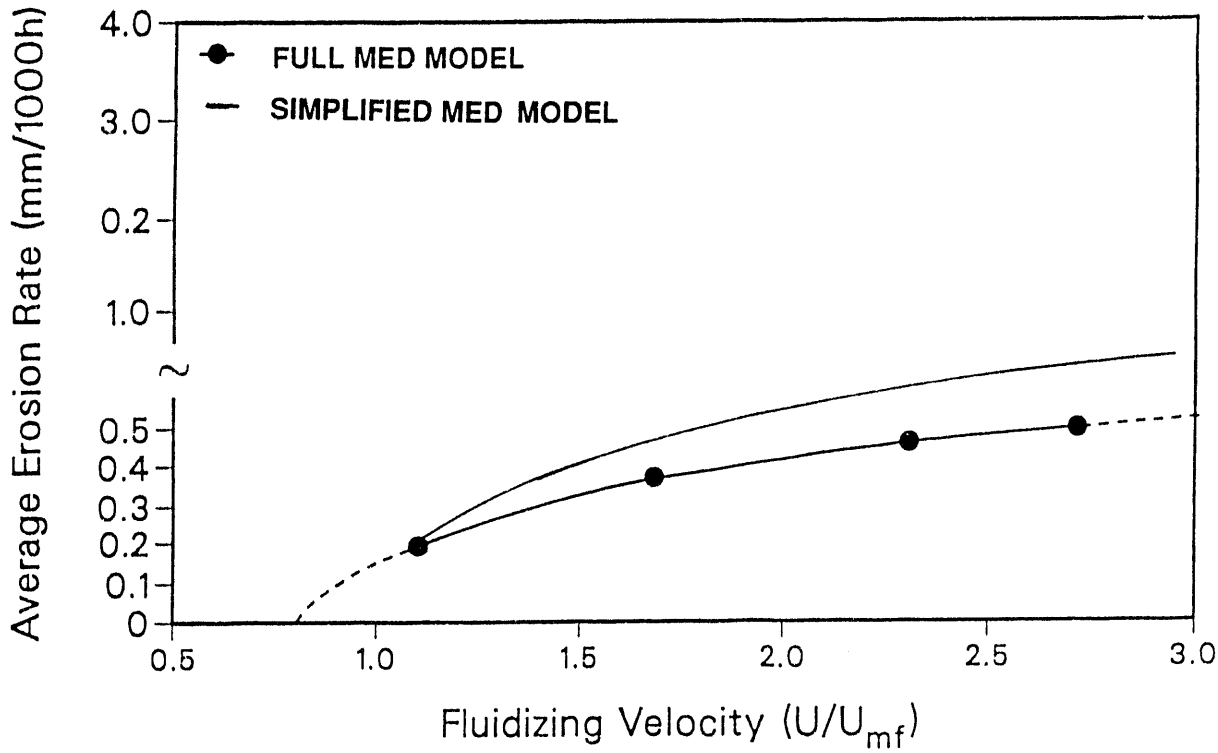

FIGURE 4.1.15 Comparison of Simplified and Full MED Erosion Model Using Renormalization at $U/U_{mf} = 1.12$

4.2 Particle Size

4.2.1 Discussion

The apparent dependency of metal wastage on particle size is a function of how its rate is plotted as a function of the other independent variables. This is clearly illustrated in Figs. 4.1.1-4.1.4 for the Parkinson et al.[4.2.1] PVC wear data. The maximum erosion rates indicated in Figures 4.1.1 and 4.1.4 may indicate a regime transition to "turbulence" as discussed by Zhu et al.[4.2.2,4.2.3] and Parkinson et al.[4.2.1] Figure 4.1.1 shows that the erosion rate decreases above a fluidizing velocity of 2 m/s for 0.7-mm particles and levels off for 1.0-mm particles.

Figure 4.1.2 shows that when the average erosion rate is plotted versus U/U_{mf}, the particle size dependency is quite pronounced; the separate curves are clearly distinct for the four sizes of particles. The same general curve shape is predicted by the full MED erosion model (as shown in Fig. 4.1.7), and the same general trend is predicted for the other erosion models, including the simplified MED erosion model, for a given particle size (as shown in Figures 4.1.5 and 4.1.16).

The effect of particle size on erosion wear in fluidized beds was investigated by Wood and Woodford.[4.2.4] Three size grades of sand were used, 0.1, and 0.93, and 1.9 mm in diameter, and fluidized with superficial air-flow velocities of 1.9, 3.0, and 4.0 m/s, respectively. The flow velocities were adjusted to give a constant void fraction, 0.7, in the 0.2×0.2-m cross-section fluidized bed that was operated at room temperature. Erosion-wear losses after 100 h are summarized in Table 4.2.1, as taken from Raask.[4.2.5] Figure 4.2.1 is a plot of the erosion rate for the four softest metals (aluminum, copper, nickel, and iron). As can be seen in the figure, there is a very nearly linear dependency of erosion rates upon particle diameter over the factor of 20 particle size range.

Clearly, the erosion wear of all materials increased with particle size, but, at the same time, the flow velocity was increased to keep the same bed density (void fraction) in the fluidized zone. It is therefore not feasible to distinguish the relative effect of particle size from that of superficial fluidizing velocity on erosion wear. Raask[4.2.5] claimed that the data in Table 4.2.1 could be fit to an equation of the form:

$$\dot{E} = \alpha (m_p)^{1.3} \qquad (4.2.1)$$

where m_p is the particle momentum given by $m_p = \rho_p V_p \pi d_p^3/6$; where ρ_p, V_p, and d_p are the particle density, velocity, and diameter, respectively; and α is an erosion wear coefficient (unfortunately, not given).

Cross-plotting the Parkinson et al.[4.2.1] erosion rate from Fig. 4.1.2 at a fixed U/U_{mf} also shows a nearly linear dependency (as shown in Fig. 4.2.2), which predicts that increasing the particle size from 500 μm to 2000 μm (a factor of four) will increase the erosion rate by a factor of three. The full MED-erosion model, few-tube approximation of this experiment, predicts this increase as shown in Fig. 4.2.3 at $U/U_{mf} = 1.7$, indicating a particle size dependency to the 0.8 power. As shown in Fig. 4.2.4, Eq. 4.1.5 in Sec. 4.1 is a reasonable fit of the data except for the 400-μm diameter particles. This equation states that the wear rate depends upon the 1.5 power of particle diameter.

Figure 4.1.3 shows that when the Parkinson et al. erosion rate data are plotted versus (UU_{mf}), a particle size dependency persists. The curve fit given by Eq. 4.1.6 ignores this fact. If all of the excess gas velocity goes into bubble production according to the two-phase theory of fluidization, one would expect no explicit particle size dependence. The full MED erosion model results tend to show a higher erosion rate for the larger particles, as shown in Fig. 4.2.5. The calculations are in the low velocity range where the particle size dependency is less pronounced, as shown in Fig. 4.1.3. Further calculations should be performed to elucidate this phenomenon.

Figure 4.1.4 shows that to the left of the maximum, the erosion rate decreases with increasing particle size, while to the right of the maximum, the erosion rate increases with particle size as expected.

Wheeldon[4.2.6] refit the Parkinson et al.[4.2.1] average PVC tube wear data with an extension of Eq. 4.1.6 as follows:

$$\Delta W/(U - U_{mf}) = 0.98\,(d_p)^{1.74} \qquad (4.2.2)$$

where

ΔW = average weight loss, g;
dp = particle diameter, mm;
U = fluidizing velocity, m/s; and
U_{mf} = minimum fluidization velocity, m/s.

The data are replotted in Fig. 4.2.6, along with a plot of Eq. 4.2.2. The correlation coefficient, r, is 0.91, and the estimate of $\Delta W/(U-U_o)$ has 95% confidence limits of ± 0.32. When the correlation coefficient is divided by its standard error of 0.04, it gives a value greater than 2. This shows the relationship to be significant and not occurring by chance. Two points that fell appreciably away from a group of data obtained with sand of similar size were considered outliers.

To confirm the validity of describing the data by means of a relationship in the form of Eq. 4.2.2, similar data obtained from CRE's 1.0-m × 0.5-m cold model[4.2.7] were processed in the same manner.[4.2.6] These data are presented in Fig. 4.2.7, along with the best fit given by the power law expression

$$\Delta W/(U - U_o) = 2.07\,(d_p)^{1.93} \qquad (4.2.3)$$

The units are the same as those for Eq. 4.2.2. The correlation coefficient, r, is 0.98, and its standard error is 0.01; dividing the former by the latter yields a value greater than 2 and shows the relationship to be significant. The 95% confidence limit for the expression is ±0.36. The constant in Eq. 4.2.3 is greater than that in Eq. 4.2.2 because of the longer tube lengths used. Although the exponents are different, tests show that the difference is not statistically significant.

Zhu et al.[4.2.2,4.2.3] studied the effect of the particle diameter on erosion using six different silica sands, keeping the excess gas velocity, ($U - U_{mf}$), constant at 1.31 m/s. The results are shown in Fig. 4.2.8. The erosion rates increase significantly with increased particle diameter, which agrees with the findings of Wood and Woodford.[4.2.4]

The dependence of the erosion rates on particle size was curve fit by Zhu et al.[4.2.3] using least squares to an equation of the form:

$$\dot{E} = C (d_p^n) \qquad (4.2.4)$$

where

$\dot{E}$ = erosion rate, mm/100 h, and
dp = particle diameter, mm.

The values of C and n in Eqs. 4.1.11 and 4.2.4 are not the same. The fitted values of C and n for the different materials tested are listed in Table 4.2.2, along with the correlation coefficients. The average value of n was found to be 1.2, not too different from a linear dependence, but somewhat lower than a 1.5 power dependence from their drop-tube erosion experiments.[4.2.2]

Lee[4.2.8] studied two sizes of sand particles under similar operating conditions. Large particles (1.09 mm in diameter) were found to cause about 200% higher weight loss of in-bed tubes than small particles (0.55 mm in diameter); see Sec. 5.1 for more information.

4.2.2 Recommended Design Guidelines and Procedures

The only practical qualitative guideline with respect to particle size effects is to keep up bed maintenance, i.e., make sure that "rocks" do not accumulate in the unit.[4.2.9] Particles no larger than 2000-3000 μ m in diameter diameter should be excluded. On the basis of this analysis, it is clear that the wear rate depends on the particle diameter raised to a power between 1 and 2. Since particle size and fluidizing velocity are interrelated, a large change in particle size without a corresponding change in fluidizing velocity can adversely affect fluidization characteristics.

The evaluation of erosion rates from Eq. 3.4 for the simplified MED erosion model for different particle diameters is presented in Figures 4.1.5 and 4.1.6.[4.2.10] As can be seen in the figures, the erosion rate increases with particle diameter for all operating conditions. An alternative to using these curves is to use the correlations discussed above to assess the erosion rate dependency upon the erosion rate.

The in-kind data reports received from the British Coal Corporation's Coal Research Establishment, addressing the dependence of the erosion rate, found that when the fluidizing velocity, U, was reduced from 0.8 to 0.6 m/s and the mean particle size of the bed material, d_p, was reduced from 0.75 to 0.4 mm, a large reduction (~60%) in the tube loss was recorded.[4.2.11] For these conditions, the highest tube loss was about the same as that measured for the tubes in the lowest rows of the 'D' bank when U was 0.8 m/s and d_p = 0.75 mm. However, it was felt that further tests needed to be done to ascertain whether the large decrease in tube wear is caused principally by the reduction in fluidizing velocity or in mean particle size. Localized wastage of tubes should also be studied in greater detail.

Test Series 1 showed that there was a large increase in tube wear rate with an increase in bed particle size, which coincides with the predicted change in bed behavior associated with the change from Geldart Group B to D.[4.2.12] It was proposed that changing the operating conditions in the Grimethorpe PFBC (U decreased from 0.8- to 0.6 m/s and d_p from 0.96 to 0.7-mm) should reduce the wear from those tubes most prone to wastage by a factor of about three. Further cold

model tests were recommended to confirm the validity of the assumptions made in scaling the results from this work.

Cold model tests were subsequently performed for tube bank "E."[4.2.13] Those cold model tests quite clearly showed that if particle size were reduced from 750 to 440 μm (and fluidizing velocity from 1.0 to 0.8 m/s), then a reduction in wear rates of between 23-50% on the vertical diameter and between 35-40% on the diagonal diameter could be obtained. However, it was not expected that the fuel preparation plant at Grimethorpe could be changed to produce the same reduction. The mean bed material particle size of 950-μm may only be reduced to around 700-μm. Assuming a linear relationship between the reduction in size and the reduction in wear, a reduction in combustor wear rates of between 18-40% on the verticle diameter and 28-36% on the diagonal diameter would be achieved. This reduction in particle size moved the calculated combustor fluidizing conditions from the border line of Geldart Groups B/D to firmly inside Group B. The actual fluidizing velocity for the combustor would be 0.6 m/s to match 0.8 m/s in the cold model.

Cold model test series A2 showed that the change in mean particle size corresponding to a change from the fluidized bed behavior associated with Geldart Group B material to that of Group D material yielded a large increase in tube wear rate, which confirmed earlier results.[4.1.14]

In cold model test series 11 to 16, the reduction in peak wear rates between cold model Test 1 and Test 11 was by a factor of 4 on the verticle dimension.[4.1.15] This reduction was the result of a combination of reduced particle size, reduced fluidizing velocity, reduced bed height, and changes to tube bank geometry.

Several design guideline procedures are now given in the form of step-by-step examples.

Example 1: Estimate Increased Tube Lifetime by Decreasing Particle Size Using the Simplified MED Erosion Model

The simplified MED erosion model given by Eqs. 3.1 or 3.4 may be used with experimental field data on bed expansion and fluidizing velocity in a manner similar to Example 1 in Sec. 4.1 to estimate the effect of particle size on erosion. The CRE 0.3-m × 0.3-m maximum PVC wear data were analyzed in just this way, as shown in Figs. 4.1.5 and 4.1.6.[4.2.10] In this case, Steps 1 and 2 in Example 1, Sec. 4.1, were eliminated. As can be seen in Figure 4.1.5, erosion rates can be reduced roughly three-fold by reducing the particle diameter from 1.3 to 0.7 mm.

Evaluate Eq. 3.1 with the various particle diameters, 0.7, 1.0, and 1.3 mm and $E_{sp} = 40$ MPa. The other parameters in Step 3, Example 1, Sec. 4.1 remain the same. The solids velocity is computed from[4.2.10]

$$V_s = [g\, x_d\, (\varepsilon - \varepsilon_{gd})/(1 - \varepsilon)]^{1/2} \qquad (4.2.5)$$

instead of setting it to the fluidizing velocity. As can be seen, the agreement with the maximum wear data is good and the correct trend is predicted — increased particle diameter increases the wear rate. For details about the generation of Figures 4.1.5 and 4.1.6, refer to Bouillard and Lyczkowski.[4.1.10] Alternatively, Wheeldon's or Zhu's correlations (Eqs. 4.2.2-4.2.4) may be used.

Example 2: Estimate Tube Lifetime from Zhu's Correlation

Estimate the increased life of a 32-mm carbon-steel (CS1020) tube if the particle size is reduced to 500-μm from 1000-μm at a fixed excess fluidizing velocity of 1.31 m/s.

Using Zhu's correlation (Eq. 4.2.4 and Table 4.2.1), the wear rate for the 1000-μm particles is given by:

$$\dot{E} = 2.10\ (1.0)^{1.09};$$
$$= 2.1\ \mu m/100\ h;\ \text{and}$$
$$= 0.184\ mm/yr.$$

Assuming a 50% safety factor, for a 4.5-mm-tube wall thickness,

$$\text{life} = \frac{4.5 \times 0.5}{0.184} = 12.22\ \text{yr.}$$

If the particle size is reduced to 0.05 mm,

$$\text{life} = 12.22 \times \left(\frac{1.0}{0.05}\right)^{1.09}$$

$$\text{life} = 26.0\ \text{yr.}$$

Example 3: Assess Tube Bundle Erosion Rate for Babcock-Hitachi Fluidized Bed

Babcock-Hitachi (Japan) designed a cold FBC model equipped with a tube bundle geometry (as shown in Figure 4.29) to measure tube bundle erosion rates.[4.2.16] These tubes are made of aluminum, and preliminary erosion data indicate tube losses of about 4 μm after 38 h of operation.

1. Estimate predicted maximum erosion rates from MED Model.
2. Compare prediction with Babcock-Hitachi experimental data.
3. Estimate stainless-steel tube lifetime, assuming the same operating conditions.
4. Assess effect of particle diameter on erosion rates.

(1) Predicted Maximum Erosion Rates From MED Model

First estimate the minimum fluidizing for the 0.7-mm-diameter (d_p) particles from Figure B.1, which is about 50 cm/s. An operating fluidizing velocity of 3 m/s represents a U/U_{mf} ratio of 6. To estimate the tube erosion rate, one can refer to Figure 4.1.5 for $d_p \sim 0.7$ mm. A maximum erosion rate of about 4 mm/1000 h for PVC tubes can be inferred. Note that these erosion rate computations were made for a vertical tube spacing of 160 mm. Since the erosion rate is proportional to the vertical spacing, the erosion rate for the Babcock-Hitachi tube bundle would be about 4 mm/1000 h × 0.35 × E_{sp_p}/E_{sp_a}, where E_{sp_p}/E_{sp_a} is the hardness ratio between PVC and aluminum. Assuming a hardness ratio of about seven, a maximum erosion rate of about 0.2 mm/1000 h is predicted.

(2) Comparison with Data

The experimental erosion rate is about (4×10^{-3} mm/38 h) $\times$ 1000 h, or approximately 0.1 mm/1000 h. Hence, we find, to our satisfaction, that

$$\dot{E}_{exp} = \frac{0.1\text{m}}{1000\text{ h}} < \text{max predicted (Fig. 4.1.5) } \dot{E} \sim \frac{0.3\text{ mm}}{1000\text{ h}}.$$

(3) Estimate Stainless-Steel Tube Lifetime

If the aluminum tubes were replaced by stainless-steel tubes with the same operating conditions, one can assess the tube lifetime, assuming a tube thickness of 3.5 mm. The stainless steel tube would wear away after

$$\frac{1000\text{ h}}{4} \times \frac{1}{0.35} \times 70 \times 3.5 = 1.7 \times 10^5 = 7{,}252 \text{ days} \equiv 20 \text{ years},$$

assuming a hardness ratio between stainless steel and PVC of about 70.

(4) Assess Effect of Particle Size

If unsuspectedly larger 1.3-μm-diameter particles are introduced in the unit, let us try to assess what erosion rate increase we can expect. From Figure B.1, we estimate that the minimum fluidization velocity for these particles is about twice that for 0.7-μm-diameter particles. Assuming that the two particle sizes act independently, and that the fluidizing velocity remains the same, U/υ_{mf} is approximately 3. From Figure 4.15, it is seen, therefore, that the erosion rate roughly doubles, thereby reducing the unit lifetime to about 10 years. Costly maintenance, repairs, and downtime could occur after 10 years of service and have to be factored into the plant management and planning. In this example, it is clear that by keeping the inventory of large particles to a minimum in the fluidized bed, one could expect a much longer tube lifetime.

References

4.2.1 Parkinson, M.J., A.W. Jury, B.A. Napier, T.J. Kempton, and J.C. Holder, *Cold Model Erosion Studies in Support of Pressurized Fluidized Bed Combustion*, Electric Power Research Institute Draft Final Report for Project 1337-2 (April 1986).

4.2.2 Zhu, J., *Tube Erosion in Fluidized Beds*, Ph.D. Thesis, Department of Chemical Engineering, The University of British Columbia (May 1988).

4.2.3 Zhu, J., J.R. Grace, and C.J. Lim, *Tube Wear in Gas Fluidized* Beds—I. *Experimental Findings*, Chemical Engineering Science, *45*(4):1003-1015 (1990).

4.2.4 Wood, R.T., and D.A. Woodford, *Tube Erosion in Fluidized-Beds*, ERDA Report 81-12 911-ET-FUC/79, prepared for New York State Energy Research and Development Authority by General Electric Co., Schenectady, NY (Dec. 1980).

4.2.5 Raask, E., *Erosion Wear in Coal Utilization*, Hemisphere Publishing Corp., Washington, D.C. (1988).

4.2.6 Wheeldon, J M., *A Re-Evaluation of Tube Wastage Data Collected from a Bubbling Fluidised Bed Cold Model*, Proceedings of the Fourth Berkeley Conference on Corrosion-Erosion-Wear of Materials at Elevated Temperatures, Berkeley, CA, Jan. - Feb. 2, 1990, A.V. Levy, ed., pp. 41-1 to 41-13, National Association of Corrosion Engineers, Houston, Texas (1991).

4.2.7 Parkinson, M.J., *Current Work on Cold Modelling of Fluid Bed Systems*, in EPRI Workshop Proceedings: Wastage of In-Bed Surfaces in Fluidized Bed Combustors, held at Argonne National Laboratory, Nov. 2-6, 1987. Available from Electric Power Research Institute (1987).

4.2.8 Lee, S.W., *Analysis and Modeling of In-Bed Tube Erosion in a Gaseous Fluidized Bed*, Doctoral Dissertation, The Catholic University of America, Washington, D.C. (Feb. 1989).

4.2.9 Stringer, J., *Current Information on Metal Wastage in Fluidized Bed Combustors*, Proceedings of the 9th International Conference on Fluidized Bed Combustion, J.P. Mustonen, ed., Vol. 2, pp. 685-696, American Society of Mechanical Engineers, New York (1987).

4.2.10 Bouillard, J.X., and R.W. Lyczkowski, *On the Erosion of Heat Exchanger Tube Banks in Fluidized Bed Combustors*, Powder Technology, *68*:37-51 (1991).

4.2.11 British Coal Corporation, Coal Research Establishment, *Cold Model Studies of Tube Wear in Support of PFBC (December 1985-February 1986)*, PFBC/MOA/P9, Stoke Orchard, Cheltenham, U.K. (April 9, 1987).

4.2.12 Parkinson, M.J., A.W. Jury, B.A. Napier, N.C. Moon, and C.M. Barrety, *Cold Model Studies on the Effect of Fluidizing Velocity and Mean Particle Size on Tube Wear, Test Series 1*, PFBC/MOA/P15, British Coal Corporation, Coal Research Establishment, Stoke Orchard, Cheltenham, U.K. (June 12, 1987).

4.2.13 British Coal Corporation, Coal Research Establishment, *Results of the First Ten Cold Model Tests at Grimethorpe Leading to the Design of Combustor Tube Bank 'E'*, PFBC/MOA/P21, Stoke Orchard, Cheltenham, U.K. (Nov. 6, 1987).

4.2.14 British Coal Corporation, Coal Research Establishment, *Cold Model Studies on the Effect of Fluidizing Velocity and Mean Particle Size on PFBC Tube Wear, Test Series A2*, PFBC/MOA/P28, Stoke Orchard, Cheltenham, U.K. (April 21, 1988).

4.2.15 British Coal Corporation, Coal Research Establishment, *Grimethorpe Cold Model Tests 11 to 16: Evaluation of the Tube Bank 'E' Final Design and Assessment of the Benefit of Further Tube Diameter Increases*, PFBC/MOA/P29, Stoke Orchard, Cheltenham, U.K. (April 28, 1988).

4.2.16 Kaneda, H., and K. Oki, *A Plan for Studying Erosion in a CFB Furnace Using a 15 Meter High, 0.7 Meter Square CFB Cold Model*, in Proceedings of the Workshop on Materials Issues in Circulating Fluidized-Bed Combustors, pp. 14-1 to 14-21, Electric Power Research Institute Report GS-6746 (Feb. 1990).

TABLE 4.2.1 Erosion Wear of Metal and Alloy Specimens in Fluidized Sand Bed[4.2.4,4.2.5]

Specimen	Erosion wear (mm/100 h)		
	Test 1[a]	Test 2[b]	Test 3[c]
Metals			
Aluminum	4	51	117
Copper	0.8	9	31
Nickel	0.8	5	20
Iron	0.7	4	14
Cobalt	0.5	2	9
Alloys			
SA 213-T11 alloy	0.5	3	9
SS 316 steel	0.9	2	4
6B stellite	0.6	2	5
A 286 alloy	0.4	2	4
High-speed steel	0.9	2	4

[a]Particle size 0.1 mm; fluidizing velocity 1.9 m/s.
[b]Particle size 0.93 mm; fluidizing velocity 3.0 m/s.
[c]Particle size 1.9 mm; fluidizing velocity 4.0 m/s.

TABLE 4.2.2 Constants from Least Squares Fitting of Eq. 4.2.4[4.2.3]

Material	C	n	Correlation Coefficient
Brass	14.42	1.58	0.98
Copper	9.50	1.15	0.96
A12011	15.05	1.09	0.96
SS304	1.18	1.13	0.94
CS1020	2.10	1.09	0.97
Mean value		1.2	
Standard deviation		0.21	

Conditions:

Sample size: 24 data points for every material.
Excess air velocity: 1.31 m/s.
Particles: silica sand
Particle sphericity: 0.89.

The units on C are $(\mu m/100\ h)/(mm^n)$.

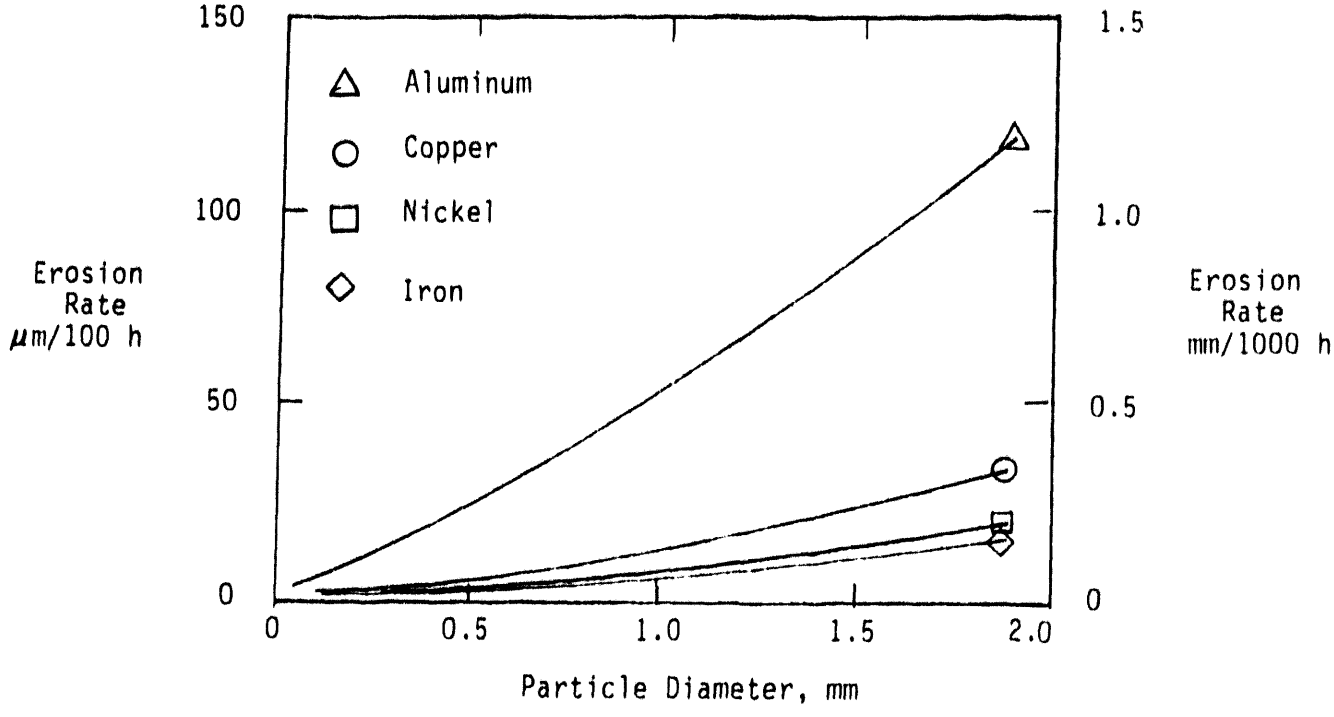

FIGURE 4.2.1 Erosion Rate as a Function of Particle Parameter[4.2.4]

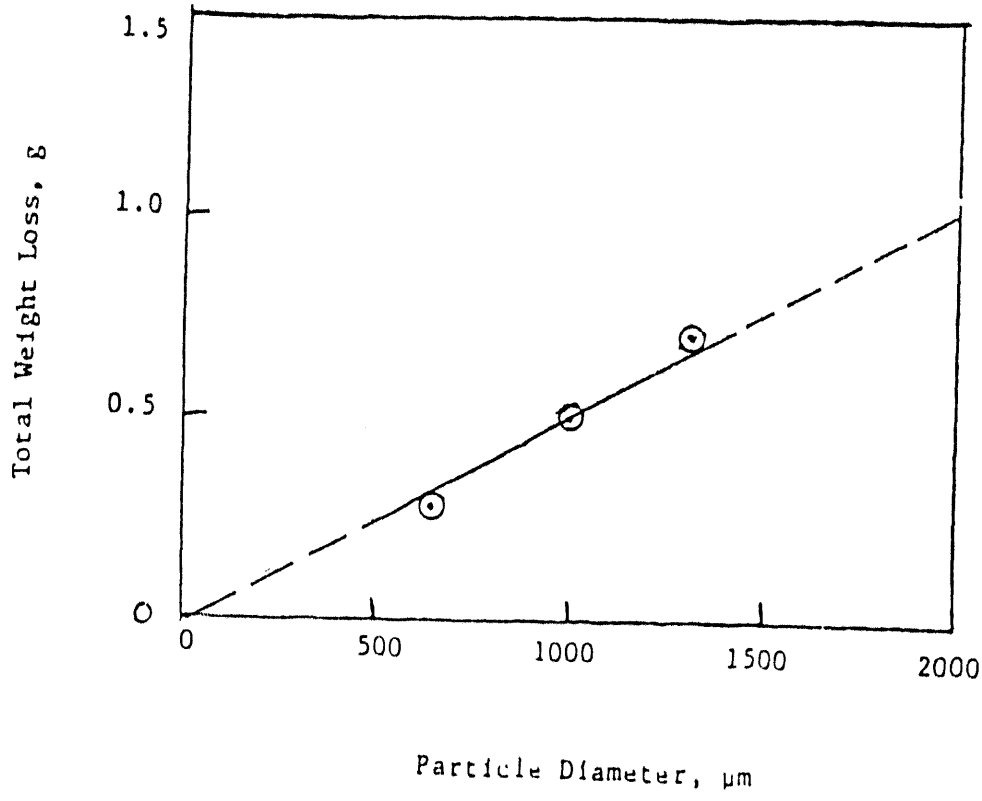

FIGURE 4.2.2 Effect of Particle Diameter on Erosion for PVC Tubes at $U/U_{mf} = 1.7$[4.2.1]

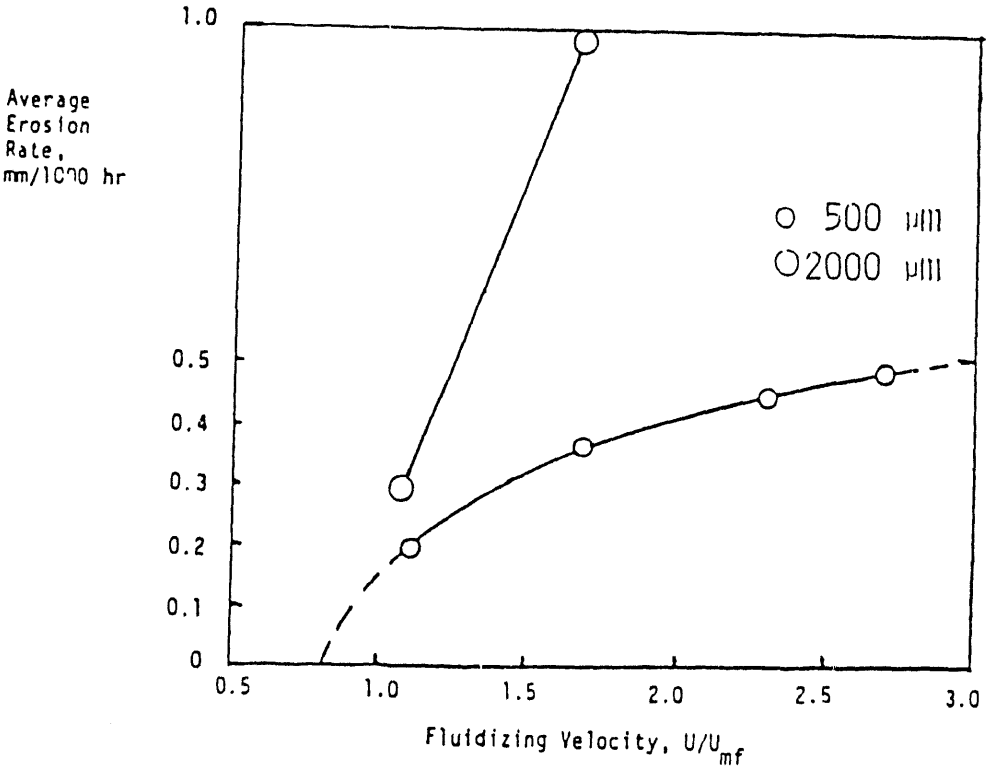

FIGURE 4.2.3 Comparison of Time-Averaged Transient Erosion Rates for Aluminum (3 Tubes) for the Monolayer Energy Dissipation Erosion Model for 500- and 2000-mm-Diameter Particles versus (U/U_{mf})

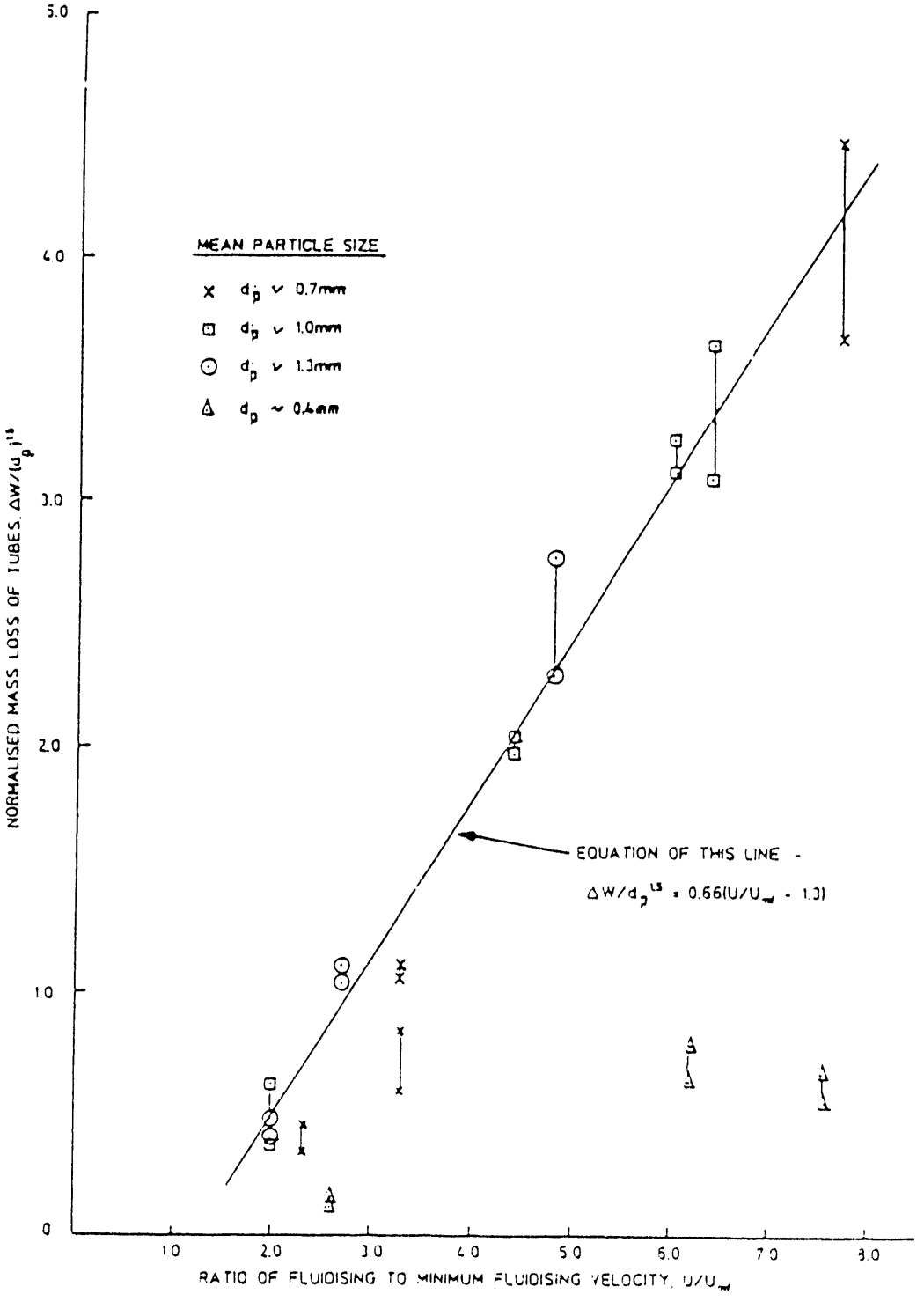

FIGURE 4.2.4 Normalized Tube Mass Loss versus $(U/U_{mf})^{(4.2.1)}$

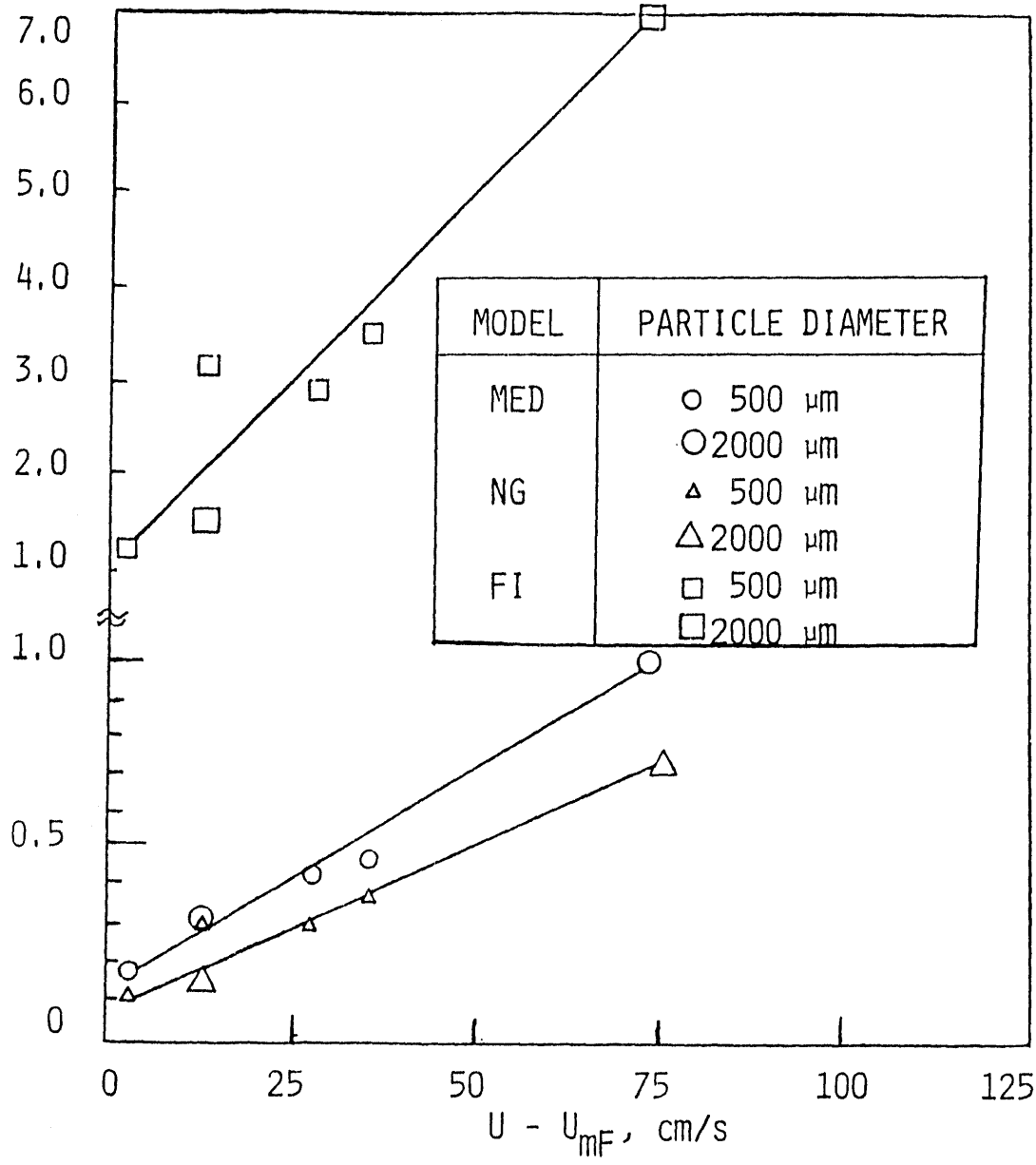

FIGURE 4.2.5 Comparison of Time Averaged Transient Erosion Rates for the Monolayer Energy Dissipation (MED), Neilson-Gilchrist (NG), and Finnie Impaction (FI) Erosion Models for 500- and 2000-mm-Diameter Particles versus ($U-U_{mf}$)

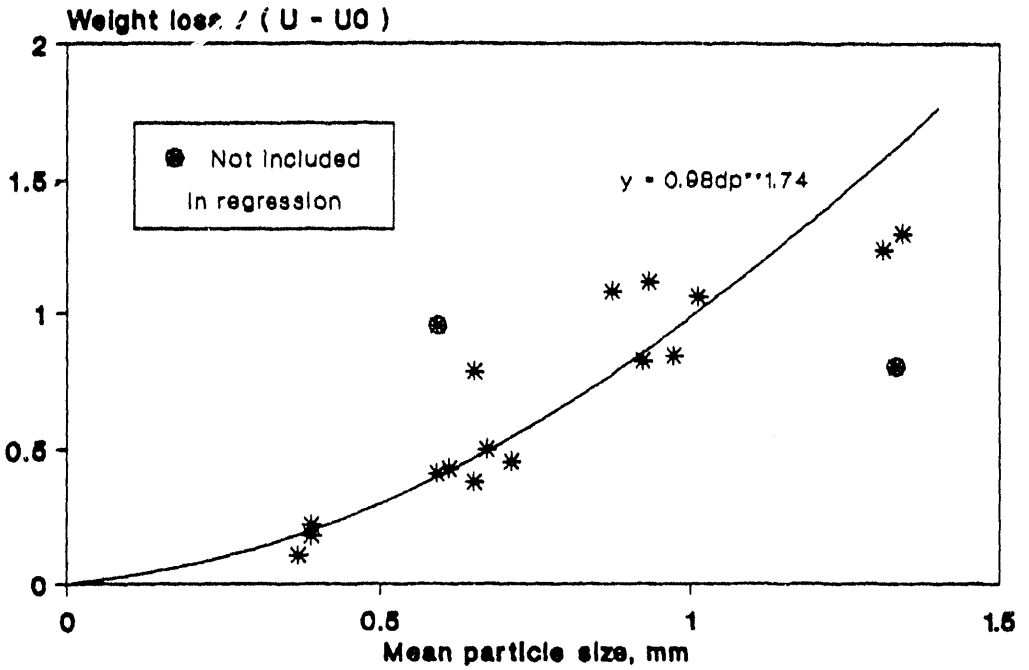

FIGURE 4.2.6 CRE 0.3 m x 0.3 m Cold Model Wastage Particle Size Dependency[4.2.6]

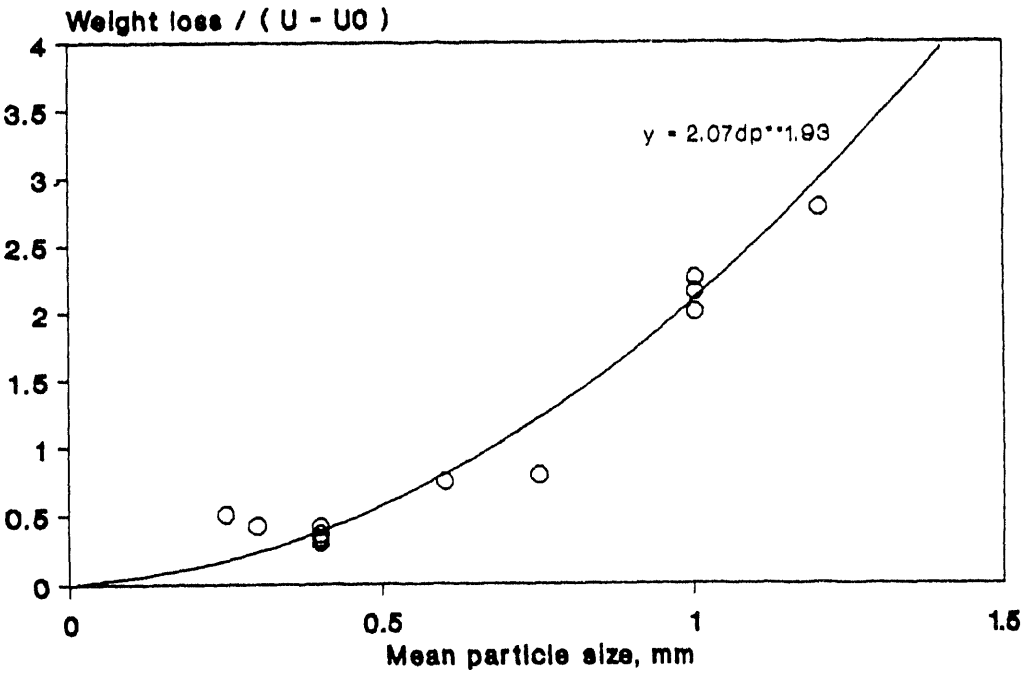

FIGURE 4.2.7 CRE 0.5 m x 1.0 m Cold Model Wastage Particle Size Dependency[4.2.6]

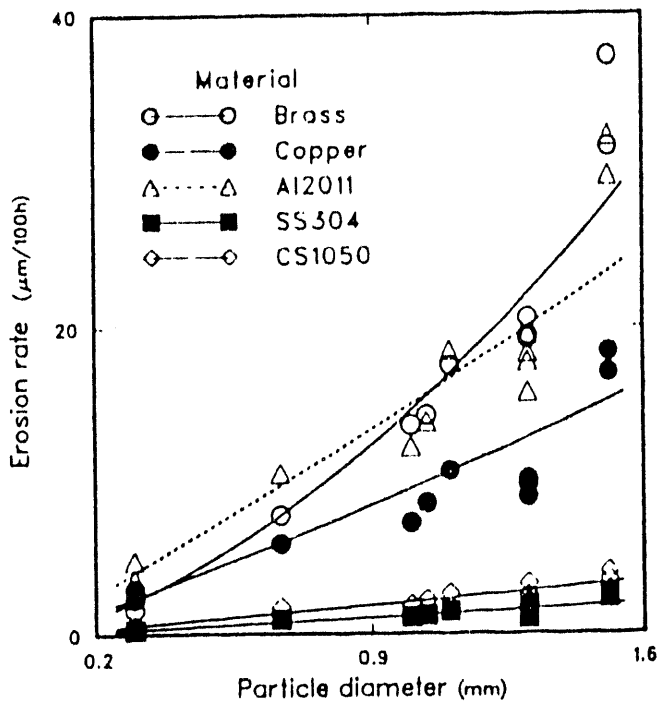

FIGURE 4.2.8 Erosion Rate versus Particle Diameter for Single 32-mm-o.d. Tube Exposed to Silica Sand (Shape Parameter 0.89) at $(U - U_{mf}) = 1.31$ m/s[4.2.2,4.2.3]

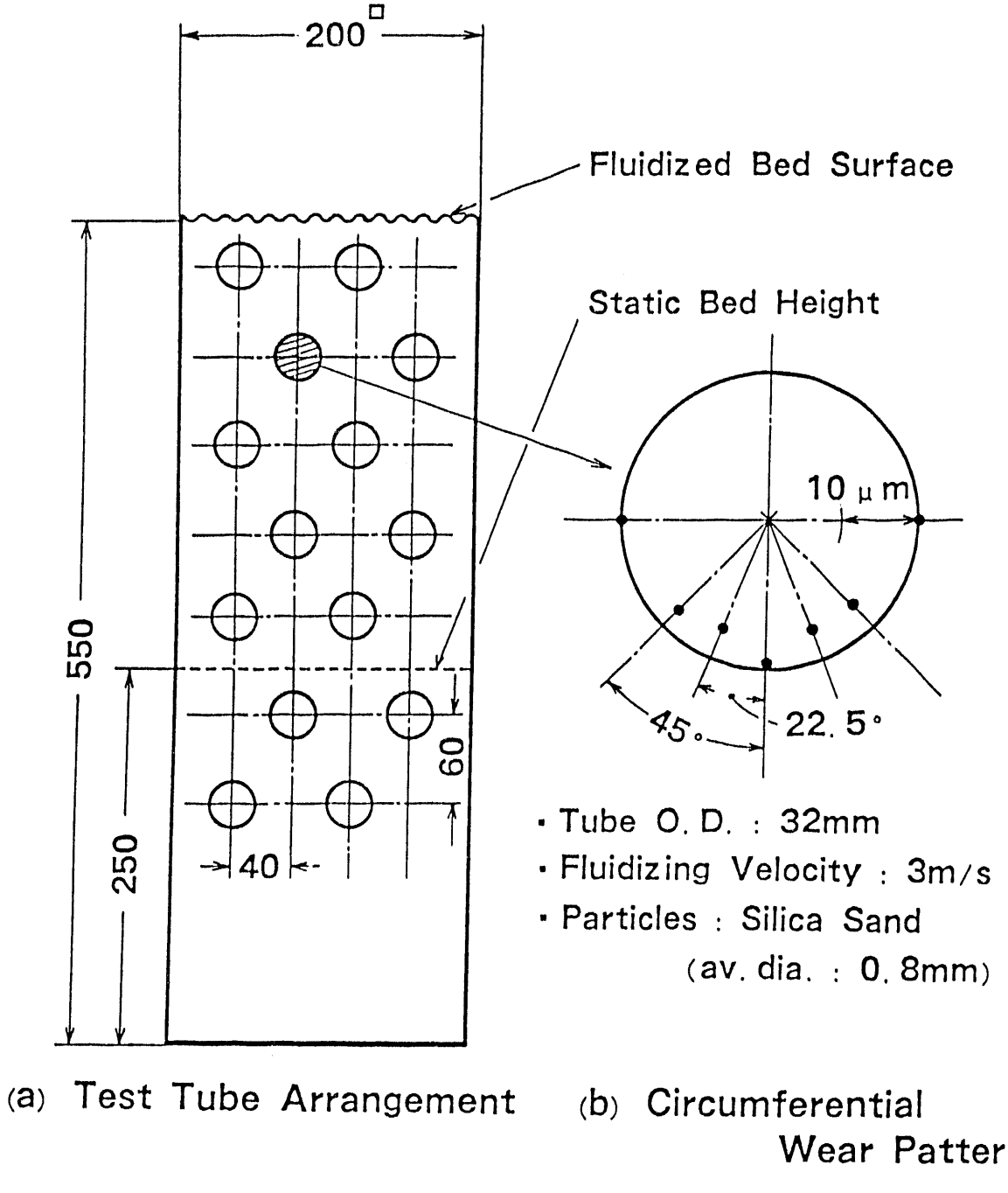

FIGURE 4.2.9 Arrangement of Test Tubes and an Example of the Measured Wear[4.2.16]

4.3 Particle Angularity or Sphericity

4.3.1 Discussion

A particle having an extremely rough surface and a sphericity close to unity, such as quartz sand, may cause significantly increased metal wastage. On the other hand, a particle such as silicon carbide or molochite that is highly angular and that does not have an extremely rough surface may also cause significantly increased metal wastage. In the absence of other quantitative information, sphericity will be used as a first approximation to characterize increased metal wastage caused by angular particles. The concept of sphericity was introduced by Wadell[4.3.1] and is defined as the square root of the projected area of the particle divided by the area of the smallest circumscribing circle. For extremely rough particles, the surface area per area of an equivalent sphere may be a measure of the increased metal wastage caused by such particles.

In order to study the effect of various particle properties affecting metal wastage, Zhu et al.[4.3.2,4.3.3] used six different silica sands and kept the excess gas velocity, $(U-U_{mf})$, constant at 1.31. m/s. The experimental setup is described in Sec. 4.1.1. Five experiments were run using 1.0-mm-diameter particles having different shape parameters. The shape parameter was characterized by an approximation to the sphericity determined from enlarged photographs.[4.3.2] The shape parameter was varied by wearing the particles for increasing experiment times. The particles became rounder as they accumulated more time in the fluidized bed.

The results are shown in Fig. 4.3.1. The results for a sphericity of 1.0 were obtained by using glass beads with a diameter of 0.89 mm. The hardness of the glass beads is 340 kgf/mm^2 (3332 MPa), which is very close to that for silica sand, 350 kgf/mm^2 (3430 MPa). The erosion rates were "corrected" for particle size by using Eq. 4.2.4 in Sec. 4.2. That is, the erosion rates for the 0.89-mm-diameter glass beads were renormalized to those for 1.0-mm-diameter glass beads according to the formula:

$$\dot{E}_{1.0\ mm} = \dot{E}_{0.89\ mm}\,(d_{p\ 1.0\ mm}/d_{p\ 0.89\ mm})^{n} \qquad (4.3.1)$$

where n is between 1-1.5. Any units may be used in Eq. 4.3.1.

Clearly, the erosion rate increases significantly as the particles become more angular, i.e., the sphericity becomes smaller as shown in Fig. 4.3.1. This same phenomenon was noted in Zhu's drop-tube metal wastage experiments.[4.3.2] Figure 4.3.1 indicates that even spherical glass beads $(\phi_s = 1)$ can produce wear rates comparable with those of angular sand particles $(\phi_s < 1)$. Other investigators, including Tilley,[4.3.4] Drennen and Zera[4.3.5], and Ninham et al.[4.3.6] Zhu et al.[4.3.2, 4.3.3] noted similar findings in that the wastage rate of fresh angular particles was higher than that for particles that were in the bed for some time. These observations are consistent with the findings of Ninham et al.[4.3.6]

The dramatically increased metal wastage rates for the ABB/CE drop-tube data for crushed quartz versus sand is shown in Fig. 4.3.2.[4.3.5] The wastage rate increases more at the higher velocities for the crushed quartz than it does for sand. Only runs 2 and 7 held the velocity and particle diameter constant. The sphericity was not measured. Zhu's drop-tube data[4.3.2] taken at 5 m/s for brass target material suggest that the crushed quartz sphericity in the ABB/CE drop-tube experiment was less than 0.8. This estimate was obtained by equating the roughly factor of 10 increase in wastage rate at 5 m/s in Fig. 4.3.2 with a similar increase for the Zhu[4.3.2] drop-tube data. Zhu found a much higher wastage rate for the drop-tube experiment, but the velocity was

higher (5 m/s) than in any of the fluidized bed experiments. If Eq. 4.1.11 (Sec. 4.1) is extrapolated to 5 m/s, a wastage rate of about one-half to one-third of the drop-tube data results. Raask[4.3.7] has tables of particles and their associated sphericities that can be used to estimate this parameter.

Zhu[4.3.2] correlated the metal wastage data as a function of sphericity with an equation of the form:

$$\dot{E} = C_3(C_4-\phi_s) \qquad (4.3.2)$$

where

$\dot{E}$ = erosion rate, μm/100 h.

The fitted values of C_3 and C_4 are listed in Table 4.3.1, along with the correlation coefficients. The curve fits are plotted in Fig. 4.3.2. The sphericity correlation given by Eq. 4.3.4 can be thought of as a correlation for the parameter involving the restitution coefficient $(1-e^2)$ in the simplified MED erosion model discussed in Sec. 3. The less spherical the particle, the lower the restitution coefficient, e, and hence the higher the erosion rate. The implication is that more energy is transferred from the particles to the target as they become more angular because of the increased possibility of tumbling, which produces gouging and subsequent material removal. Two parameters used to characterize the increased metal wastage caused by angular particles are the asperity, which is the inverse of the sphericity,[4.3.7] and the abrasivity index.[4.3.7,4.3.8] The coefficient of restitution, e, may be thought of as an implicit function of these two parameters, as shown in Example 2.

4.3.2 Recommended Design Guidelines and Procedures

Guidelines of a qualitative nature indicate that the abrasivity index of the bed material must be taken into account.[4.3.8] Results of a range of used bed materials from different FBCs varied by a factor of up to 1.6.

Because of a lack of quantitative data for fluidized beds, Eq. 4.3.2 and the values in Table 4.3.1 are recommended as a first approximation to estimate the increased erosion propensity for angular particles. Even though sphericity may not completely reflect particle angularity and/or surface roughness effects on metal wastage, it can be used in place of the parameter $(1-e^2)$ in the simplified MED erosion model developed in Sec. 3. Figures 2.4 and 2.7 in Raask's book[4.3.7] containing various particle shapes can be used to quickly estimate particle sphericities. A detailed discussion of sphericity, roundness, and asperity is also presented.

Example 1: Estimate Increased Metal Wastage due to Decreasing Particle Sphericity

Estimate the increased metal wastage produced by changing the particle sphericity, ϕ_s, from $\phi_{s1} = 1.0$ to $\phi_{s2} = 0.9$ for carbon steel (CS1020) tubes at an excess fluidizing velocity of 1.31 m/s for 1-mm silica sand ($U_{mf} = 0.36$ m/s).

From Eq. 4.3.2 and Table 4.3.1

increase in wear $= (C_4 - \phi_{s2}) / (C_4 - \phi_{s1})$
$= (1.07 - 0.9)/(1.07 - 1.0)$
$= 2.43.$

Therefore, less round sand particles would erode at a rate 2.43 times the wastage rate for particles having a sphericity of 1.0.

Example 2: Estimate Coefficient of Restitution from Zhu's Experiment

Zhu's[4.3.2] correlation given by Eq. 4.3.2 can be used to estimate the restitution coefficient as a function of spericity. We will use aluminum alloy A12011-T3 as an example. At a spericity of 1.0, the factor $C_4 - \phi_S = 0.10$. Equating this value to $1 - e^2$ yields $e^2 = 0.9$, in agreement with the typical value used to generate Figs. 4.1.5 and 4.1.6.[4.3.9, 4.3.10] The erosion rate at a spericity of 0.8 would yield $C_4 - \phi_s = 1.10 - 0.8 = 0.3$, or a factor of 300% higher. In this case, $e^2 = 0.7$. This same technique can be used for the other materials in Table 4.3.1. Lacking any other data, this technique should be used to estimate e^2.

References

4.3.1 Waddell, H., *Sphericity and Roundness of Rock Particles,* J. Geol., *41*:310-331 (1933).

4.3.2 Zhu, J., *Tube Erosion in Fluidized Beds,* Ph.D. Thesis, Department of Chemical Engineering, The University of British Columbia (May 1988).

4.3.3 Zhu, J., J.R. Grace and C.J. Lim, *Tube Wear in Gas Fluidized Beds—I. Experimental Findings,* Chemical Engineering Science, *45*(4):1003-1015 (1990).

4.3.4 Tilley, G.P., *Erosion Caused by Impact of Solid Particles,* Treatise on Materials Science and Technology, Vol. 13: Wear, S. Douglas, ed., pp. 287-320, Academic Press, New York (1979).

4.3.5 Drennen, J.F., and J. Zera, *Erosion Limit Study Final Report, Task 1 of Argonne National Laboratory's Erosion in Fluidized Bed Combustors Joint Venture Program,* ABB Combustion Engineering, Inc., Report MSE-90-2, Windsor, CT (January 1990).

4.3.6 Ninham, A.J., M.J. Entwisle, I.M. Hutchings, and J.A. Little, *A Laboratory-Scale Fluidized Bed Rig for High-Temperature Tube Wastage Studies,* Proceedings of the 10th (1989) International Conference on Fluidized Bed Combustion, A.M. Manaker, ed., Vol. 1, pp. 583-589, American Society of Mechanical Engineers, New York (1989).

4.3.7 Raask, E., *Erosion Wear in Coal Utilization,* Hemisphere Publishing Corp., Washington, D.C. (1988).

4.3.8 Ellis, F., and C. Armitage, *Combating Metal Wastage in Fluidized Bed Combustors,* in 1988 Seminar on Fluidized-Bed Combustion Technology for Utility Applications, Vol. 1: Atmospheric Fluidized-Bed Combustion, Electric Power Research Institute (May, 1988).

4.3.9 Bouillard, J.X., and R.W. Lyczkowski, *On the Erosion of Heat-Exchanger Tube Banks in Fluidized-Bed Combustors,* Powder Technology, *68*:37-51 (1991).

4.3.10 Savage, S.B., *Granular Flow at High Shear Rates,* pp. 339-357, Academic Press, New York (1982).

Table 4.3.1 Constants from Least Squares Fitting of Eq. 4.3.2.[4.3.2]

Material	C_3	C_4	Correlation Coefficient
Brass	65.1	1.07	0.98
Copper	28.0	1.13	0.91
A12011-T3	56.4	1.10	0.95
SS304	5.5	1.06	0.96
CS1020	12.5	1.07	0.92
Mean Value		1.1	
Standard Deviation		0.03	

Conditions:

Sample Size: 12 data points for every material.
Particles: 1.0-mm silica sand and 1.0-mm glass beads.
Excess air velocity: 1.31 m/s.

The units of C_3 are $\mu m/100$ h.

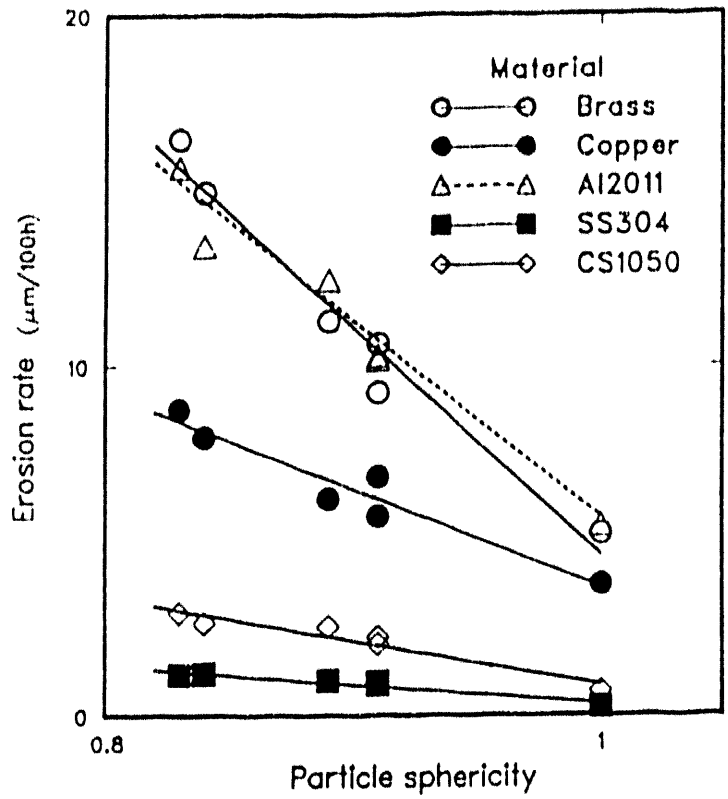

Operating conditions:

Particles: *1.0 mm silica sand and glass beads*
Excess air velocity: *1.31 m/s*
Tube: *32 mm single tube*
Duration: *41 – 120 h*

*Note erosion data for particle sphericity = 1 is for 0.8-mm-diameter glass beads corrected to 1.0 mm. All the remaining erosion data are for silica sand.

FIGURE 4.3.1 Erosion Rate versus Particle Shape Parameter for Single 32-mm-o.d. Tube Exposed to Silica Sand and Glass Beads at $(U-U_{mf})$ = 1.31 m/s[4.3.2,4.3.3]

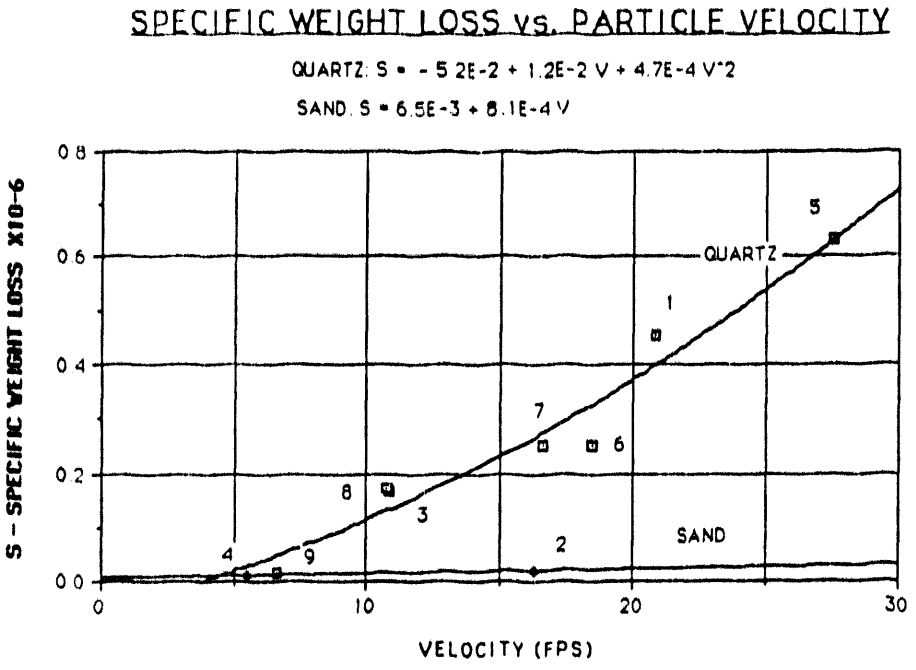

Figure 15

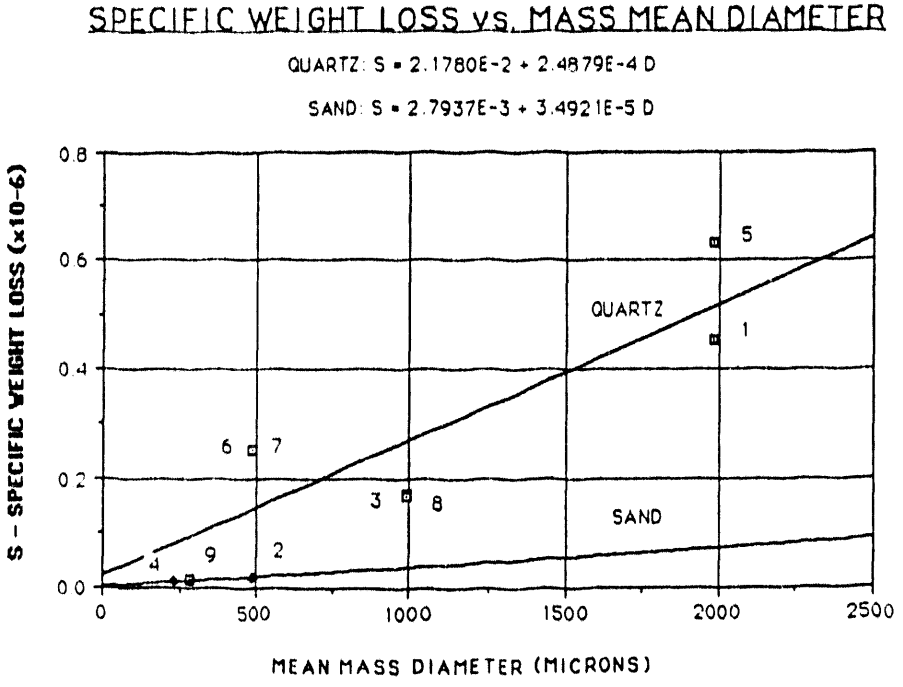

FIGURE 4.3.2 Specific Weight Loss versus Particle Velocity (Top) and Mean Mass Diameter for the ABB CE Drop-Tube Experiment[4.3.5]

4.4 Particle Hardness

4.4.1 Discussion

The basic assumption in the erosion models developed thus far is that the particle hardness is much greater than that of the target. When this is true, there is *no* effect of particle hardness on the erosion rate. This was first studied systematically by Wellinger and Uetz.[4.4.1] Figure 4.4.1, reproduced from Engel,[4.4.2] illustrates this phenomenon. For particles harder than the target material, therefore, changes in sphericity, angularity, or abrasivity would not increase erosion rates, implying no correlation exists between these parameters and particle hardness. When the particle hardness drops below the hardness of the target, the erosion rate decreases.

The work of Tsai et al.[4.4.3] suggests that at least for slurries, the overall effect of particle and target hardness on erosion is approximately

$$\dot{E} \propto \frac{E_p^{1/2}}{E_t}, \quad E_p<E_t \tag{4.4.1}$$

where E_p is the particle hardness and E_t is the target hardness.

Zhu et al.[4.4.4,4.4.5] studied the effect of particle hardness in the fluidized-bed experiment described in Sec. 4.1. Hard silicon carbide was used as the bed material. Results for these tests are shown in Fig. 4.4.2. Zhu et al. concluded that for nonferrous materials, the particle hardness did not appear to affect the metal wastage rates appreciably. However, for the ferrous metals, an increase in particle hardness caused an increase in erosion rates. These findings are generally consistent with the findings of Wellinger and Uetz[4.4.1] shown in Fig. 4.4.1.

Wood and Woodford,[4.4.6] studying limestone, silica sand, and alundum (synthetic Al_2O_3), found essentially no particle hardness dependence, even though the measured particle hardnesses varied over an order of magnitude.

4.4.2 Recommended Design Procedures

If the particle hardness is less than the target material hardness, use. Eq. 4.4.1 to renormalize the metal wastage rate upwards but only up to the point where the particle hardness equals the target hardness. Tables of tube and particle hardness are listed in Appendix B.

References

4.4.1 Wellington, K., and H. Uetz, Wear, *1*:225-231 (1957).

4.4.2 Engel, P.A., *Impact Wear of Materials*, Elsevier Scientific Publ. Co., Amsterdam (1978).

4.4.3 Tsai, W., J.A.C. Humphrey, I. Cornet, and A.V. Levy, *Experimental Measurement of Accelerated Erosion in a Slurry Pot Tester*, Wear, *68*:289-303 (1981).

4.4.4 Zhu, J., *Tube Erosion in Fluidized Beds*, Ph.D. Thesis, Department of Chemical Engineering, The University of British Columbia (May 1988).

4.4.5 Zhu, J., J.R. Grace, and C.J. Lim, *Tube Wear in Gas Fluidized Beds–I. Experimental Findings*, Chemical Engineering Science, *45*(4):1003-1015 (1990).

4.4.6 Wood, R.T., and D.A. Woodford, *Tube Erosion in Fluidized-Beds*, ERDA Report 81-12 911/FT-FUC/79, prepared for New York State Energy Research and Development Authority by General Electric Co., Schenectady, NY (Dec. 1980).

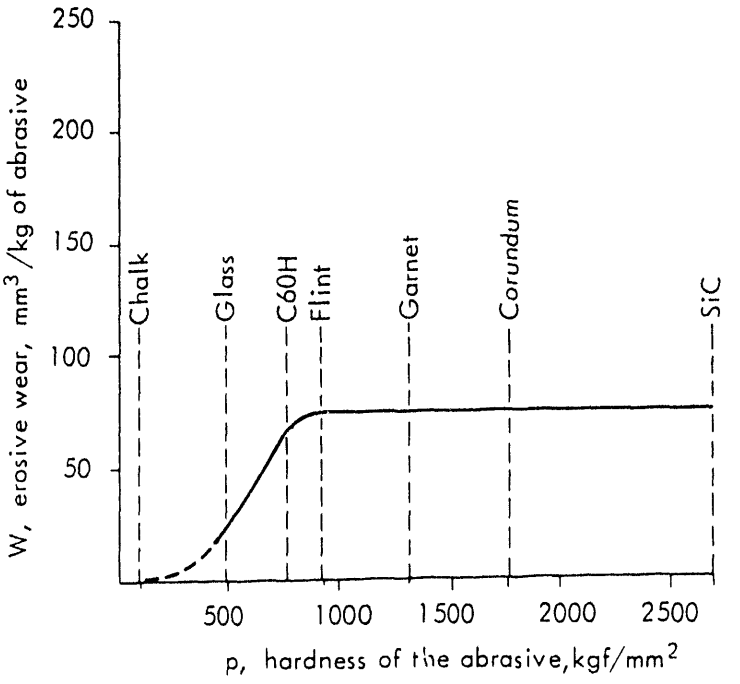

FIGURE 4.4.1 Dependence of the Erosive Wear of C60H Steel (Hardness =750 kgf/mm^2) on the Hardness of Abrasives, Impact Angle = 90°(4.4.1,4.4.2)

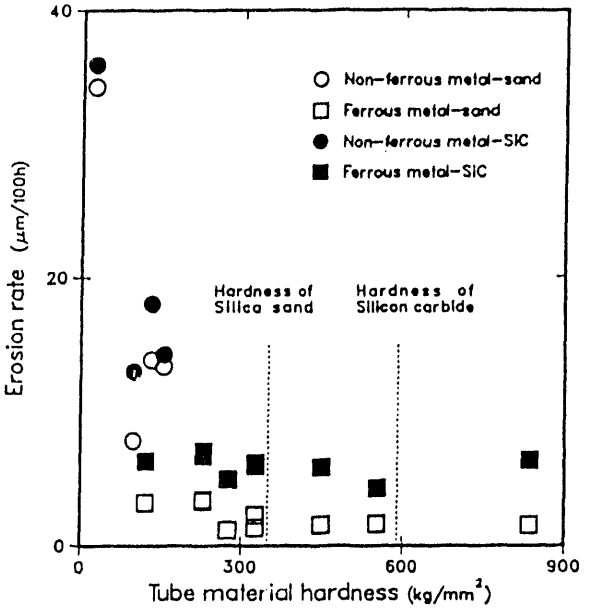

FIGURE 4.4.2 Erosion Rate versus Tube Material Hardness for Silica Sand and Silicon Carbide for a Single 32-mm-o.d. Tube, 1-mm-Diameter Particles, Sphericity = 0.89 and (U - U_{mf}) = 1.3 m/s(4.4.4,4.4.5)

4.5 Bed/Tube Temperature

4.5.1 Discussion

Zhu conducted nine tests in the lower part of a CFB at four different tube temperatures to test the effect of temperature on the erosion of different materials. Seven materials (brass, copper, Al 011, SS304, SS316, CS1020, and CS1050) were tested.[4.5.1] The outside diameter of each tube was 32 mm. The superficial gas velocity was 1.83 m/s; 0.92-mm silica sand particles (ϕ_s = 0.89) were employed as the bed material, and the static bed height was 410 mm in all cases.

All high-temperature tests lasted about 30 h, except for one that ran for 74 h. Because of the limited number and duration of the tests, they must be regarded as preliminary in nature. For convenience in comparing the results at high temperature with those at room temperature, the erosion rates were all corrected for particle size by using Eq. 4.2.4 in Sec. 4.2. Table 4.5.1 and Figs. 4.5.1 and 4.5.2 summarize the data as a function of bed and tube surface temperatures for the nonferrous and ferrous metals, respectively.

For nonferrous metals, the erosion rate increased with temperature because of a decrease of Young's modulus and of material hardness. No oxidation was observed because of the temperature increase, except for copper, when the tube surface temperature was 145°C and the fluidized bed temperature was 750°C.

For ferrous metals, Zhu et al.[4.5.1] observed an apparent erosion rate decrease with temperature because oxidation increased the tube weight, which offset the material loss. The presence of an oxide layer made it impossible to obtain accurate measurements of true erosion in the limited time available for high-temperature experiments. However, the data obtained by Zhu et al. and data from other studies appear to indicate that the actual erosion rate at high temperature is higher than that at room temperature under the same operating conditions. Zhu et al. further concluded that more tests were clearly needed to clarify the influence of high temperature on erosion and on combined erosion/corrosion synergism of ferrous metal surfaces.

Stringer[4.5.2] reported that the erosion rate at Grimethorpe for low-alloy steels decreased dramatically for a small (50°C) temperature increase.

4.5.2 Recommended Design Guidelines and Procedures

If one knows the effective tube material hardness as a function of temperature, the simplified MED erosion model described in Sec. 3, together with the worked examples (Example 5, Sec 4.1 and Example 3, Sect. 4.2), can be used to assess the increased erosion rates for nonferrous metals and the decreased erosion rates for ferrous metals caused by oxide formation at elevated temperatures.

References

4.5.1 Zhu, J., *Tube Erosion in Fluidized Beds,* Ph.D. Thesis, Department of Chemical Engineering, The University of British Columbia (May 1988).

4.5.2 Stringer, J., *Current Information on Medal Wastage in Fluidized Bed Combustors,* Proceedings of the 9th International Conference on Fluidized Bed Combustion, J.P. Mustonen, ed., Vol. 2, pp. 685-696, American Society of Mechanical Engineers, New York (1987).

TABLE 4.5.1 Erosion Rates of Nonferrous Metals at Different Temperatures[4.5.1]

Bed Temperature (°C)	25	400	750
Tube Surface Temperature (°C)	25	120	145
	Erosion rate (μm/100 h)		
Brass	4.57	7.95	13.2
	3.43	9.79	
	3.68		
Copper	2.91	23.5	22.8
	3.03		
	4.22		
Al2011	5.55	6.86	17.8
	5.88	8.14	

Other operating conditions:

Excess air velocity: 1.31 m/s.
Particles: 1.00-mm silica sand.
Particle sphericity: 0.89.

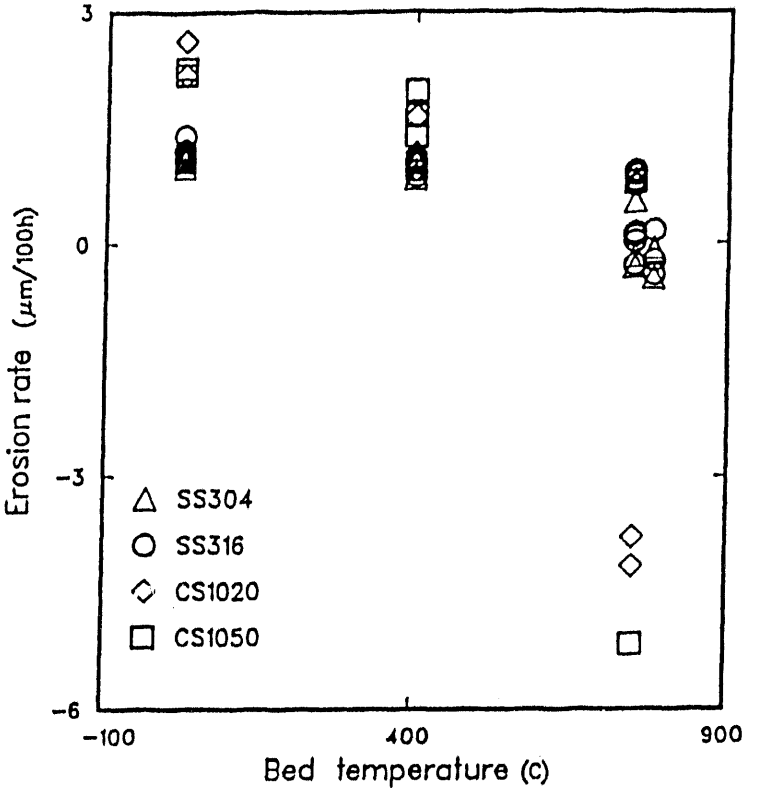

FIGURE 4.5.1 Erosion Rate versus Bed Temperature for 1.00-mm Silica Sand Particles with 32-mm-o.d. Tube at U - U_{mf} = 1.31 m/s[4.5.1]

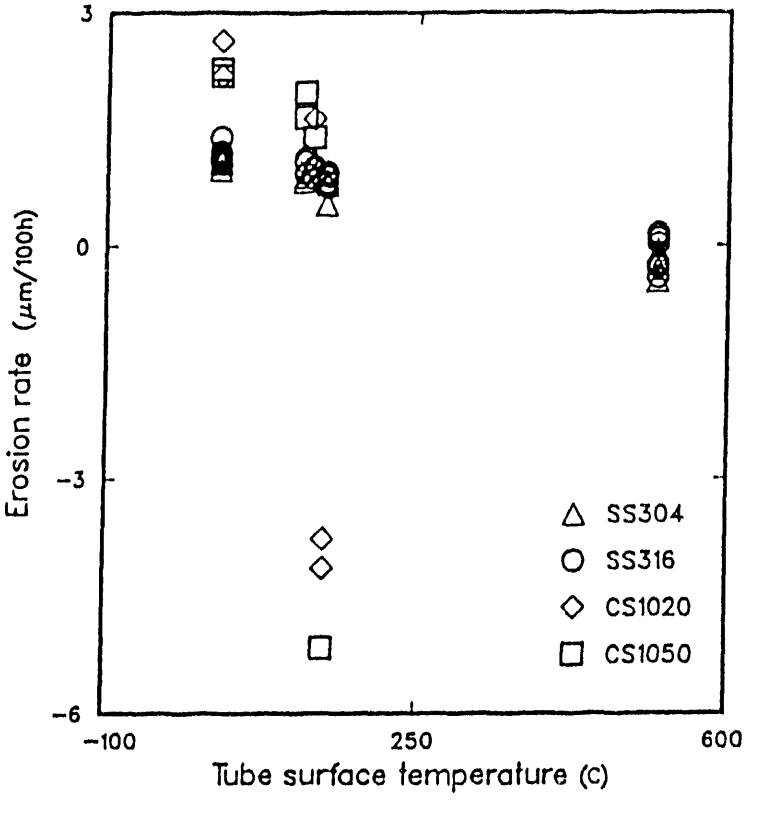

FIGURE 4.5.2 Erosion Rate versus Tube Surface Temperature for 1.00-mm Silica Sand Particles with 32-mm-o.d. Tube at U - U_{mf} = 1.31 m/s[4.5.1]

5 Design Parameters

Design parameters (such as bed depth, distance between air distributor and bottom of the tube bundle, tube diameter, staggered or in-line tube arrangement, and tube material hardness) are thought to play a role in tube wear. As in Sec. 4, the sensitivity of the erosion models to changes in each of these parameters is determined and, where possible, compared with data.

The shallow beds employed in the United Kingdom (U.K.) define the shallowest fluidized bed in use, around 200-300 mm. An AFBC air heater experiment[5.1] employed an 8-ft-deep bed, while at the upper end, typical PFBC beds are around 12 ft deep.

The distance between the air distributor and the bottom of the tube bundle varies between about 200 mm, as found in the Stork FBC unit at AKZO Chemicals, to about 900 mm, as first used at Grimethorpe.[5.2] The minimum distance is not only defined by fluidization/erosion considerations, but also by the need to perform maintenance on the air distributor and lower sections of the tube bundle.

The tube diameter ranges from as small as 34 mm in the Grimethorpe PFBC to the 2-1/2 in. tubes in the Great Lakes AFBC unit. The Curtis-Wright PFBC air-heater employed 3-in. vertical tubes.

Horizontal and inclined tubes can be arranged in a triangular (staggered) or a square (in-line) pitch, or in any number of asymmetrical configurations. The two variations considered here are staggered and in-line.

Tube material surface hardness can vary widely — some tubes have been coated with wax or with different layers of paint in order to assess wear in accelerated tests. PVC tubes define the low end of tube material hardness (Shore hardness of A80-A90, ~ 4.1 HV), while carbon steel defines the upper end of the range of tube hardness, around 750 HV.

Distributor design can have a profound effect upon erosion. Inspite of this, few data are available to guide designers.

In the following section, the effects of design parameters on metal wastage of a qualitative and quantitative material are discussed. The empirical/qualitative approach has been validated by performing a sensitivity study using the detailed hydraulic and erosion models. The simplified models, can in principle, be further extended to incorporate detailed results of the sensitivity study.

References

5.1 Podolski, W.F., R.W. Lyczkowski, E. Montrone, J. Drennen, Y.H. Ai, and B.T. Chao, *A Study of Parameters Influencing Metal Wastage in Fluidized Beds Combustors*, Proceedings of the 11th (1991) International Conference on Fluidized Bed Combustion, E.J. Anthony, ed., *2*:609-618, American Society of Mechanical Engineers (1991).

5.2 Parkinson, M.J., A.W. Jury, B.A. Napier, T.J. Kempton, and J.C. Holder, *Cold Model Erosion Studies in Support of Pressurized Fluidized Bed Combustion*, Electric Power Research Institute Draft Final Report for Project 1337-2 (April 1986).

5.1 Distance of Tube/Tube Bundle to Air Distributor and Bed Height

5.1.1 Discussion

The distance of the bottom row of a tube bundle to the distributor and the height of the bed address the same issue, since there is no need to have a significant amount of bed material above the tubes. In fact, the slumped bed height is usually lower than the top of the tube bank in order to improve load turndown characteristics.[5.1.1]

5.1.1.1 Parkinson et al. Experiments

Parkinson et al.[5.1.2] studied the effect of tube bundle height in the 0.5-m × 1.0-m cross-section cold model of Tube Bank "C" at Grimethorpe. The bed material consisted of an equal mixture of 1- to 2-mm and 0.5- to 1.0-mm sand for which the average particle diameter was 0.86 mm. The depth of the slumped bed was 1.5 m for both runs. The tube bank consisted of 60 tubes (35 mm o.d.), 12 rows high and 5 tubes per row. The distributor consisted of 72 standpipes, each with four rows of eight holes, 3 mm in diameter.

The weight loss was obtained after 48 hours of operation. The results for test runs 1 and 2, bare aluminum tubes, are shown in Fig. 5.1.1. Reducing the height of the tube bank from 0.9 m (26 tube diameters) to 0.45 m (13 tube diameters) reduced the metal wastage of the lowest row by a factor of three, while the tubes in the upper portion of the tube bank showed a roughly 25% increase. The overall metal wastage rate decreased from about 0.1 mm/1000 h to about 0.075 mm/1000 h, or roughly 25%. The reason for the increase in the erosion rate of the top several rows of tubes for the 0.45-m distance may be that at the 0.9-m distance, they were above the slumped bed height, while at the 0.45-m height, they were totally submerged. Wood and Woodford[5.1.3] also observed the erosion rate to increase with bed height.

5.1.1.2 Nieh et al. and Lee Experiments

Nieh et al.[5.1.4] and Lee[5.1.5] studied the effect on erosion of the distance of a single tube to the distributor as well as tube bundle height in their cold model. The single tube studies used wax, PVC, and aluminum tubes 17 mm in diameter. Other studies used tube bundles consisting of 14-mm-diameter wax cylinders. The fluidized-bed cross-sectional area was 21 by 21 cm. Both staggered and in-line tube arrangements were studied. The tube bank for the staggered configuration consisted of 11 tubes in three rows, four on the top, three in the middle, and four on the bottom. The vertical pitch was 30 mm (2.2 tube diameters), and the horizontal pitch was 21 mm (1.5 tube diameters). The in-line configuration consisted of 12 tubes in three vertical rows, four in each row. In this case, both the vertical pitch and horizontal pitch were 30 mm. The bed material consisted of 0.55-mm glass beads having a minimum fluidization velocity of 19 cm/s. The fluidizing velocities for the single tube studies were 26, 67, and 85 cm/s (1.37, 3.5, and 4.5 U/U_{mf}). For the tube bundle studies, the fluidizing velocity was 68 cm/s, 3.5 U/U_{mf}. The slumped bed height was 12.5 cm, and the expanded bed height was 20.5 cm. The distributor consisted of a perforated plate having 1,025 orifice holes, each with a diameter of 0.8 mm arranged in a triangular pattern.

Figure 5.1.2 shows the effect of the single tube to distributor clearance (for fixed bed height) on tube specific weight loss for low, medium, and high superficial velocities.[5.1.5] The average specific erosion rates were 0.4, 0.2, and 0.1 $mg/cm^2/h$ for the 4-h tests at 3-, 5-, and 7-cm clearances, respectively. These distances are far smaller than those typical of commercial FBCs, as already discussed above. Therefore, the conclusions may be of limited use for design of industrial-scale FBCs.

The tube-specific weight loss decreased with increasing tube-to-distributor clearance. This was interpreted as being due to high velocity jets from the orifices near the distributor carrying more bed particles to strike on the lower half of the tubes, causing higher erosion. The influence of local air jets diminished as they penetrated the bed. This could be seen by examining the bottom surface condition of the eroded tubes. The local jetting effect may explain the problems of severe erosion of in-bed tubes that were close to solids reinjection ports, pneumatic feeding points, and damaged air nozzles. The velocity effect is also indicated in Fig. 5.1.2. Higher fluidizing velocities produced higher tube erosion at each tube-to-distributor distance, which is consistent with the findings in Sec. 4.1. It was also found that erosion in the splash zone could be double that on the in-bed tubes, depending on tube location.

Figure 5.1.3 shows the results of the case of a staggered tube bundle with a horizontal pitch of 21 mm (close pitch). As can be seen in the figure, there is a distinct maximum in the erosion rate as the tube bank is lowered from 50 mm (3.6 tube diameters) to 15 mm (1.1 tube diameters) from the distributor. The average erosion rate doubled when the distance was reduced from 50 to 30 mm but then decreased over 50% at a distance of 15 mm.

The outer tubes in both top and bottom rows (solid data points) were found to have weight losses about 45% to 100% higher than the inner tubes (open data points) at all heights. In the tube bundle, the outer top tubes had the largest weight loss, followed by outer bottom tubes, middle tubes (averaged), inner bottom tubes and inner top tubes. This phenomenon is attributed to (1) the higher particle and air velocities around the tube bundle and the outer tubes and (2) the lower particle and air velocities within the tube bundle due to the frictional drag imposed by the immersed tubes.

5.1.1.3 Lockwood's Experiment

Lockwood's qualitative studies, which were performed in a thin room-temperature fluidized bed having a cross-sectional area of 5.1 cm × 51 cm, offer an alternative explanation.[5.1.6] The tubes were 5.1 cm in diameter. The bed material consisted of either dolomite (with a 569-μm particle diameter) or limestone (with a 1379-μm particle diameter). The slumped bed height was 45 cm. The tube array consisted of 14 (staggered pitch) and 15 (square pitch) tubes having various horizontal and vertical pitches with two different distances of the tube bundle to the air distributor, 15 and 25 cm (approximately 3 and 5 tube diameters). The fluidizing velocities varied from about 1.5 to 6 times U_{mf}.

The quality of fluidization appeared better when the arrays were close to the distributor plate. Bed stability, as manifested by small pressure fluctuations, was better with the array 2.5 cm (1 in.) above the distributor plate than with the array 15 or 25 cm (6 to 10 in.) above the distributor. When the tube array was positioned 15 to 25 cm (6 to 10 in.) above the distributor, increasingly rapid bubble growth occurred below the array, which caused irregular pressure fluctuations. However, it was noted that large bubbles were generally split into smaller ones upon entering the array. When the tube array was positioned 15 to 25 cm (6 to 10 in.) above the distributor, several rows of tubes were above the slumped bed height. In these instances, fewer solids entered the freeboard above the tube array, thus helping to limit entrainment.

5.1.1.4 Zhu et al. Experiment

Zhu et al.[5.1.7, 5.1.8] lowered a brass tube (see Sec. 4.1) from a height of 308 mm (10 tube diameters) to 30 mm, keeping the slumped bed height constant at 320 mm. The metal wastage rate increased about 1.8 times. The wear also became nonuniform along the tube. It was

thought that the tube was in the jetting zone of the orifice holes. A series of tests was performed in which the static bed height was lowered from 320 mm to 180 mm while the tube was maintained "close to the surface of the bed." The erosion rates for the materials tested decreased anywhere from 3% to 40%, as shown in Table 5.1.1. The reduction in erosion rates was interpreted as being due to the reduction in bed height. The lower bed height likely reduced the amount of bubble coalescence in the vicinity of the tube, thereby reducing the particle impact velocities and erosion rate.

5.1.1.5 Foster Wheeler Ash Bed Heat Exchanger Sensitivity Study: Effect of Tube Bubble Geometry and Distance to Distributor

A bubbling bed equipped with a tube bundle consisting of 18 tubes plus a single tube placed some distance below it was specified by ANL, as shown in Fig. 5.1.4. The bed was divided in half (front to back) to run two beds simultaneously and at different fluidizing velocities. At first, the single tube was to be placed along the centerline of the bed as indicated, very close to the distributor. In effect, four experiments were to be conducted simultaneously. Later, the single tube was specified to be two tubes, located symetrically and aligned with the second column of tubes from the sidewalls.

Computer simulations of this bed were conducted prior to the experiment. However, the tube arrangement actually used in the experiment differed from that used in the simulations. The final experimental configuration is shown in Fig. 5.1.5. This arrangement made it impossible for a one-to-one comparison between predicted and experimental erosion rates. Furthermore, the hardness of the PVC tube used in the experiment was not available at the time of the simulation, thus leading to additional uncertainty. A PVC-tube specimen was subsequently sent to ANL for hardness determination and a value of 38 MPa was found, a value close to that used in the analyses (40 MPa) and the same value as in Sec. 4.1. The mean particle diameter was 185 μm, with a spread of from about 60 to 1000 μm.[5.1.9] Particle sphericity was measured by The Shapespeare Corp. to be 0.801, with a standard observation of ±0.064.

In the following discussion, the fluidized bed was simulated for about two seconds of real time. Two tube bundle arrangements were analyzed by using our FLUFIX/MOD2 and EROSION/MOD1 software packages. Operating conditions for these simulations are presented in Table 5.1.2. The tube bank and bed height for the second simulation were lowered by 25 cm and 18 cm, respectively. In the second simulation, the tube placed near the distributor was removed. Typical transient porosity contours are shown in Figures 5.1.6 and 5.1.7 for both tube bundle simulations. As can be seen in Figure 5.1.6 for the first simulation (lower tube bundle) bubbles are deflected by the tube placed just above the distributor and move upward preferentially between the tube bundle and the bed wall. Similar patterns are computed in the second simulation shown in Figure 5.1.7, but the jet penetration seems to reach higher distances, penetrating the lower row of the bundle. The extent of the jet penetration distance can be estimated by using Merry's[5.1.10] correlation, for example. Predicted erosion rates for aluminum tubes are shown in Table 5.1.3. These predictions show that by lowering the tube bundle and removing the tube near the distributor, erosion rates are increased by about twofold. As discussed above, the tube bundle is more prone to erosion in the second simulation because it is placed within the jetting region of the distributor. This computer simulation clearly shows that lowering a tube bundle in the jetting region of the distributor likely results in higher wear rates.

5.1.1.6 Parkinson et al. Shallow Fluidized-Bed Sensitivity Study

A shallow few- (five-) tube version of Parkinson's[5.1.2] cold model experiment was modeled with the FLUFIX/MOD2 and EROSION/MOD1 computer programs, approximating the tube pitch configuration and spacing of Grimethorpe tube bank C1.

Results from the full MED erosion model for all three rows of tubes are plotted in Fig 5.1.8 as a function of fluidizing velocity. At U/U_{mf} = 2.3, the tube highest in the bed has the highest erosion rate; if the trends were to continue, it appears that the erosion rate at the middle tube may overtake that of the lowest tube. This is the same trend that occurs when the tube bank is closer to the distributor, as shown in Fig. 5.1.1 where U/U_{mf} = 4.3. The time-averaged solids flow patterns are shown in Fig. 5.1.9 to aid in interpreting the results.

Another study was performed with the FLUFIX/MOD2 and EROSION/MOD1 codes for an approximately round tube placed at two different locations in a two-dimensional fluidized bed, as shown in Figure 5.1.10. In the first case, Figure 5.1.10(a), the tube was located 357 mm above the distributor (three tube diameters), and the bed height was 510 mm. In the second case, Figure 5.1.10(b), the tube was located 211 mm (slightly less than two tube diameters) from the distributor, and the initial bed height was 374 mm. The bed material was 0.5-mm glass beads. The fluidizing velocity was 31.3 cm/s (U/U_{mf} = 1.5). The time-averaged erosion rates computed for aluminum tube material from the MED erosion model decreased slightly from 0.37 mm/1000 h to 0.31 mm/1000 h, or a ratio of 0.84, in reasonable agreement with the results of Zhu et al.[5.1.8] As shown in Fig. 5.1.6, the fluidized bed expanded less for the same fluidizing conditions as the tube was lowered. This may explain the decreased metal wastage rate.

A third case was run with increased bed height above the tube. The erosion rate decreased from 0.33 mm/1000 h to 0.1 mm/1000 h. Figure 5.1.11(a) shows that a second vortex formed above the lower one and less bubbling occurred under the tube, resulting in a lower erosion rate.

A fourth case was run in which fluidizing velocity was increased from 1.5 U_{mf} (30 cm/s) to 2.0 U_{mf} (40 cm/s), as shown in Fig. 5.1.11(b). The erosion rate tripled to 0.3 mm/1000 h, which yields a dependency on erosion or fluidizing velocity to the 2.5 power, in good agreement with the results of Zhu et al. (see Sec. 4.1), which indicate a mean value of 2.1 power, depending upon fluidizing velocity.

In shallow beds, which are infrequently used in the United States but are commonly used in the U.K., the "classic" Type "A" erosion pattern does not appear; that is, the maximum wear is on the underside at 30 to 45° from the bottom center.[5.1.11] The tubes do not display the Type A "flats" located at 20-30° from the bottom center.[5.1.12] In addition, the wear is higher on the top row of tubes. This phenomenon was predicted with the FLUFIX/MOD2 code and the MED erosion model for the CRE few-tube model and recently with the new Foster Wheeler Development Corp. fluidized bed described in Sec. 5.1.1.7.

5.1.1.7 Analysis of Foster Wheeler Development Corp. Shallow Fluidized Bed

During the Cooperative R&D Venture, Foster and Wheeler Development Corp. (FWD) also performed several erosion tests in fluidized beds having different thicknesses. In these experiments, PVC, aluminum, and carbon steel tubes were used in beds 0.1 m, 0.83 m and 1.65 m thick. This was accomplished by using a movable partition perpendicular to the tube bank. The carbon steel tubes did not show significant wear after as much as 400 h of operation and were thus excluded from consideration. Podolski et al.[5.1.11] summarized the results of these

experiments, as well as those of a similar experiment performed at the University of Illinois at Urbana-Champaign (UIUC). In all these tests, the pitch and height of the tubes above the distributor was maintained the same, as was the distribution of the tube material, as shown in Fig. 5.1.12. The UIUC bed, which used a square 30.4 × 30.4-cm bed cross section, could only accommodate three central tubes and two half tubes attached to the side walls.

In the FWDC experiments, fluidizing air was supplied by a two-stage, air-cooled, 100-KW, two-cylinder compressor. The compressed air was blown into the air plenum through PVC pipes at a nominal temperature of 338 K. The static frame of the bed was made of carbon steel sheets covered by 0.75-in.-thick Lexan sheets and had a total rectangular cross section of 164 cm × 72.4 cm with a height of 67.3 cm.

Above the air plenum, a flat, perforated steel plate distributor, 3.2 mm thick, was used. To ensure good gas distribution, a total of 7403 orifice holes, each having a diameter of 2.8 mm, were drilled in a square pattern through the distributor plate. The front side of the fluidized bed was made of Lexican to facilitate the visual observations of bubble motion. The system had a freeboard height of 26.3 cm to keep the particles from elutriating. Fixed horizontal and vertical pitches of respectively 15.2 cm and 7.6 cm were maintained within the tube array. The tube array consisted of two rows, the lower row being placed 23 cm above the distributor. The expanded bed height was maintained at 41 cm above the distributor, yielding a bed layer 8 cm above the tube bundle. The tubes were made of plastic, aluminum, and carbon steel. All test runs were conducted with the bed initially filled with molochite particles to a slumped bed height of 36 cm. Published chemical analysis of molochite indicates that molochite is composed of 52-53% of SiO_2, 44% of Al_2O_3, and small traces of TiO_2, CaO, MgO, and Na_2O. The molochite particles are irregularly shaped, brittle, and have a wide particle-size distribution. The particle-size weight-fraction distribution was determined by sieving at ANL, and the weight-averaged mean diameter was 1.3 mm. When fluidized at 1.22 m/s, the beds expanded to a bed height of 41 cm and intense bubbling was observed, although the beds were only fluidized at $1.25 \times U_{mf}$. Slugs and bubbles were observed through the plastic front panel. Hence, for these Type D particles, the bed behavior was not only bubbling, but also slugging.

Table 5.1.4 summarizes the experimentally determined maximum tube erosion rates anywhere in the beds for the four runs performed by FWDC. The maximum tube erosion rates for PVC tubes are about five times higher than aluminum. The average experimental erosion rates from the FWDC "medium bed," 0.83-m-thick by 0.74-m-wide Run B,[5.1.11] are shown in Fig. 5.1.13. This FWDC bed was chosen to be analyzed because its aspect ratio closely matched the square 0.3 × 0.3-m UIUC bed that used the same tube geometry and bed material. The average erosion rates for PVC tubes are comparable with those for aluminum, and the variations for both tube types are about the same. Note that the spread in the average erosion rates for PVC and aluminum tubes is about the same as the maximum.

The FWDC bed was simulated using FLUFIX/MOD2 and EROSION/MOD1. The computational domain of the FLUFIX model shown in Figure 5.1.14 is 36.55 cm wide by 102.0 cm high. The cell size is $\Delta X = \Delta Y = 0.85$ cm. Thus, the computational cell is 43 in the x-direction and 120 in the y-direction for a total of 5160 nodes. The simulated tubes consist of two rows of obstacles, 5.08 cm in diameter, in a triangular pitch arrangement. The horizontal spacing was 15.3 cm and the vertical spacing was 7.65 cm. The static bed height was 40.64 cm. Symmetry was assumed.

The simulation conditions are summarized in Table 5.1.5. The inlet superficial gas velocity was first maintained at 0.9 times the minimum air fluidizing velocity, U_{mf}, where U_{mf} was taken

to be 97.3 cm/s as determined from the Ergun equation programmed in the FLUFIX computer program. This was done to obtain a reasonable initial condition for the subsequent run at $U/U_{mf} = 1.25$. The compaction gas volume fraction was set equal to 0.47. The time step used in the simulation was 5×10^{-5}s for the first second; it was then decreased to 2.5×10^{-5} to avoid a high number of iterations. Hydrodynamic model B was used with a solids viscosity of Pa·s.

As can be seen, the predicted erosion rate averaged about 0.38 mm/1000 h, which is also about the maximum value experimentally recorded in Table 5.1.4. This relative good agreement between experiment and predictions reinforces our confidence in our computer models. The variability in the predicted average erosion rates is due to uncertainties in material properties, restitution coefficients, and lack of accounting of three-dimensional hydrodynamic effects.

The UIUC experimental erosion rate data are also shown in Fig. 5.1.13. As can be seen in the figure, there is general consistency with the experimental FWDC erosion rates, and agreement is closer to the computed predictions. Also shown are predictions using a two-dimensional model of the UIUC bed as described by Lyczkowski et al.[5.1.12] The primary reason for the inconsistency between the experiments and the data was an over-prediction of solids velocities in the vicinity of the tubes.

The molochite particles were characterized before and after one of the FWDC runs by The Shapespeare Corp. A fifty-times magnification of some representative particles is shown in Fig. 5.1.15. Some smoothing of the particles' edges is evident. The sphericity changed from 0.839 ± 0.063 to 0.801 ± 0.064, both somewhat lower than that estimated for use in the simulation (0.89). Although the sphericity of the particles changed little, a significant amount of fines was produced, which, in the UIUC experiments, clogged the filtering system after only several hours. A bag collector had to be installed.

For a quick evaluation of the maximum erosion rate, one can refer to Figure 4.1.5 to obtain an estimate of about 1 mm/1000 h for 1.5-μm-diameter particles at $U/U_{mf} = 1.25$. The vertical spacing used to produce Fig. 4.1.5 was 16 cm. In the FWDC experiment, a vertical spacing of about 8 cm was used, as shown in Fig. 5.1.12; hence, the estimated maximum erosion rate is about 0.5 mm/1000 h for this tube bundle. This erosion rate is exactly that experimentally measured in the FWDC unit, as indicated by Table 5.1.4. Again, Figure 4.1.5 is most useful for estimating maximum erosion rates of tube bundles in fluidized beds. To determine the location of the maximum, the EROSION/MOD1 computer program must be run.

5.1.2 Recommended Design Guidelines and Procedures

A guideline of a qualitative nature, well accepted in the FBC community, is that the tube bank should be as close to the distributor as possible.[5.1.13-5.1.16] Bain and Michner[15.1.16] state that the shallowest static bed depth permissible that satisfies other design criteria should be used. A realistic constraint in the United States is that a person must be able to fit under the tube bundle (approximately 0.5 m). In addition, the bed depth should be minimized.

The apparently contradictory results found in the literature may be attributed to the coalescence phenomena discussed in Sec. 6.1 or the jetting phenomena from the distributor discussed by Zhu et al. and Lockwood. Another parameter to consider is the position of the tubes – above, partially submerged, or completely below the slumped bed height. Thus, it appears that the distance of the tube bundle to the distributor should be close to about 0.45 m. It would appear that if the tube or tube bundle to distributor spacing is less than about 5 tube diameters, the erosion

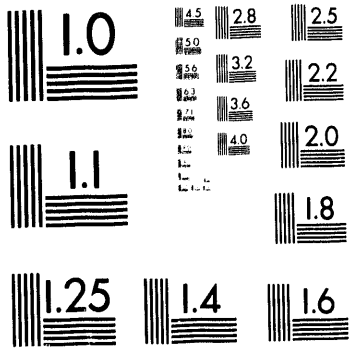
1.0
1.1
1.25
1.4
1.6
1.8
2.0
2.2
2.5
2.8
3.2
3.6
4.0
4.5
5.0
5.6

2 of 2

rate will actually begin to increase. Reducing the tube bundle to distributor distance at distances above 5 tube diameters reduces the erosion rate slightly. These findings agree with the experience of Stork Boilers,[5.1.17] which recommended tube bundle to distributor spacing of 150 to 200 mm, and with the experience of Rogers et al.,[5.1.18] who found metal wastage to increase with decreasing bed height in shallow beds.

Another qualitative guideline is that the top row of tubes should be covered when the bed is slumped, since erosion rates for tubes in the splash zone increase significantly. Submerging the top row of tubes completely within the slumped bed is recommended.

Our interpretation of the results is that the tube bank should be located well above the jetting region and below the region of bubble coalescence. Estimates of the location of these two regions can be made by reference to Merry[5.1.10] (jetting) and Levy et al.[5.1.19] (coalescence; see Sec. 7.3). The extent of these regions depends upon distributor design and tube bundle geometry.

The in-kind data reports received from the British Coal Corporation Coal Research Establishment addressing the dependence of the erosion rate upon location of the tube bundle in the fluidized bed found that tube wastage in the cold model was found to be greatest between heights of 1.5 and 2 m above the air distributor. In the Grimethorpe combustor, maximum losses were found at a height of about 2.5 m.[5.1.20]

Experience in test series involving tube bank "E" showed that a reduction in bed height produces a reduction in plastic wear rate throughout the whole tube array in direct proportion to the reduction in height.[5.1.21]

A second benefit of reducing the bed height is that a point may be reached at which the legs of the "Eiffel Tower"-shaped wear pattern will not have joined together within the height of the bed. This means that bubble streams have not coalesced into one strong stream within the bed. The top of the bed would then show two areas of moderate wear rather than a central peak wear.

Clearly it is advantageous to reduce bed height and, hence, tube bank height on the grounds of tube bank wear. However, the choice of bed height is dictated by overall combustor performance, which is predominantly a function of the gas residence time within the bed.

Later tests showed that the presence of two areas of peak wear in Test 11 at the top of the bed (row 8) could be explained by a reduction in bed height when viewed in the light of the wear pattern observed in Test 1.[5.1.22] This pattern is thought to be linked with bubble paths.

The effect of increasing fluidizing velocity from 0.6 to 0.9 m/s and raising the bed depth from 2.7 to 3.1 m as required for the second period of Test Series A2 showed no significant increase in the peak diagonal wear rate.[5.1.22] However, the profile of wear at the top of the tube bank had changed: instead of decreasing in the top rows of the tube bank, the wear rate increased monotonically. This is thought to be connected with the increase in bed depth.

Operation of Tube Bank "E" with only the two lower rows fully submerged in the bed showed that the submerged rows suffered slightly higher wear (17% more) than they would have in a deep bed. The wear rate on all the rows above the bed was less than that below the bed, with the wear rate decreasing with increasing distance above the bed.

References

5.1.1 Divilio, R.J., and R.R. Reed, *Turndown Studies for Utility Fluidized-Bed Boilers*, Electric Power Research Institute Report CS-3237, Palo Alto, CA (1984).

5.1.2 Parkinson, M.J., J.F.G. Grainger, A.W. Jury, and T.J. Kempton, *Tube Erosion at IEA Grimethorpe: Cold Model Studies at CRE*, in Reports Commissioned by the Project from Outside Consultants and Others, Vol. 2, NCB (IEA Grimethorpe) Ltd., Barnsley, S. Yorkshire, U.K. (Sept. 1984).

5.1.3 Wood, R.T., and Woodford, *Tube Erosion in Fluidized-Beds*, ERDA Report 81-12 911-ET-FUC/79, prepared for New York State Energy Research and Development Authority by General Electric Co., Schenectady, NY (Dec. 1980).

5.1.4 Nieh, S., S.Y. Lin, S.W. Lee, and T.T. Fu, *Measurements of In-Bed Tube Bundle Erosion and Particle-Tube Frequency in a Gas Fluidized Bed*, Particulate Science and Technology, *6*:269-283 (1988).

5.1.5 Lee, S.W., *Analysis and Modeling of In-Bed Tube Erosion in a Gaseous Fluidized Bed*, Doctoral Dissertation, the Catholic University of America, Washington, D.C. (Feb. 1989).

5.1.6 Lockwood, D.W., *Effects of Heath Exchanger Tube Spacing and Arrangement on the Quality of Fluidization*, Proc. Second Pacific Chemical Engineering Congress, American Institute of Chemical Engineers, New York, Vol. II, pp. 1177-1181 (Aug. 1977).

5.1.7 Zhu, J., *Tube Erosion in Fluidized Beds*, Ph.D. Thesis, Department of Chemical Engineering, The University of British Columbia (May 1988).

5.1.8 Zhu, J., J.R. Grace, and C.J. Lim, *Tube Wear in Gas Fluidized Beds—I. Experimental Findings*, Chemical Engineering Science, *45*(4):1003-1015 (1990).

5.1.9 Lehn, C.S., *Low and High Fluidizing Velocity Erosion in 3-D Tube Bundles with Included Video,* Foster Wheeler Development Corp. Report FWC/FWDC/TR-91/09, Livingston, NJ (Oct. 1991).

5.1.10 Merry, J.M.D., *Penetration of Vertical Jets into Fluidized Beds,* AIChE Journal, *21*:507-510 (1975).

5.1.11 Podolski, W.F., R.W. Lyczkowski, E. Montrone, J. Drennen, Y.H. Ai, and B.T. Chao, *A Study of Parameters Influencing Metal Wastage in Fluidized Beds Combustors,* Proceedings of the 11th (1991) International Conference on Fluidized Bed Combustion, E.J. Anthony, ed., Vol. 2, pp. 609-618, American Society of Mechanical Engineers (1991).

5.1.12 Lyczkowski, R.W., I.K. Gamwo, F. Dobran, Y.H. Ai, B.T. Chao, and M.M. Chen, *Comparison of Experimental and Computed Solids Motion and Bed Dynamics for Fluidized Beds Containing Obstacles,* Proceedings of the 11th (1991) International Conference on Fluidized Bed Combustion, E.J. Anthony, ed., Vol. 1, pp. 325-333, American Society of Mechanical Engineers, New York (1991).

5.1.13 Ellis, F., and C. Armitage, *Combating Metal Wastage in Fluidized Bed Combustors,* in 1988 Seminar on Fluidized Bed Combustion Technology for Utilization Application Volume I: Atmospheric Fluidized Bed Combustion, Electric Power Research Institute (May 1988).

5.1.14 Stockdale, W., F. Ellis, and C. Armitage, *Wastage of In-Bed Surfaces in Fluidized Bed Combustors, Experience in Practice with 3 Industrial AFBC Units in the U.K.,* Paper No. 2.5 in Proceedings Wastage of In-Bed Surfaces in Fluidized-Bed Combustors, workshop held at Argonne National Laboratory, Nov. 2-6, 1987. Available from Electric Power Research Institute (1987).

5.1.15 Stringer, J., *Current Information on Metal Wastage in Fluidized Bed Combustors,* Proceedings of the 9th International Conference on Fluidized Bed Combustion, J.P. Mustonen, ed., Vol. 2, pp. 685-696, American Society of Mechanical Engineers, New York (1987).

5.1.16 Brain, S., and A. Michner, *Minimization of Wastage in Bubbling Atmospheric Fluidized Bed Boilers,* in Proceedings Corrosion-Erosion-Wear of Materials at Elevated Temperatures, Berkeley, Calif., Jan. 31-Feb. 2, 1990, A.V. Levy, ed., pp. 40-1 to 40-16, National Association of Corrosion Engineers, Houston, Texas (1991).

5.1.17 Verhoeff, F., and G.J. Holtzer, *Metal-Wastage in the 90-MWth AKZO SFBC Installation,* Proceedings: Workshop on Wear Potential of FBC Bed Material, in Fluidized-Bed Combustors, pp. 275-292, Electric Power Research Institute Report No. TR-10056, Palo Alto, CA (November 1991).

5.1.18 Rogers, E.A., T.D. Rantell, S.A. Brain, and B. Atkinson, *Minimizing Erosion in U.K. Fluidized Bed Boilers,* manuscript received from E. Addis, British Coal Board (1991).

5.1.19 Levy, E.K., and F. Bayat, *The Bubble Coalescence Mechanism of Tube Erosion in Fluidized Beds,* in Fluidization VI, J.R. Grace, L.W. Shemilt, and M.A. Bergougnou, eds., pp. 603-611, Engineering Foundation, New York (1989).

5.1.20 British Coal Corporation, Coal Research Establishment, *Cold Model Studies of Tube Wear in Support of PFBC (December 1985-February 1986),* PFBC/MOA/P9, Stoke Orchard, Cheltenham, U.K. (April 9, 1987).

5.1.21 British Coal Corporation, Coal Research Establishment, *Results of the First Ten Cold Model Tests at Grimethorpe Leading to the Design of Combustor Tube Bank "E",* PFBC/MOA/P21, Stoke Orchard, Cheltenham, U.K. (Nov. 6, 1987).

5.1.22 British Coal Corporation, Coal Research Establishment, *Grimethorpe Cold Model Tests 11 to 16: Evaluation of the Tube Bank "E" Final Design and Assessment of the Benefit of Further Tube Diameter Increases,* PFBC/MOA/P29, Stoke Orchard, Cheltenham, U.K. (April 28, 1988).

TABLE 5.1.1 Comparison of Erosion Rate between Beds of 320- and 180-mm Static Bed Depth[5.1.8]

Material	Erosion Rate (μm/100 h) Static Bed Height (320 mm)	Static Bed Height (180 mm)	Ratio
SS 340	0.98	0.95	0.97
	1.07	0.95	0.89
CS050	2.75	2.39	0.87
	2.72	2.49	0.92
Brass	16.6	7.85	0.47
	13.9	7.74	0.56
Copper	7.24	5.76	0.80
Al 2011	14.9	8.84	0.59
	13.5	7.90	0.58

TABLE 5.1.2 FWDC Low- and High-Velocity Erosion Experiment Operating Conditions Used in the Computer Simulations

Material	CFB Entrainment Ash
Particle mean diameter	0.0185 cm
Particle density	2.16 g/cm^3
Particle sphericity	0.9
Minimum fluidization porosity	0.44
Fluid carrier	Air
Temperature	339K
Pressure (top of bed)	101.3 kPa
Minimum fluidization velocity, U_{mf}	4 cm/s
Fluidizing velocity, U	18 cm/s
U/U_{mf}	4.5

TABLE 5.1.3 Predicted Erosion Rates for Aluminum Tubes (mm/1000 h)

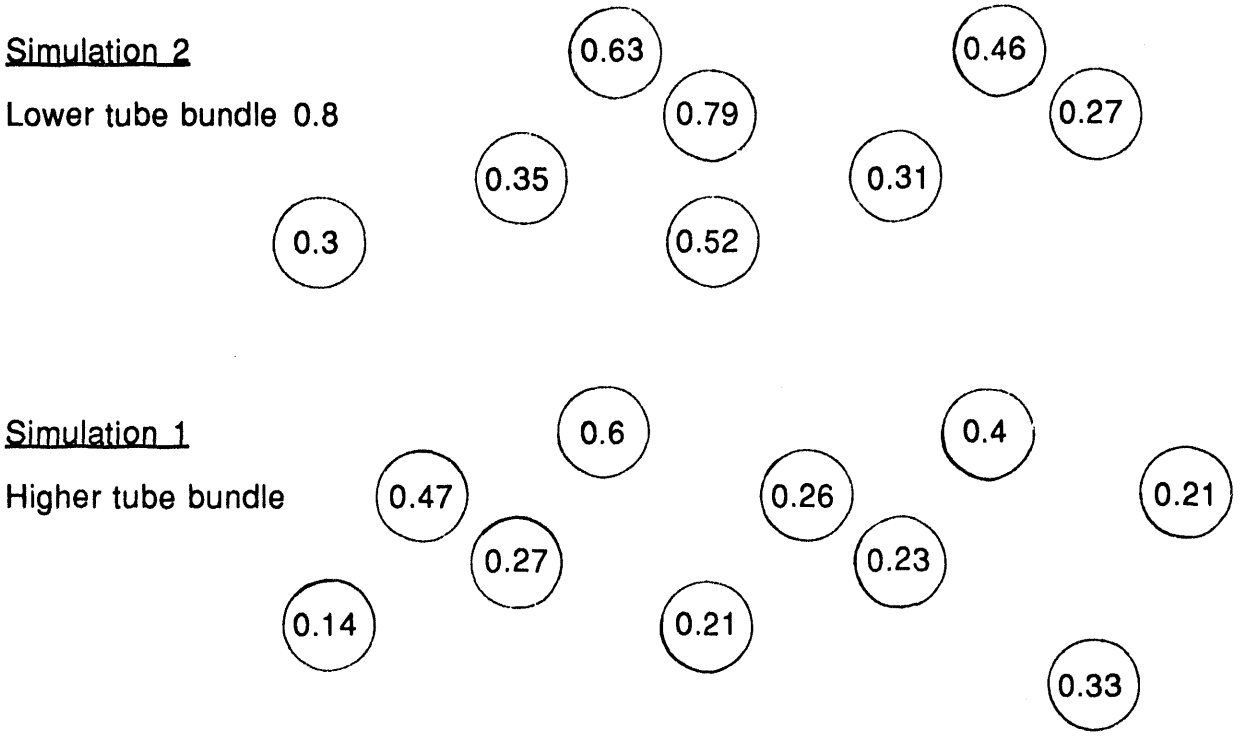

TABLE 5.1.4 Maximum Erosion Rates in FWDC Fluidized Beds

PVC	Aluminum	Units
100	20	mil/1000 h
25	0.5	mm/100 0 h

Table 5.1.5 Simulation Operating Conditions for Bed with Nine Tubes

Material	Molochite
Particle mean diameter, mm	1500
Particle density, g/cm^3	2.48
Particle sphericity	0.86
Minimum fluidization porosity	0.45
Fluid carrier	Air
Temperature, K	338.55
Pressure, KPa (top of bed)	108.92
Minimum fluidization velocity, U_{mf}, cm/s	97.3
Fluidization velocity, U, cm/s	121.9
U/U_{mf}	1.25

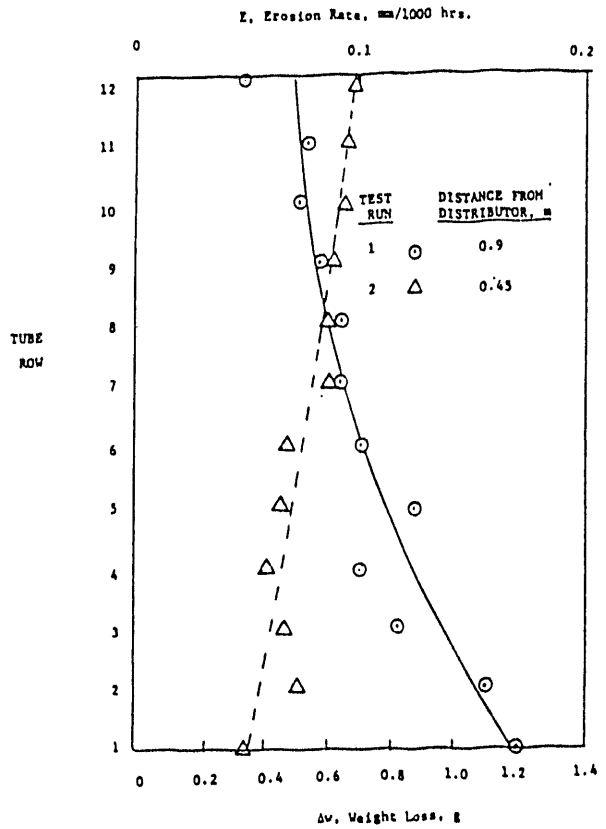

FIGURE 5.1.1 Average Weight Loss and Metal Wastage Rate of Bare Aluminum Tubes after Parkinson et al.[5.1.2]

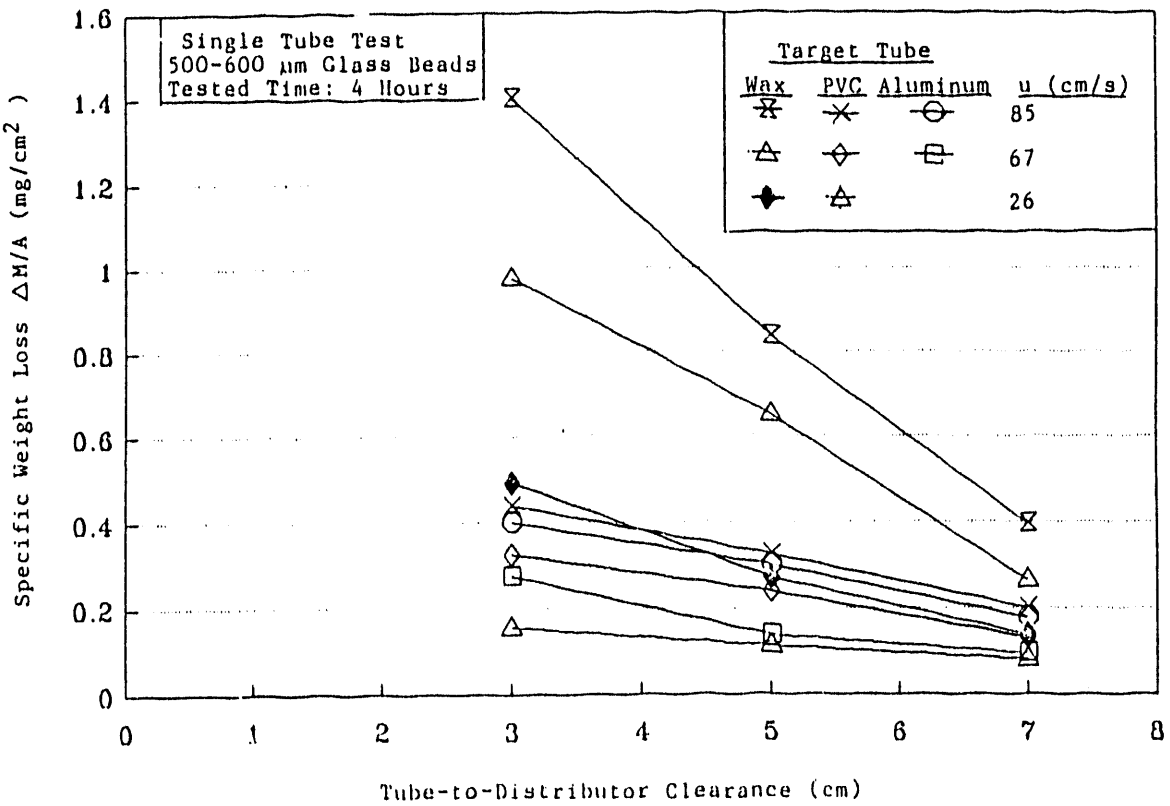

FIGURE 5.1.2 Effect of Tube-to-Distributor Clearance on In-Bed Tube Erosion at Different Fluidization Velocities[5.1.5]

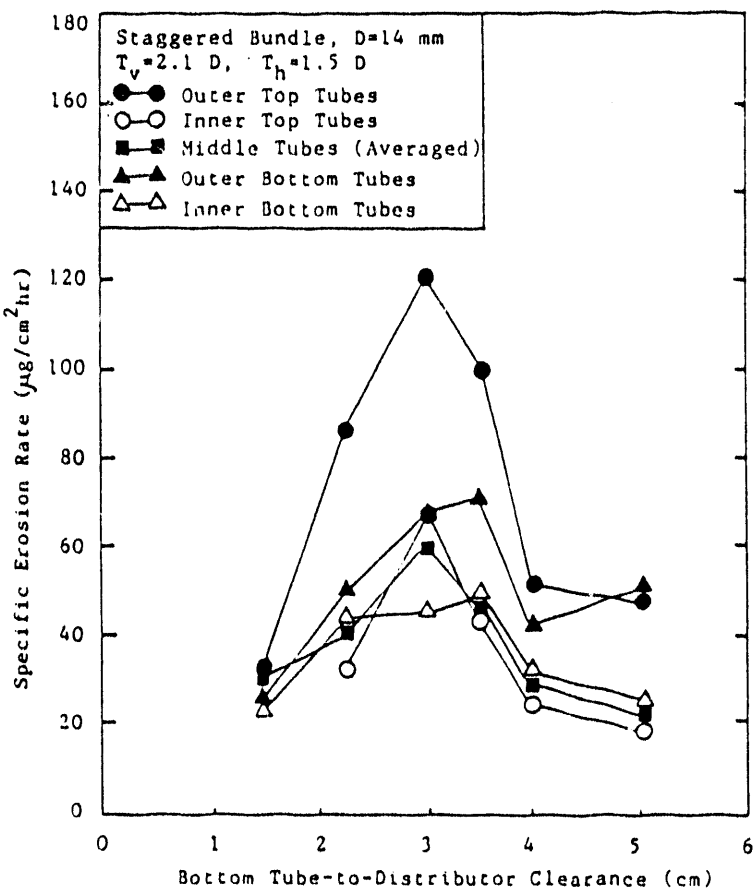

FIGURE 5.1.3 Effect of Bottom Tube-to-Distributor Distance for a Staggered Tube Bundle[5.1.4]

LOW AND HIGH FLUIDIZING VELOCITY

PURPOSE:
TO VERIFY COMPUTER GENERATED DATA FOR TWO BUBBING BEDS IN TWO SINGLE TESTS.

TEST SETUP:
THE TUBE BUNDLE CONSISTS OF 18 STAGGERED 2" PVC PIPES IN ALTERNATING ROWS OF 4 AND 5. THE TUBE PATTERN IS SHOWN BELOW IN FIG.1

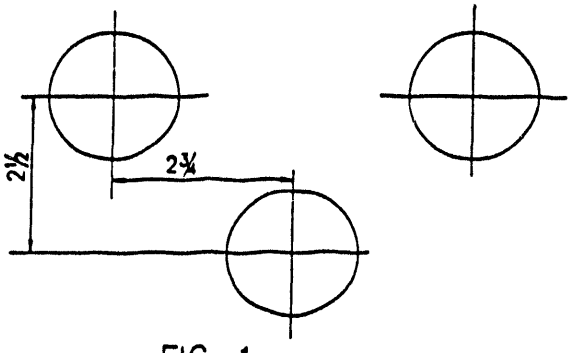

FIG. 1

APPROXIMATELY 18" BELOW THE BOTTOM ROW OF THE BUNDLE, A SINGLE TUBE WILL BE INSTALLED. THIS WILL DETERMINE WHETHER OR NOT JJHEIGHT IS A DETERMINING FACTOR OF TUBE EROSION. FIG 2 SHOWS A SIDE VIEW OF THE TEST CHAMBER RETROFITTED WITH THE TUBES, SUPPORT PLATES (FIG. 3), DISTRIBUTOR PLATES (FIG.4) AND THEIR NOZZLES (FIG.5)

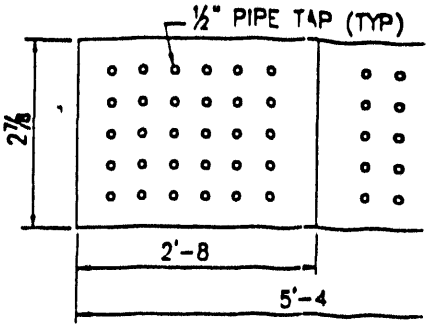

FIG. 4
GRID PLATE

TWO MACHINED DISTRIBUTOR PLATES SI
BE TACK WELDED TO THE FLOOR OF TH
THREADED AIR NOZZLES WILL BE SCRE
EACH PLATE WILL HAVE 30 NOZZLES I
6 x 5 MATRIX. THE PLATE IN AREA "A"
WITH A ⅜" NOZZLE AND AREA "B" WI
THE MIDDLE SUPPORT PLATE WILL ACT
PLATE BETWEEN THE TWO TEST AREAS.
THE TWO TYPES OF AIR NOZZLES USED

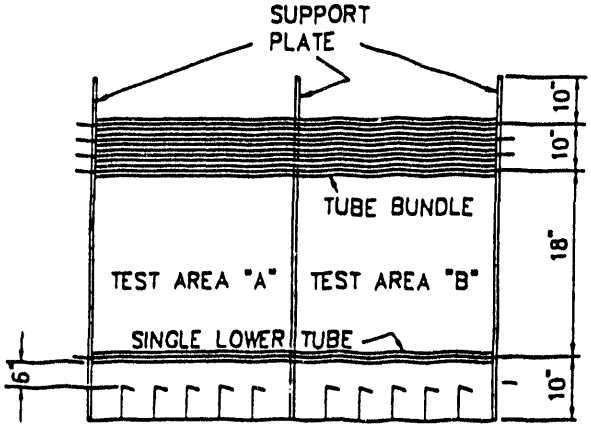

FIG. 2
GEORGE TOWN ELEVATION

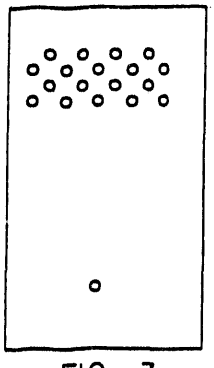

FIG. 3
TUBE SUPPORT PLATE

TEST ARE

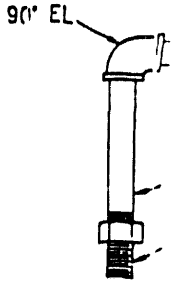

ZING VELOCITY EROSION TEST

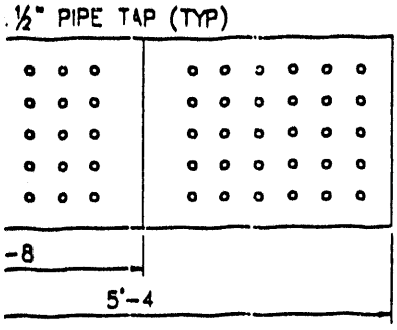

FIG. 4
GRID PLATE

DISTRIBUTOR PLATES SHOWN IN FIG. 4 WILL
) TO THE FLOOR OF THE BED CHAMBER.
IOZZLES WILL BE SCREWED INTO EACH HOLE .
L HAVE 30 NOZZLES IN A STANDARD
'HE PLATE IN AREA "A" WILL BE FITTED
ZLE AND AREA "B" WITH A ½".
PORT PLATE WILL ACT AS SEPAPARATING
THE TWO TEST AREAS. SHOWN BELOW ARE
OF AIR NOZZLES USED FOR AREA "A" AND "B".

TEST CONDITIONS

BED HEIGHT: APPROX. 3"-4" ABOVE TUBE BUNDLE (EXPANDED)
BED MATERIAL: CFB ENTRAINMENT ASH
GAS VELOCITY: TEST AREA "A"-.6 FT/SEC
TEST AREA "B"-1 FT/SEC

MEAN DIAMETER OF MATERIAL: 150 MICRON-220 MICRON RANGE*
UP STREAM PRESSURE: 6 PSI
TUBE MATERIAL: PVC
TUBE SIZE: 2" PIPE (2⅜")

* BED SAMPLE FOR SIZE WILL BE TAKEN DURING TEST

MEASURED PARAMETERS

DIFFERENTIAL PRESSURE TRANSDUCERS WILL BE MOUNTED DIRECTLY ABOVE AND BELOW THE TUBE BUNDLE WITH THREE OTHERS WITHIN THE BUNDLE. ALL WILL BE COMMON TO A VERTICAL LINE. THESE WILL ACCOUNT FOR BUBBLE SPEED AND SIZE. BUBBLE FREQUENCY CAN BE MEASURED BY MOUNTING THE FIVE TRANSDUCERS HORIZONTALLY USING THE ATMOSPHERE AS A REFERENCE 10" BELOW THE TUBE BUNDLE. BOTH AREAS WILL BE MONITORED.

TEST AREA "A" FLUIDIZING NOZZLES

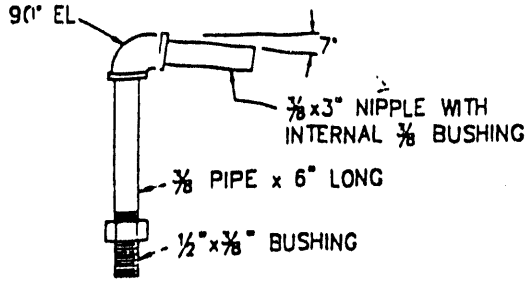

TEST AREA "B" FLUIDIZING NOZZLES

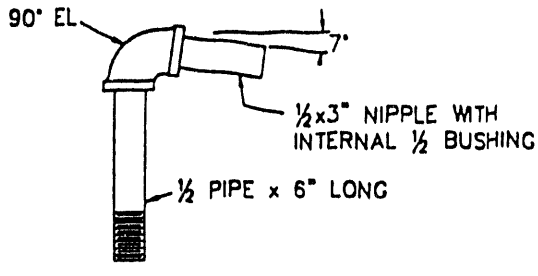

FIG. 4 5
FLUIDIZING NOZZLES

\rd\9032

FIGURE 5.1.4 Schematic and Operating Conditions for Foster Wheeler Development Corp. Cold Model of a CFB External Heat Exchanger

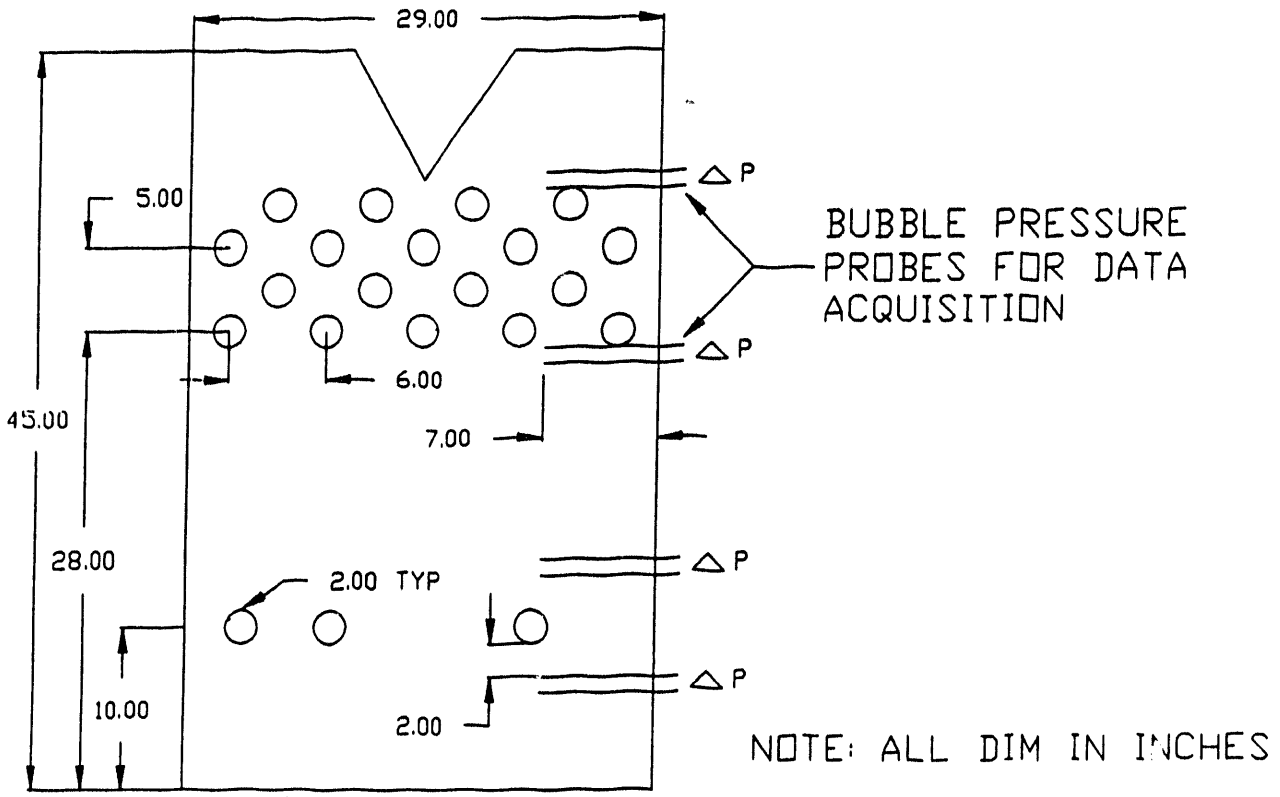

FIGURE 5.1.5 Final Foster Wheeler Development Corp. Cold Model of a CFB External Heat Exchanger[5.1.9]

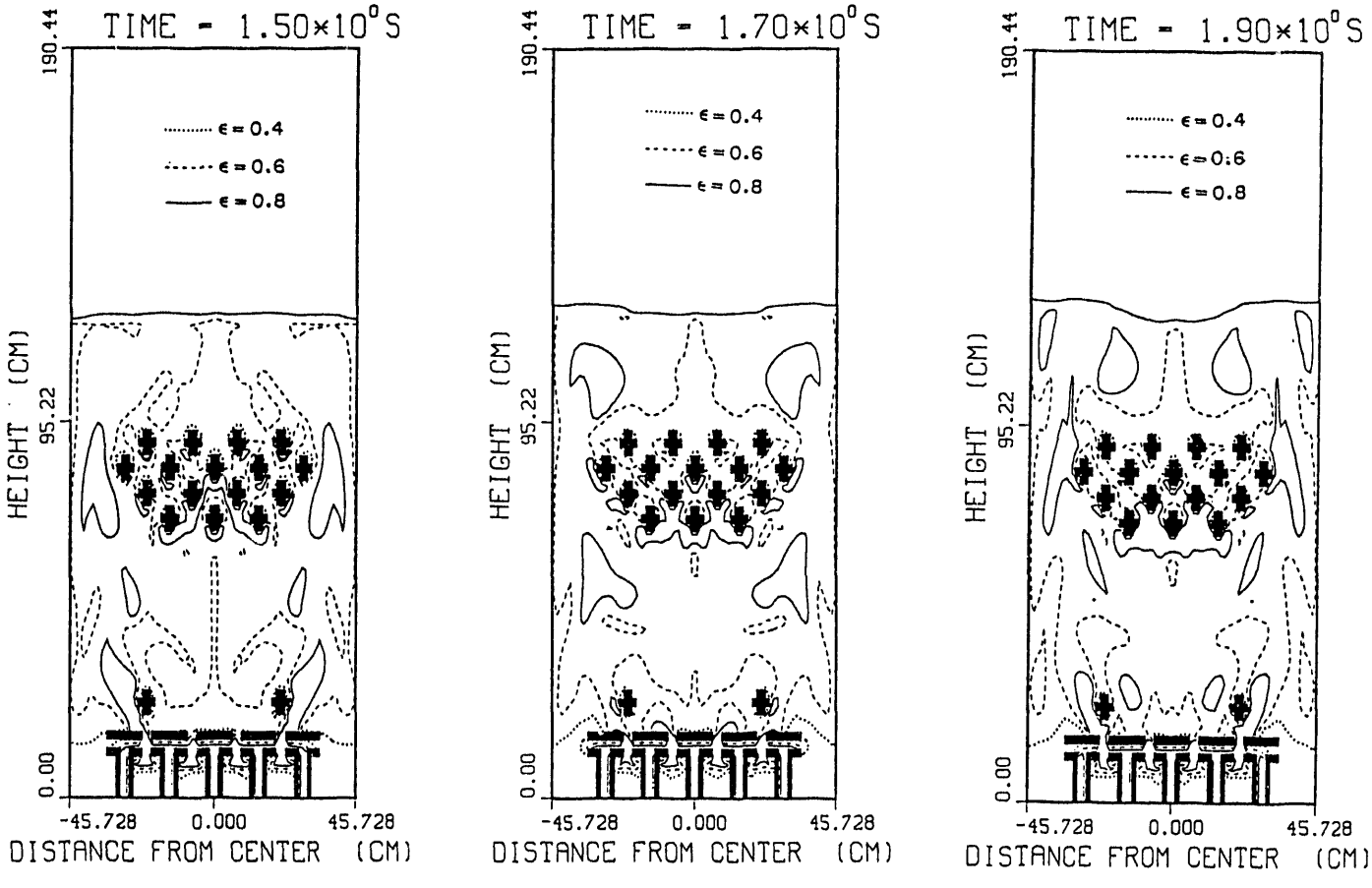

FIGURE 5.1.6 Transient Porosity Contours for Simulation 1 (tube bundle raised with tube near t-shaped distributor)

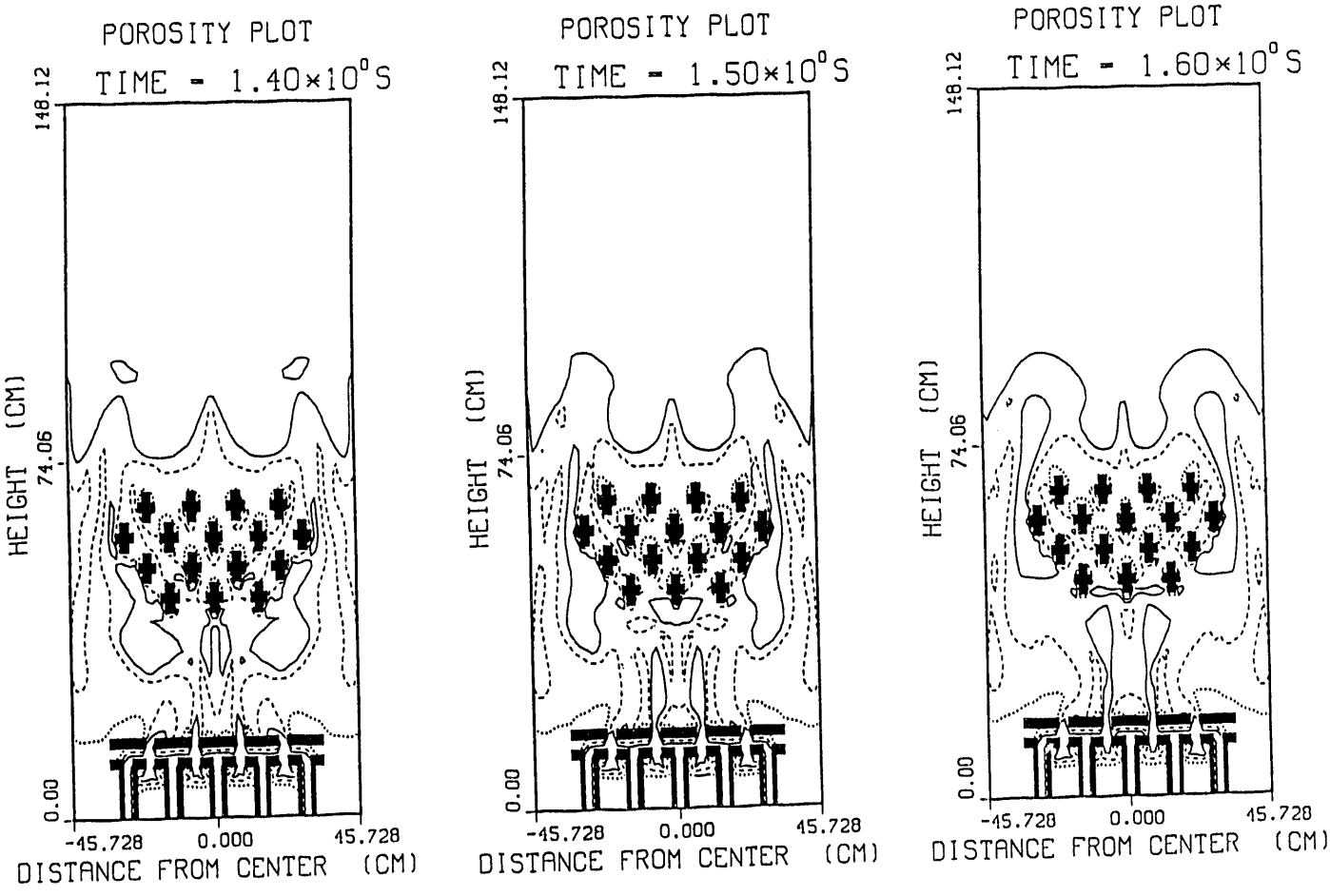

FIGURE 5.1.7 **Transient Porosity Contours for Simulation 2 (tube bundle lowered with tube near t-shaped distributor removed)**

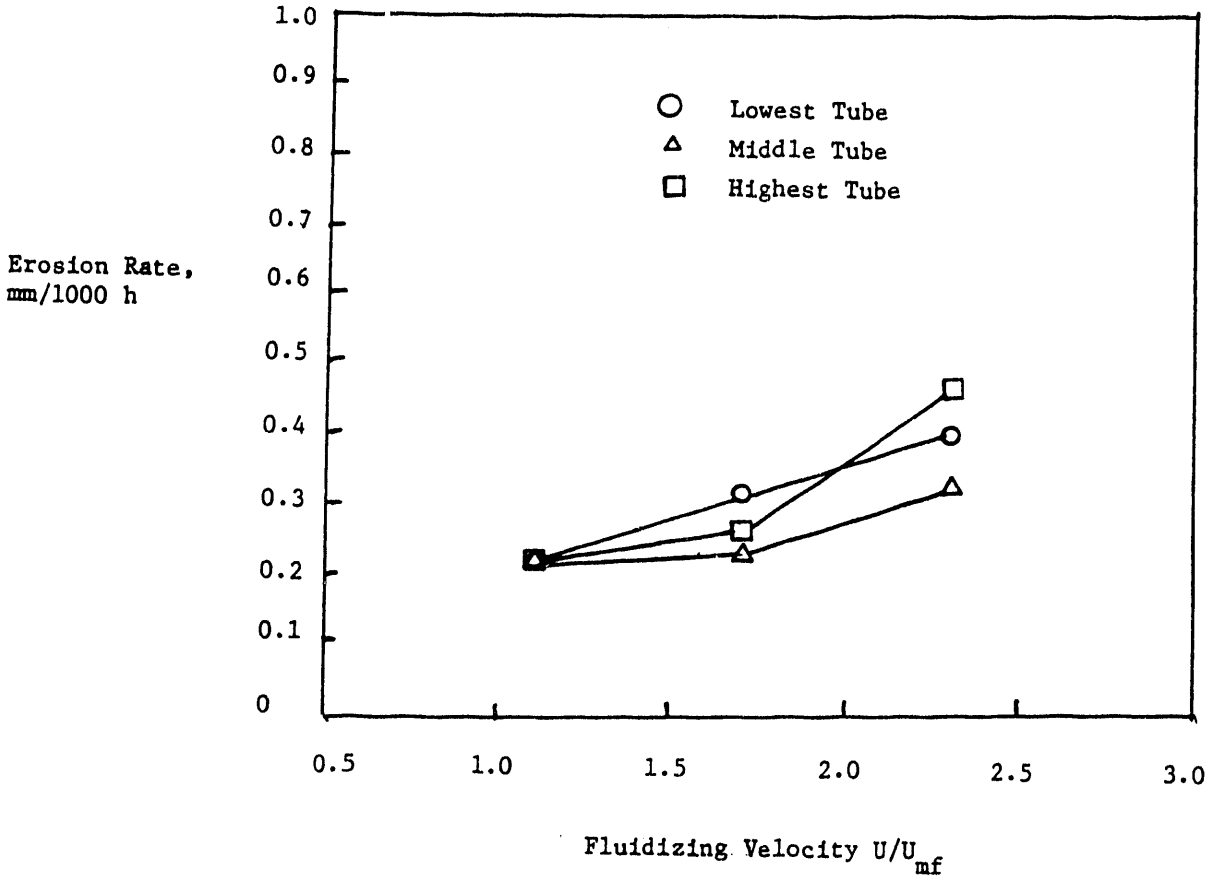

FIGURE 5.1.8 Generic Few- (5) Tube-Geometry Comparison of Time-Averaged Erosion Rates for Aluminum Tubes for the MED Erosion Model

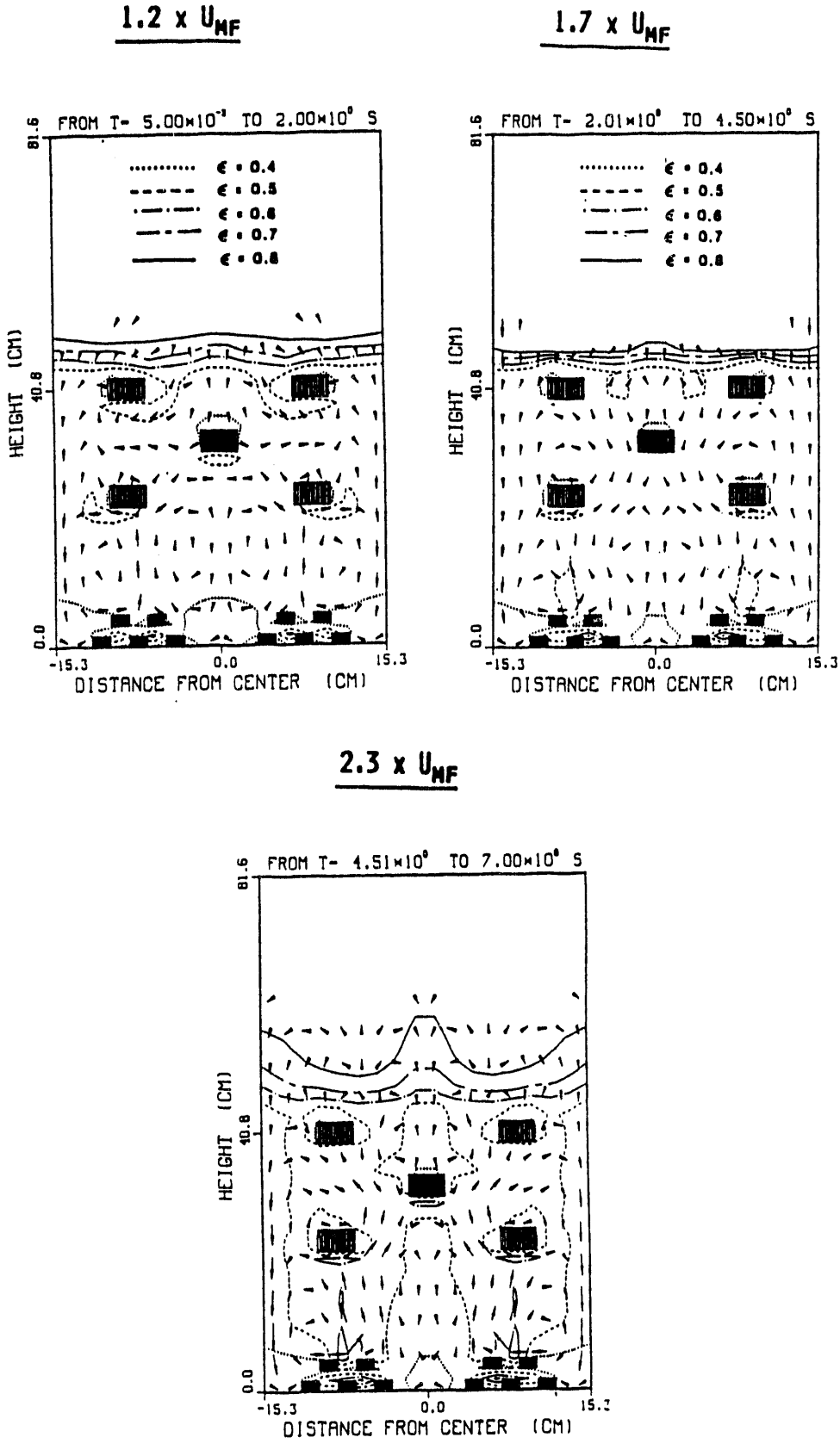

FIGURE 5.1.9 CRE Few Tube (5 Tubes) Generic FBC Geometry Time-Averaged Porosity Contours and Solids Velocity Vectors

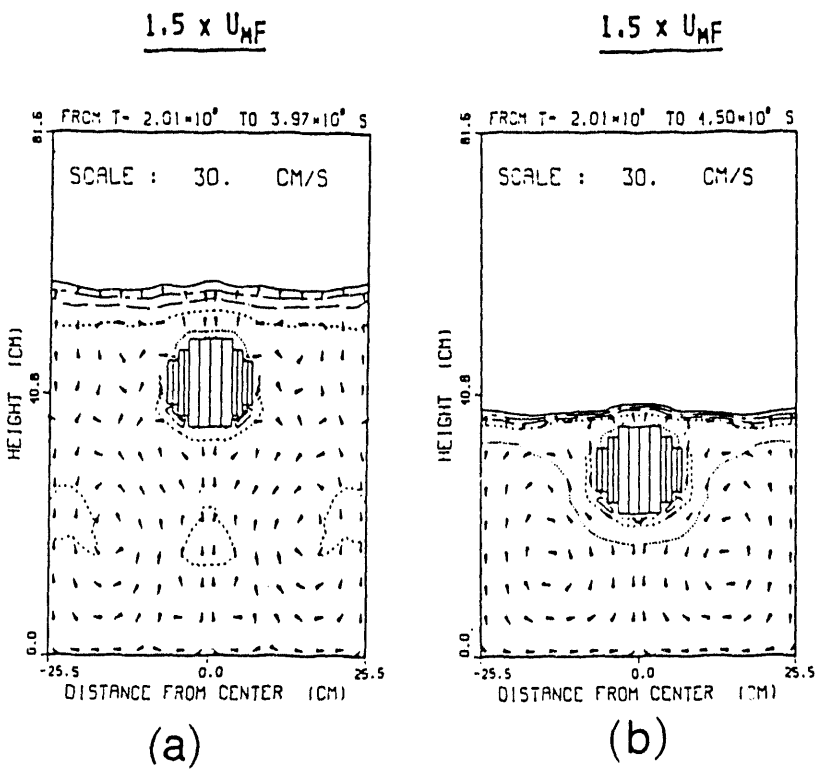

FIGURE 5.1.10 Time-Averaged Solids Velocity Vectors and Porosity Contours for an Approximately Round Tube at Two Different Heights above the Gas Distributor.

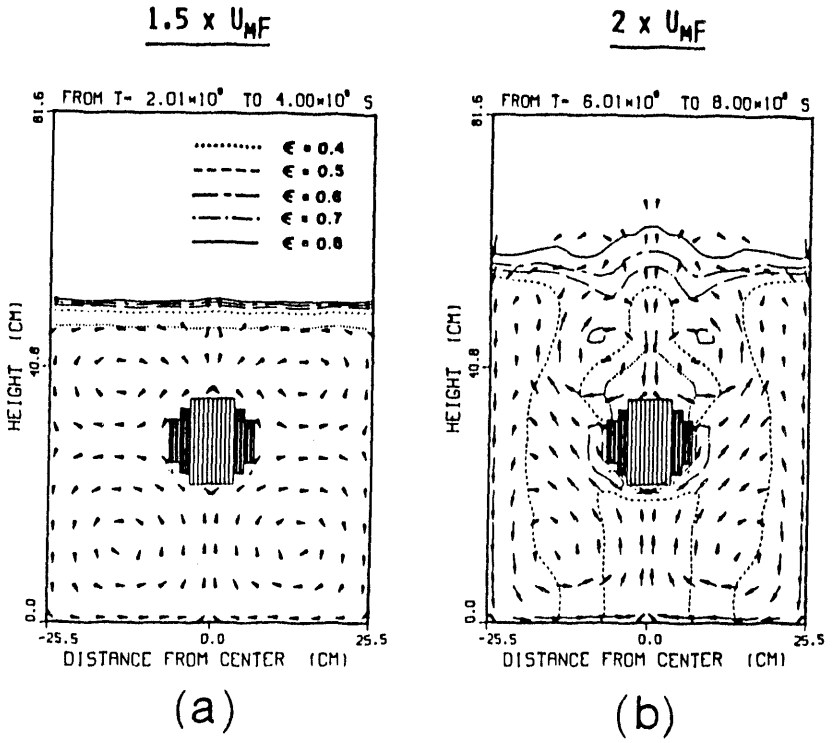

FIGURE 5.1.11 Time-Averaged Solids Velocity Vectors and Porosity Contours for an Approximately Round Tube at 1.5 and 2.0 × U_{mf}

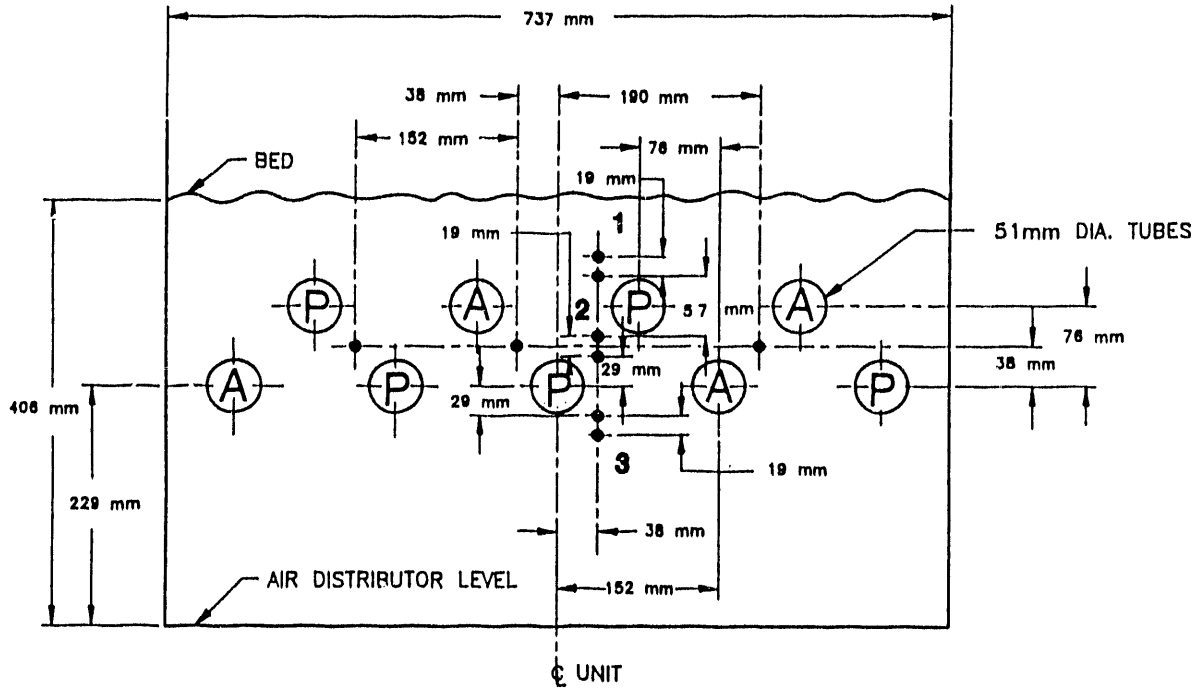

FIGURE 5.1.12 Schematic of Foster Wheeler Variable Thickness Fluidized-Bed Experiment

P2	A4	P6	A8
0.13	0.08	0.08	0.17
0.46	0.41	0.41	0.46
	0.05	0.23	
	0.47	0.30	

P1	P3	P5	A7	P9
0.08	0.08	0.17	0.09	0.06
0.30	0.36	0.38	0.36	0.30
	0.16	0.14	0.03	
	0.35	0.38	0.31	

Key:

FWDC "Medium Bed" Experiment

EROSION/MOD1 Predictions (Aluminum)

UIUC Experiment

EROSION/MOD1 Predictions (Aluminum)

Units are mm/1000 h

FIGURE 5.1.13 Predicted Average Erosion Rates for the FWDC "Medium" Bed Run B and the UIUC Bed

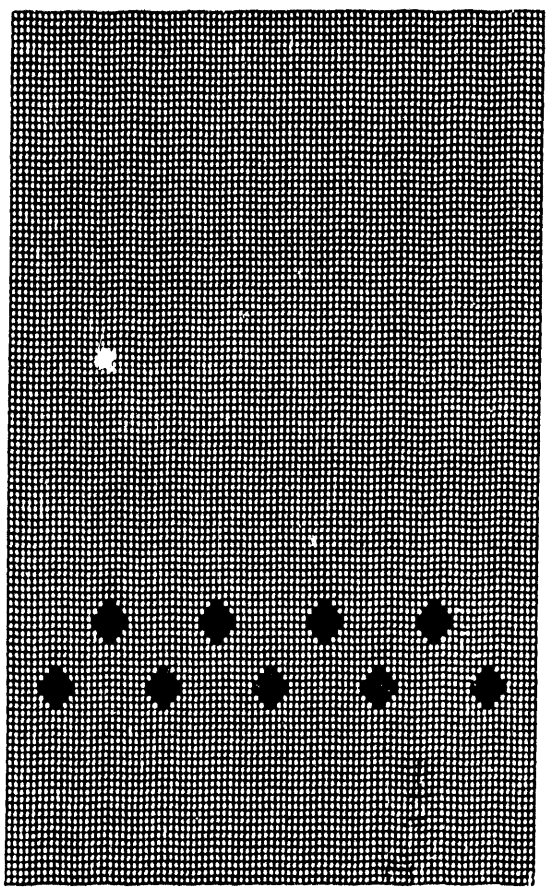

FIGURE 5.1.14 Computational Domain for FWDC Experiments

(a)

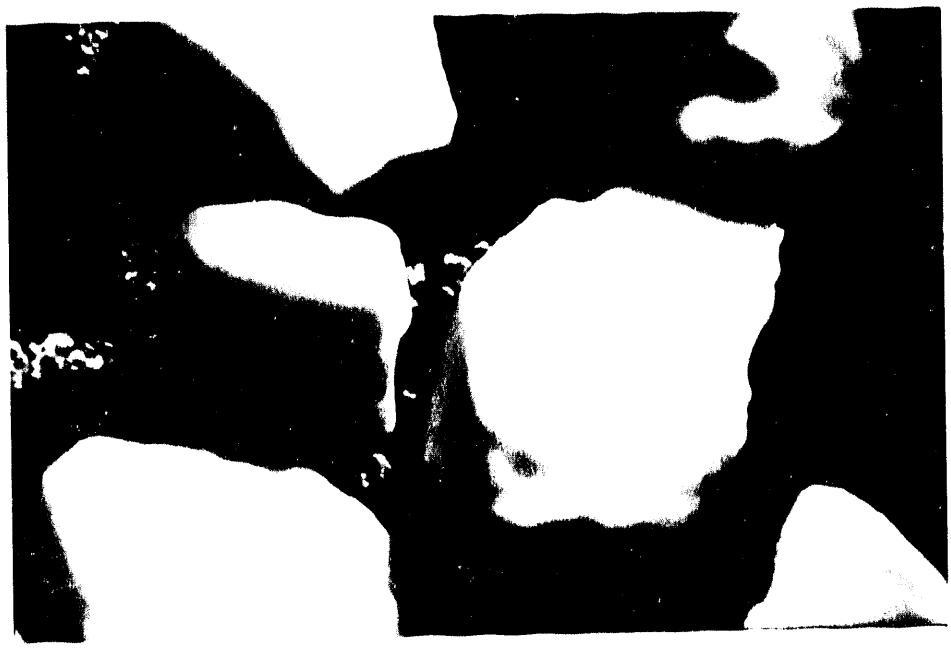

(b)

FIGURE 5.1.15 Representative Molochite Particles before (a) and after (b) a Typical FWDC Erosion Test (200-400 h)

5.2 Tube Material Hardness

5.2.1 Discussion

Zhu et al.[5.2.1] and Wood and Woodford[5.2.2] studied a variety of tube materials having a wide range of hardness. Zhu's data are plotted in Fig. 5.2.1 as a function of tube hardness and in Fig 5.2.2 as a function of Young's modulus (see also Fig. 4.4.2). The conclusion reached was that the Young's modulus appeared to be the major tube material property that influences the erosion rate — the higher the Young's modulus, the higher is the resistance to wear. The erosion rate was relatively insensitive to changes in material hardness, yield strength, and tensile strength. However, there appeared to be a threshold value of hardness (and yield strength) below which erosion increases dramatically.[5.2.1]

The Wood and Woodford[5.2.2] data in Table 4.2.1 are shown graphically in Fig. 5.2.3. The hardnesses measured are listed in Appendix B, Table B.1. The conclusion was that there is a strong material sensitivity and some link to hardness, although clearly other properties such as strain hardening and strain-rate hardening were involved.

Stringer[5.2.3] summarized the Grimethorpe experience, indicating that for steels, only minor difference in wear rates was observed for a range of materials, including plain carbon steel and Incoloy 800H.

As a gross check of consistency (and more should be performed), the wear rate data of Zhu et al. and Wood and Woodford were compared for copper at a fluidizing velocity of 3 m/s. Zhu's correlations indicates about 0.2 mm/1000 h and Wood and Woodford obtained about 0.1 mm/1000 h.

For the shallow UK bed tests, cold model tests showed that the highest losses were from the mild steel specimens, while the stainless steels showed lower weight losses (typically by a factor of two to three), with the low-chromium steel (2 1/4%Cr1%MO) approximately midway between.[5.2.4] There was no significant difference in performance between the stainless steels.

Tests at elevated temperatures were carried out using an alloy abrasion rig.[5.2.4] In these isothermal tests with bed and tube specimens at the same temperature (up to 400°C), the competing mechanisms of wastage and particle imbedment were found to be due to the changing properties of the metal surfaces. Thus, under some conditions, a net weight gain was found, while at others, a weight gain was found at low tube/particle contact velocities and a weight loss at higher velocities. In tests where significant wastage was measured, type 304 stainless steel again outperformed mild steel by a factor in the range of 2 to 5.

5.2.2 Recommended Design Guidelines and Procedures

Type 304 stainless steel is recommended. However, it is not clear that there is any significant effect of tube material hardness on metal wastage for ferrous metals in operating FBCs because of the formation of hard, tenacious oxide layers. Carbon steel may be the exception because of metal substrate softening as compared with stainless steels.

References

5.2.1 Zhu, J., J.R. Grace, and C.J. Lim, *Tube Wear in Gas Fluidized Beds—I. Experimental Findings*, Chemical Engineering Science, *45*(4):1003-1015 (1990).

5.2.2 Wood, R.T., and Woodford, *Tube Erosion in Fluidized-Beds*, ERDA Report 81-12 911-ET-FUC/79, prepared for New York State Energy Research and Development Authority by General Electric Co., Schenectady, NY (Dec. 1980).

5.2.3 Stringer, J., *Current Information on Medal Wastage in Fluidized Bed Combustors*, Proceedings of the 9th International Conference on Fluidized Bed Combustion, J.P. Mustonen, ed., Vol. 2, pp. 685-696, American Society of Mechanical Engineers, New York (1987).

5.2.4 British Coal Corporation, Coal Research Establishment, *Minimizing Erosion in Coal-Fired Boilers*, Commission of the European Communities Report EUR 12360EN, Contact No. 7220-ED/808, Final Report, Directorate-General, Telecommunciations, Information Industries and Innovation, Luxembourg (1989).

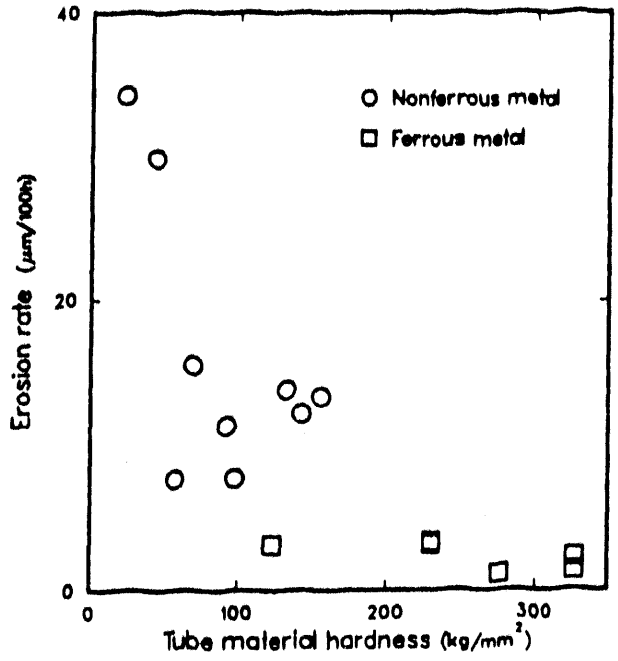

FIGURE 5.2.1 Erosion Rate versus Tube Material Hardness for 1.0-mm Silica Sand Particles (shape parameter - 0.89, U-U_{mf} = 1.31 m/s, and single 32-mm-o.d. tube)[5.2.1]

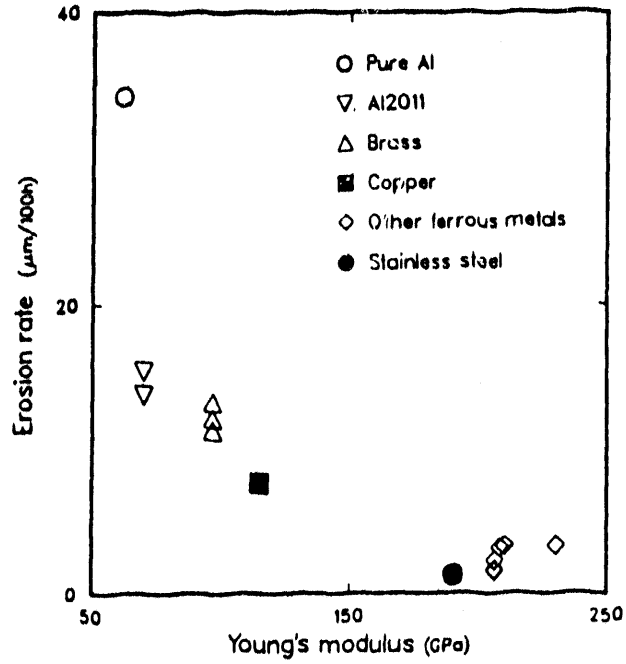

FIGURE 5.2.2 Erosion Rate versus Tube Elasticity: 23-mm-o.d. Tube, 1.0-mm Silica Sand Particles, Shape Parameter - 0.89, and U-U_{mf} = 1.31 m/s[5.2.1]

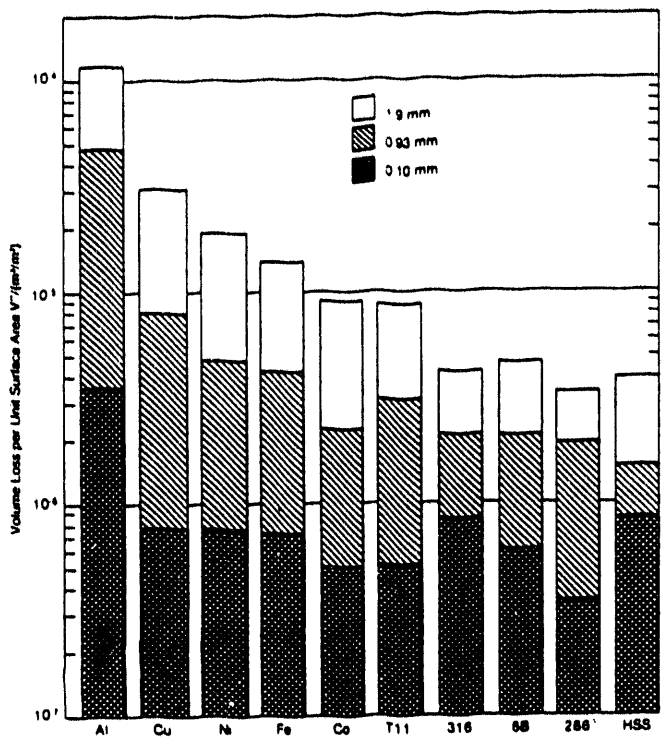

FIGURE 5.2.3 Maximum Local Volume Loss after 100 h of Bed Exposure for Three Sizes of Silica Sand[5.2.2]

5.3 Tube Pitch Spacing

5.3.1 Discussion

Nieh et al.[5.3.1] studied the effect of staggered tube bundles with the same vertical pitch (2.1 tube diameters) and two different horizontal pitches. Figure 5.3.1 shows the result of this study. The tube erosion in the tube bundle with tighter pitch (equal to 1.5 tube diameters) varied with distance of the bottom tube to the distributor in such a manner that a maximum occurred at 3 cm (2.1 tube diameters) above the distributor. The tube erosion for the looser tube pitch (2.5 tube diameters) increased linearly with increasing bundle height. At 1.5 cm (1.1 tube diameters), the erosion rates were almost equal and very low. As the tube bundles were raised to 3 cm (2.1 tube diameters) or 5 cm (3.6 tube diameters), a distinct effect of horizontal pitch on tube erosion was noted.

Lockwood[5.3.2] carried out qualitative visualization studies varying both the horizontal and vertical tube pitches from 1/2 to 1-1/2 tube diameters. He found that the horizontal spacing had the most significant effect upon fluidization quality. The quality of fluidization was determined visually and from pressure fluctuation measurements. On the basis of this study, a moderate to wide horizontal spacing is indicated (in this case, 1 to 1-1/2 tube diameters). Narrow spacing, when coupled with increasing gas velocity, tended to restrict vertical solids movement. As the bed expanded and the solids rose above the tubes, the tubes formed a barrier that prevented the solids from moving downward. The venturi effect created by the closely spaced tubes on the rising gas stream also restricted vertical solids movement downward. The net result was a dilute phase within the immersed tubes. If vertical spacing was too wide, rising bubbles expanded and coalesced into larger bubbles. Moderate to close vertical spacing (1 to 1/2 tube diameters) for triangular arrays yielded good solids circulation and bed stability. For rectangular arrays, moderate vertical spacing appeared qualitatively to be the most desirable. Wide spacing (1-1/2 tube diameter) in both directions permitted bubbles to expand and coalesce into large ones with associated instabilities and occasional slugging and increased erosion. Close spacing (1/2 tube diameter) in both directions restricted solids circulation. Higher bed differential pressures also resulted from close spacing. Considerable difficulty was experienced in fluidizing the 1379-μm (12 Tyler mesh) solids when the tubes were closely spaced in both directions, and the tube array was close (2.5 cm) to the distributor plate.

5.3.2 Recommended Design Guidelines and Procedures

It would appear from the above limited and contradictory results that the role of bubble coalescence and jetting from the distributor can affect the erosion rate when the pitch for a staggered tube bundle is varied. It appears that above about 3 tube diameters from the distributor, a tight pitch configuration (1-1.5 tube diameters) yields significantly lower metal wastage than loose pitch (greater than 1.5 tube diameters). On the other hand, it appears that for tube bundles closer than 3 tube diameters to the distributor, a loose pitch configuration (greater than 1.5 tube diameters) is recommended over a tight pitch configuration. Considering the idealizations of the experiments, these recommendations should be viewed with some skepticism until more realistic controlled experiments are performed. A realistic constraint, however, is that the temperature gradient through the tube bank may become too high with the tight pitch and therefore pitches less than 2 tube diameters are not admissable.

The in-kind data reports received from British Coal Corporation's Coal Research Establishment addressing the dependence of the erosion rate upon tube spacing found that for the

six different tube spacings studied, the bank whose tubes suffered the highest losses was that used in the Grimethorpe PFBC (the "D" array).(5.3.3) The largest decrease in tube loss measured for a change in tube spacing was obtained when using "DSH" bank. By using this array, the maximum tube weight losses were about 35% less than those measured when the "D" bank was fitted.

Further studies confirmed earlier results that showed that close-packed tube arrays suffered less wear than those with larger tube separation.(5.3.4) Tests for tube bank "E" showed that the position of peak wear and its value can be controlled by judicious variation of packing density to combat the highest wear with the greatest packing density.(5.3.5) Some scope was felt to exist for reducing wear by extreme changes in geometry, but these concepts were considered unlikely to result in a practical tube bank. A significant feature of tube bank "E" was the nearly constant peak wear rate on the diagonal tube positions as a function of height up the tube bank.(5.3.6) This observation indicates that the dense tube packing at the top of the bed had been beneficial at suppressing wear on this part of the tube.

References

5.3.1 Nieh, S., S.Y. Lin, S.W. Lee, and T.T. Fu, *Measurements of In-Bed Tube Bundle Erosion and Particle-Tube Frequency in a Gas Fluidized Bed*, Particulate Science and Technology, 6:269-283 (1988).

5.3.2 Lockwood, D.W., *Effects of Heat Exchanger Tube Spacing and Arrangement on the Quality of Fluidization*, Proc. Second Pacific Chemical Engineering Congress, American Institute of Chemical Engineers, New York, Vol. II, pp. 1177-1181 (Aug. 1977).

5.3.3 British Coal Corporation, Coal Research Establishment, *Cold Model Studies of Tube Wear in Support of PFBC (December 1985-February 1986)*, PFBC/MOA/P9, Stoke Orchard, Cheltenham, U.K. (April 9, 1987).

5.3.4 Parkinson, M.J., A.W. Jury, B.A. Napier, N.C. Moon, and C.M. Barrety, *Cold Model Studies on the Effect of Fluidizing Velocity and Mean Particle Size on Tube Wear, Test Series 1*, PFBC/MOA/P15, British Coal Corporation, Coal Research Establishment, Stoke Orchard, Cheltenham, U.K. (June 12, 1987).

5.3.5 British Coal Corporation, Coal Research Establishment, *Results of the First Ten Cold Model Tests at Grimethorpe Leading to the Design of Combustor Tube Bank "E"*, PFBC/MOA/P21, Stoke Orchard, Cheltenham, U.K. (Nov. 6, 1987).

5.3.6 British Coal Corporation, Coal Research Establishment, *Grimethorpe Cold Model Tests 11 to 16: Evaluation of the Tube Bank "E" Final Design and Assessment of the Benefit of Further Tube Diameter Increases*, PFBC/MOA/P29, Stoke Orchard, Cheltenham, U.K. (April 28, 1988).

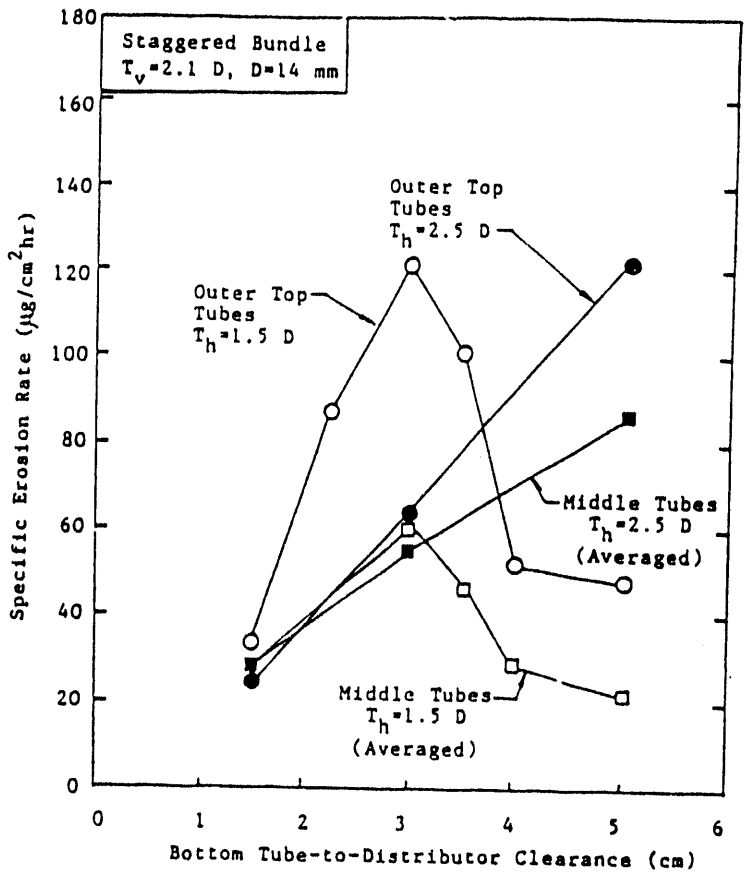

FIGURE 5.3.1 Effect of Horizontal Pitch of Staggered Tube Bundles on Specific Erosion Rate[5.3.1]

5.4 Staggered versus In-Line Tube Arrangement

5.4.1 Discussion

Nieh et al.[5.4.1] studied tube erosion of a staggered bundle (11 tubes) and an in-line bundle (12 tubes) measured under identical flow conditions (U = 75 cm/s, bottom tube to distributor distance = 3 cm, 2.1 tube diameters). The vertical pitch was 3 cm (2.1 tube diameters), and the horizontal pitch was 1.5 cm (1.5 tube diameters). From previous tests, they found the in-line tube bundle also had a characteristic maximum erosion at a tube bundle height (above distributor) of 3 cm, like the case of a narrow-pitch staggered bundle. Figure 5.4.1 summarizes the comparison of tube erosion of in-line and staggered bundles. The average erosion of the tubes at different positions in the staggered configuration was found to be consistently larger than that of corresponding tubes in the in-line configuration by approximately 45%. However, it should be noted that the two outer tubes in the middle row on the in-line bundle (no corresponding tubes in the staggered bundle) were found to experience severe erosion, 200% higher than the inner tubes at the same level. Nieh et al. believed that the higher overall erosion of the staggered bundle was due to the smaller flow resistance of the staggered bundle than the in-line bundle, thereby permitting a higher particle impinging velocity and hence greater tube erosion.

Cold model test results conducted by Ellis and Armitage[5.4.2] show that triangular pitch results in greater metal wastage than square pitch. Figure 5.4.2 compares the results of the wear rates from their studies.

CURL[5.4.3] studied the effect of altering the Grimethorpe tube bank C geometry to an in-line arrangement maintaining the same density of tubing. With the in-line arrangement, the wastage rate within the body of the tube bank was reduced by about 50%. However, the elutriation rate was excessive on this test, and any future work on in-line tube tanks should include a closely pitched section at the top to reduce the energy of bursting bubbles. This radical change in tube bank geometry was not pursued when it became evident that is was not a practical short-term solution for Grimethorpe.

Lockwood[5.4.4] found that in the rectangular arrays, channeling (gas by-passing) was a common occurrence, particularly at higher superficial velocities. As the vertical spacing was decreased, channeling became more severe. Severe channeling caused the solids to be carried higher into the freeboard and increased entrainment in the exit gas stream, just as observed at CURL. Qualitatively, channeling was also associated with smaller fluctuations in bed differential pressure with rectangular arrays than with triangular arrays. Small differential pressure fluctuations, while generally associated with a stable, uniformly fluidized bed, can be due to gross gas by-passing, an undesirable characteristic.

Triangular arrays experienced some channeling, too. In this case, channeling was either in a diagonal manner up the array between diagonal rows of tubes, or vertically in a pseudosinusoidal fashion. This form of by-passing was less frequent than in the rectangular arrays. Channeling typical of both triangular and rectangular arrays is depicted schematically in Fig. 5.4.3. Triangular arrangements provided a more uniform gas-solids mixture than rectangular ones. In general, bed differential pressure fluctuations were slightly greater with triangular arrays but were also associated with less gas by-passing. Solids circulation was more uniform throughout the bed with triangular arrays. Close vertical spacing in rectangular arrays resulted in channeling. The vertical rows of tubes effectively acted as barriers to horizontal solids movement.

5.4.2 Recommended Design Guidelines and Procedures

The consensus of investigators is that tubes should be in an in-line (square) arrangement in order to minimize erosion. The studies in this section conclude that the pitch should also be no more than 1-1.5 tube diameters. However, if the pitch is too small, channeling may occur, possibly increasing metal wastage significantly. Brain and Michner[5.4.5] recommended that whenever possible, the tubes should be arranged on a square pitch in preference to a triangular pitch. Where triangular pitch or cross-over arrangements have to be used, some protection on the underside of the upper tubes may be required. However, the British Coal Corporation's Coal Research Establishment in-kind data for cold model tests indicated that there was no significant difference between triangular and square pitching, at least at high packing densities; therefore, for ease of construction, a square pitched tube bank was developed.[5.4.6]

For the UK shallow beds, experiments carried out with two rows of tubes arranged in either a square or triangular pitch array showed that maximum wear occurred on the upper row of tubes in the triangular array.[5.4.7] The wear on these tubes was four times greater than that on the corresponding tubes in the square array. The high rate of wear of the upper row tubes in the triangular pitch can be attributed to their location in the path of high-velocity bed material passing between the lower row tubes. The upper rows in the square array tend to be sheltered by the lower row tubes.

These tests also showed how increasing horizontal tube spacing (200 to 400 mm) can be used to reduce wear, particularly on the upepr row of a triangular array. Increasing the horizontal pitch of lower row tubes reduces the inter-tube "channel" velocity and thus reduces the velocity of particles impinging on the upper row tubes.

The maximum distances from tube surface to tube surface for triangular tube pitches are larger than for square or in-line pitch tube arrays. The simplified MED erosion model given by Eq. 3.4 predicts that the erosion increases with a characteristic acceleration distance. If this distance is taken to be the maximum distance from tube surface to tube-surface, this explains the observed higher erosion rates for triangular pitch tube bundles, relative to square or in-line pitch tube bundles.

References

5.4.1 Nieh, S., S.Y. Lin, S.W. Lee, and T.T. Fu, *Measurements of In-Bed Tube Bundle Erosion and Particle-Tube Frequency in a Gas Fluidized Bed*, Particulate Science and Technology, *6*:269-283 (1988).

5.4.2 Stockdale, W., F. Ellis, and C. Armitage, *Wastage of In-Bed Surfaces in Fluidized Bed Combustors, Experience in Practice with 3 Industrial AFBC Units in the U.K.*, Paper No. 2.5 in Proceedings Wastage of In-Bed Surfaces in Fluidized-Bed Combustors, Workshop Held at Argonne National Laboratory, Nov. 2-6, 1987. Available from Electric Power Research Institute (1987).

5.4.3 Sparham, G.A., *Tube Wastage Investigations — Support Work of CURL*, in Reports Commissioned by the Project from Outside Consultants and Others, Vol. 2, NCB (IEA Grimethorpe) Ltd., Barnsley, S. Yorkshire, U.K. (Sept. 1984).

5.4.4 Lockwood, D.W., *Effects of Heat Exchanger Tube Spacing and Arrangement on the Quality of Fluidization*, Proc. Second Pacific Chemical Engineering Congress, American Institute of Chemical Engineers, New York, Vol. II, pp. 1177-1181 (Aug. 1977).

5.4.5 Brain, S., and A. Michner, *Minimization of Wastage in Bubbling Atmospheric Fluidized Bed Boilers*, Proceedings on Corrosion-Erosion-Wear of Materials at Elevated Temperatures, Berkeley, Calif., Jan. 31-Feb. 2, 1990, A.V. Levy, ed., pp. 40-1 to 40-16, National Association of Corrosion Engineers, Houston, Texas (1991).

5.4.6 British Coal Corporation, Coal Research Establishment, *Results of the First Ten Cold Model Tests at Grimethorpe Leading to the Design of Combustor Tube Bank "E"*, PFBC/MOA/P21, Stoke Orchard, Cheltenham, U.K. (Nov. 6, 1987).

5.4.7 British Coal Corporation, Coal Research Establishment, *Minimizing Erosion in Coal-Fired Boilers*, Commission of the European Communities Report EUR 12360EN, Contract No. 7220-ED/808, Final Report, Directorate-General, Telecommunications, Information Industries and Innovation, Luxembourg (1989).

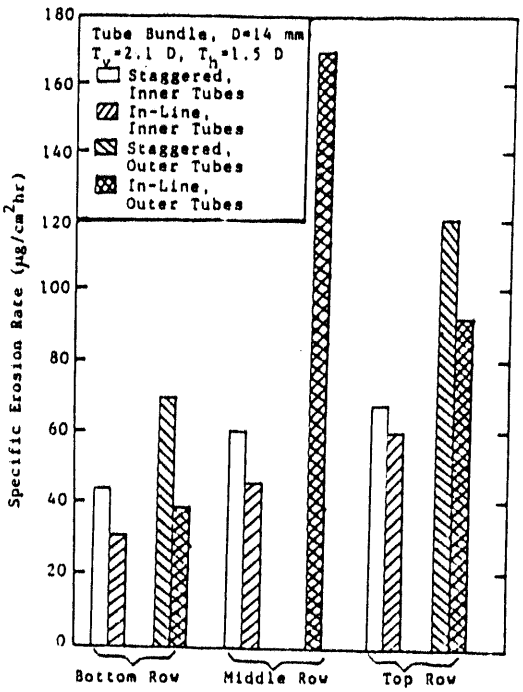

FIGURE 5.4.1 Comparison of Specific Erosion Rate of Different Bundle Configurations[5.4.1]

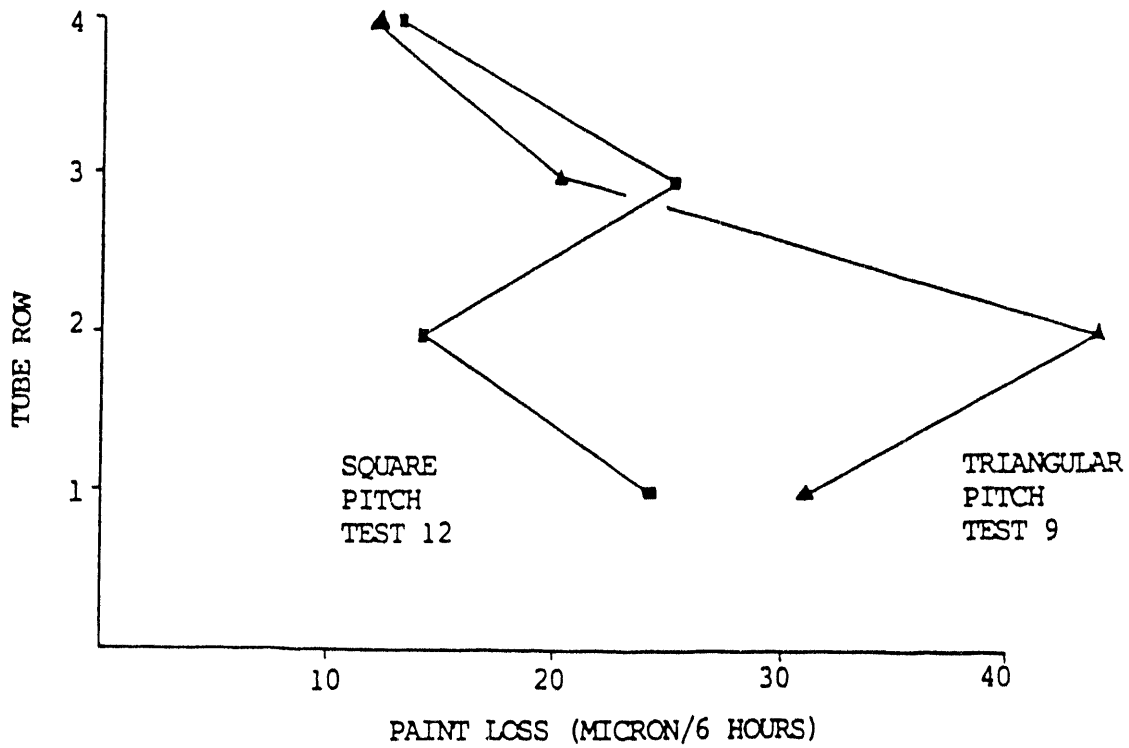

FIGURE 5.4.2 Cold Model Test Results[5.4.2]

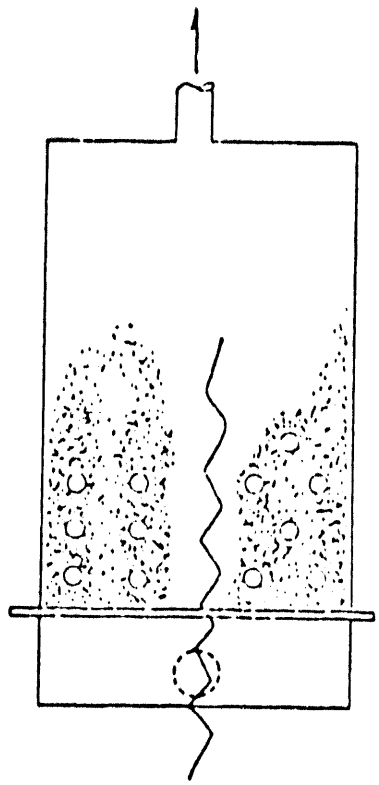

FIGURE 5.4.3 Schematic Diagram Showing Channeling in Rectangular Arrays, on the Left Segment, and in Triangular Array, on the Right Segment(5.4.3)

5.5 Tube Inclination

5.5.1 Discussion

Lee[5.5.1] studied the influence of tube orientation on in-bed tube erosion at four different inclined angles: 0°, 30°, 60°, and 90° (vertical). For successive test runs, the tube was placed horizontally and vertically at the center and vertically near the wall to quantify the effect of tube location. Figure 5.5.1 shows the averaged specific erosion rate and the specific weight loss for the immersed tube in a bed with 0.55-mm glass beads at a superficial velocity of 67 cm/s. The sample tubes were tested at the above bed conditions for three hours for different tube locations and orientations. The averaged specific erosion rates for 0°, 30°, 60°, and 90° were found to be 0.58, 0.49, 0.34, and 0.27 mg/cm^2·h, respectively. Horizontal tubes were found to experience a weight loss about 215% greater than that of vertical tubes under the same conditions. The specific erosion rate of the vertical tube near the wall was found to be only 0.15 mg/cm^2·h, 55% that of the tube in the core region. Experience with single tube inclinations may not properly reflect those for bundles of tubes. However, the trend of these results agrees well with other observations[5.5.2] that the erosion rate of horizontal tubes is greater than that of inclined and vertical tubes. The specific weight loss of tubes close to the side wall was much less than that of tubes near the center of the bed, also in agreement with other findings.[5.5.2-5.5.5] The lower erosion rate for tubes near the wall is attributed to the averaged solids flow patterns in the bed.

Wear rates measured on the vertical (and inclined) sections of the Grimethorpe C tube bank were reported to be much less than those measured on the horizontal sections. In the cold model, the wastage on the bends was about the same as that on plain horizontal tubes. However, the wear on vertical and inclined tube banks in the cold model was much more severe. It is thought that in the 2-m × 2-m combustor the "wall effect" (i.e., the low levels of wastage close to the walls observed in all the rigs) extends to about 400 mm from the wall and includes regions of the bed where the bends and the inclined and vertical sections are located. When specifying a design for tube bank C2, greater emphasis was therefore placed on the wear measurements made on tube bank C rather than on data from the cold model tests, in which the wall effect extended only about 70 mm into the bed.

5.5.2 Recommended Design Guidelines and Procedures

The situation in the open literature is somewhat confusing, but it is clear that tube inclination will produce more three-dimensional effects than a horizontal tube. The influence of bubble coalescence must be considered. This implies that the bed height be taken into consideration. The experience with shallow bed FBCs led to the conclusion that the tube bank inclination should be minimized and that horizontal tubes were preferred.[5.5.3, 5.5.4] The argument given was that inclined tubes could cause particles to track along the tube. This is consistent with Rowe and Everett's x-ray studies that showed that inclined tubes cause bubbles to rise along them.[5.5.6] Conclusions drawn from Lee's single-tube studies should be applied to a tube bundle with caution, if at all. The contradictory results for cold models of Grimethorpe[5.5.5] may be a result of improper scaling. Brain and Michner recommended that horizontal tubes should be used if possible.[5.5.7]

The British Coal Corporation's Coal Research Establishment in-kind data have clarified the situation, as has a recent report by them.[5.5.8, 5.5.9] The BCC compared tapered beds and vertical tube bundle erosion rates to those obtained using a parallel-sided bed fitted with an array of horizontal tubes and operated under the same fluidizing conditions.[5.5.8] The maximum weight

loss was a factor of 3.6 higher when a tapered bed was fitted. When an array of vertical tubes was tested, the maximum tube weight loss was more than a factor of 15 larger than that of an identical horizontal tube array. However, since the wear was spread uniformly over the surfaces of the vertical tubes in the centre of the array and was confined to about 20% of the surface area of horizontal tubes, the life expectancy of the vertical tube array was estimated to be only about three times shorter than that of the bundle of horizontal tubes.

For the UK shallow beds, results from tests with tubes inclined at 10° to the horizontal suggest that wear may be increased by as much as 50% compared with horizontal tubes.[5.5.9] A proposed explanation for this effect is that bubbles and particles have been observed, in video surveys, to "track" along sloping tubes as opposed to passing around horizontal tubes.

The simplified MED erosion model given by Eq. 3.4 predicts that erosion increases with a characteristic acceleration distance, x_d. For vertical tubes, this characteristic distance can be taken to be the tube height, which is at least an order of magnitude larger than the maximum tube pitch a horizontal tube array producing a correspondingly higher erosion rate.

References

5.5.1 Lee, S.W., *Analysis and Modeling of In-Bed Tube Erosion in a Gaseous Fluidized Bed*, Doctoral Dissertation, the Catholic University of America, Washington, D.C. (Feb. 1989).

5.5.2 Parkison, J., B.A. Napier, A.W. Jury, and T.J. Kempton, *Cold Model studies of PFBC Tube Erosion*, DOE/METC 85/6021, Vol. 2, pp. 730-738 (1985).

5.5.3 Stockdale, W.F. Ellis, and C. Armitage, *Measurements of In-Bed Tube Bundle Erosion Combustors, Experience in Practice with 3 Industrial AFBC Units in the U.K.*, Paper No. 2.5 in Wastage of In-Bed Surfaces in Fluidized-Bed Combustors, Workshop Held at Argonne National Laboratory, Nov. 2-6, 1987. Available from Electric Power Research Institute (1987).

5.5.4 Ellis, F., and C. Armitage, *Combating Metal Wastage in Fluidized Bed Combustors*, in 1988 Seminar on Fluidized-Bed Combustion, Electric Power Research Institute (May 1988).

5.5.5 Parkinson, M.J., J.F.G. Grainger, A.W. Jury, and T.J. Kempton, *Tube Erosion at IAEA Grimethorpe: Cold Model Studies at CRE*, in Reports Commissioned by the Project from Outside Consultants and Others, Vol. 2, NCB (IEA Grimethorpe) Ltd., Barnsley, S. Yorkshire, U.K. (Sept. 1984).

5.5.6 Rowe, P.N., and D.J. Everett, *Fluidised Bed Bubbles Viewed by X-rays Part I—Experimental Details and the Interaction of Bubbles with Solids Surfaces*, Trans. I. Chem. Engineers, *50*:42-48 (1972).

5.5.7 Brain, S., and A. Michner, *Minimization of Wastage in Bubbling Atmospheric Fluidized Bed Boilers*, Proceedings on Corrosion-Erosion-Wear of Materials at Elevated Temperatures, Berkeley, Calif., Jan. 31-Feb. 2, 1990, A.V. Levy, ed., pp. 40.1-40-16, National Association of Corrosion Engineers, Houston, Texas (1991).

5.5.8 Parkinson, M.J., A.W. Jury, B.A. Napier, N.C. Moon, and C.M. Barrett, *Cold Model Studies of Tube Wear with Vertical Tubes and Tapered Beds*, PFBC/MOA/P17, British Coal Corporation, Coal Research Establishment, Stoke Orchard, Cheltenham, U.K. (Oct. 8, 1987).

5.5.9 British Coal Corporation, Coal Research Establishment, *Minimizing Erosion in Coal-Fired Boilers*, Commission of the European Communities Report, Directorate-General, Telecommunications, Information Industries and Innovation, Luxembourg (1989).

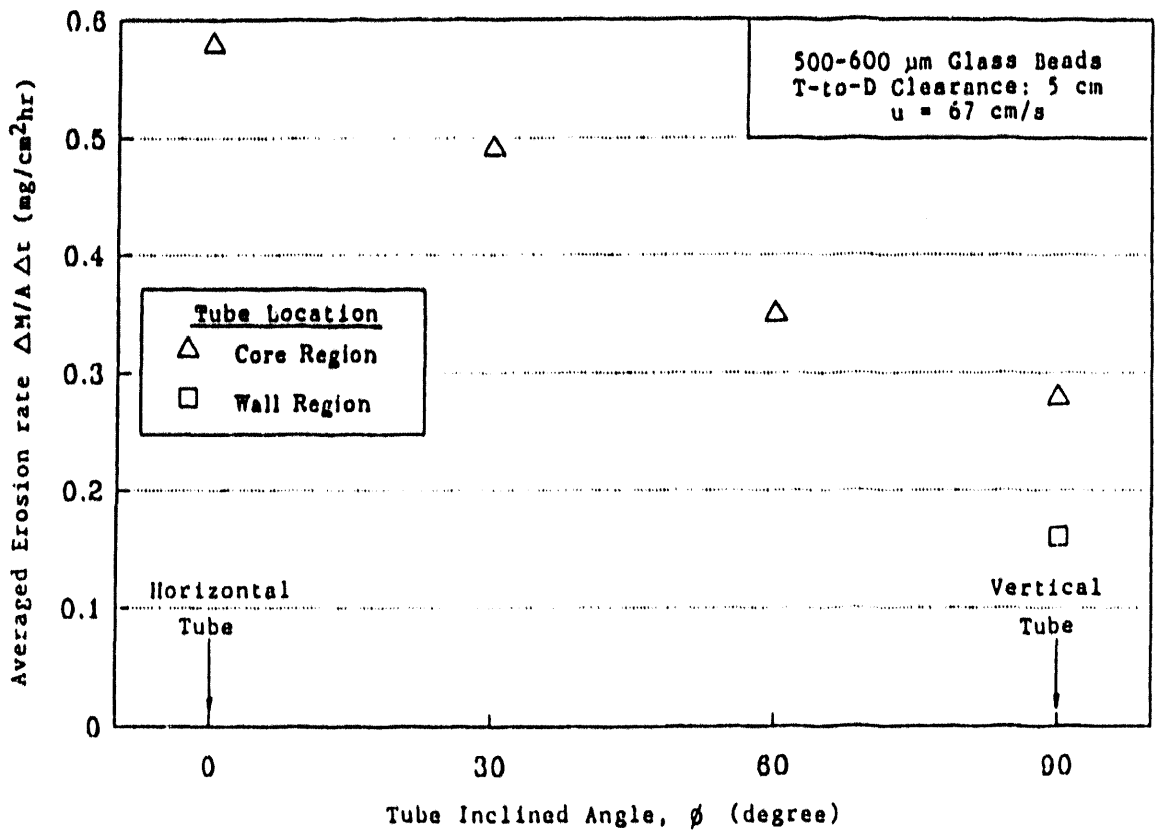

FIGURE 5.5.1 Influence of Tube Orientation and Location on In-Bed Tube Erosion (177 mm diameter)[5.5.1]

5.6 Protective Devices

5.6.1 Discussion

Lee[5.6.1] studied four different types of tube protective devices — pinned tube, ball-studded tube, finned tube, and finned and ball-studded tube — to aid the understanding of the preventive methods of an in-bed erosion. The ball-studded tube had two configurations: in-line studding pattern and staggered studding pattern.

The pins were installed on half of the tubes as shown in Fig. 5.6.1. At $U\text{-}U_{mf} \sim 70$ cm/s, the bare tube specific weight loss at 3 cm was 1.43 mg/cm^2, and the specific weight loss of the pinned tube was 0.87 mg/cm^2 at a tube-to-distributor spacing of 3 cm. This represents a reduction of 40% over that of the bare tube. Similar reductions resulted at lower fluidizing velocities. The specific weight loss versus excess fluidizing velocity exhibits the same characteristic jump at a threshold velocity (26 cm/s) slightly above the minimum fluidization velocity, similar to that shown in Fig. 4.1.8 in Sec. 4.1, indicating an erosion threshold velocity.

Lee[5.6.1] found that a ball-studded tube with the in-line pattern was less effective in reducing erosion of the ball-studded tube than the staggered pattern. Figure 5.6.2 shows the measured results of specific weight loss for the different types of protective devices. The staggered studding tube had a wastage rate that is three times lower than that of a bare tube. Erosion was reduced more than threefold by using a combination of finned and ball-studded tube, as shown in Fig. 5.6.2. The finned and ball-studded tube is the more desirable protective device. When the anti-erosion devices were applied to the three Foster Wheeler boilers, the maximum erosion rate could be reduced two or three fold by using a finned and ball-studded tube at the same fluidizing velocity.[5.6.2]

Parkinson et al.'s experimental program in support of Grimethorpe yielded a large amount of data on the erosion rate of various types of horizontal tube for a range of operating conditions.[5.6.3] A summary of the overall average weight losses for the tests is shown in Fig. 5.6.3, and this gives a clearer picture of the benefits achieved.

The total decrease in erosion rate, from that suffered under the initial test conditions (Run 1) to that achieved under the conditions adopted for Run 8, where all the means of tube protection suggested by the results of the intervening test runs were included, shows an improvement by more than a factor of 50. However, the benefit obtained from each change individually (i.e., either [1] decreasing the tube bundle to distributor distance from 0.9 to 0.45 m, [2] fitting fins or pegs to the tubes, or [3] changing the fluidizing velocity, U, from 2 to 1 m/s) is dependent on the value of the other two parameters. For example, decreasing the fluidizing velocity for plain tubes reduces wear by more than a factor of 4.5 (cf. Runs 2 and 5), whereas the same change in fluidizing velocity for pegged tubes (cf. Runs 4 and 8) gives an "improvement" by a factor of 1.8. Changing from plain to pegged tubes at 2 m/s (Runs 2 and 4) produces a reduction of more than 7.6 times, while at 1 m/s, the change is only a factor of 2.9 (cf. Runs 5 and 8). Clearly the benefit that can be achieved by a given change cannot be quantified by a single parameter since it is strongly dependent on the other operating conditions.

Stockdale, Ellis, and Armitage[5.6.4] reported on the influence of fluidizing velocity on wear rate for three types of in-bed tube surfaces tested, as can be seen in Fig. 5.6.4. It is apparent that a much higher design fluidizing velocity can be tolerated when the tube bundle is fitted with a protection system; both finned and ball-studded tubes show improved resistance to wear at fluidizing velocities up to 3 m/s. Plain steel-tube arrangements should be designed at fluidizing

velocities below 2 m/s on the basis of this work, if the same resistance against metal wastage is to be achieved.

5.6.2 Recommended Design Guidelines and Procedures

The use of protective devices appears to be effective at low fluidizing velocities. There appears to be a threshold velocity above which metal wastage increased exponentially, eventually exceeding that of bare tube. Use of these protective devices is considered to be a stop-gap measure. Figures 4.1.13 and 5.6.4 confirm this observation, since, if the fluidizing velocity is too high, protective devices such as studs and fins lose their effectiveness, producing erosion rates comparable with bare tubes.

The British Coal Corporation's Coal Research Establishment in-kind data indicate that the addition of some finned tubes to the tube bank altered the distribution of wear only slightly with some leveling off of the wear on the centre platens.[5.6.5] However, the fins did not affect the peak wear rate observed for the tube bank. The addition of four longitudinal fins at 45, 135, 225, and 315 degrees to the tubes showed a typical 8% reduction in wear on the exposed bottom measuring position, with an overall average improvement on the tube of 20%.

References

5.6.1 Lee, S.W., *Analysis and Modeling of In-Bed Tube Erosion in a Gaseous Fluidized Bed*, Doctoral Dissertation, The Catholic University of America, Washington, D.C. (Feb. 1989).

5.6.2 Montrone, E.D., *Experience with Foster Wheeler Fluidized Bed Combustors*, in EPRI Workshop Proceedings: Wastage of In-Bed Surfaces in Fluidized Bed Combustors, held at Argonne National Laboratory, Nov. 2-6, 1987. Available from Electric Power Research Institute (1987).

5.6.3 Parkinson, M.J., A.W. Jury, B.A. Napier, T.J. Kempton, and J.C. Holder, *Cold Model Erosion Studies in Support of Pressurized Fluidized Bed Combustion*, Electric Power Research Institute Draft Final Report for Project 1337-2 (April 1986).

5.6.4 Stockdale, W., F. Ellis, and C. Armitage, *Wastage of In-Bed Surfaces in Fluidized Bed Combustors, Experience in Practice with 3 Industrial AFBC Units in the U.K.*, Paper No. 2.5 in Wastage of In-Bed Surfaces in Fluidized-Bed Combustors, Workshop Proceedings held at Argonne National Laboratory, Nov. 2-6, 1987. Available from Electric Power Research Institute (1987).

5.6.5 British Coal Corporation, Coal Research Establishment, *Grimethorpe Cold Model Tests 11 to 16: Evaluation of the Tube Bank "E" Final Design and Assessment of the Benefit of Further Tube Diameter Increases*, PFBC/MOA/P29, Stoke Orchard, Cheltenham, U.K. (April 28, 1988).

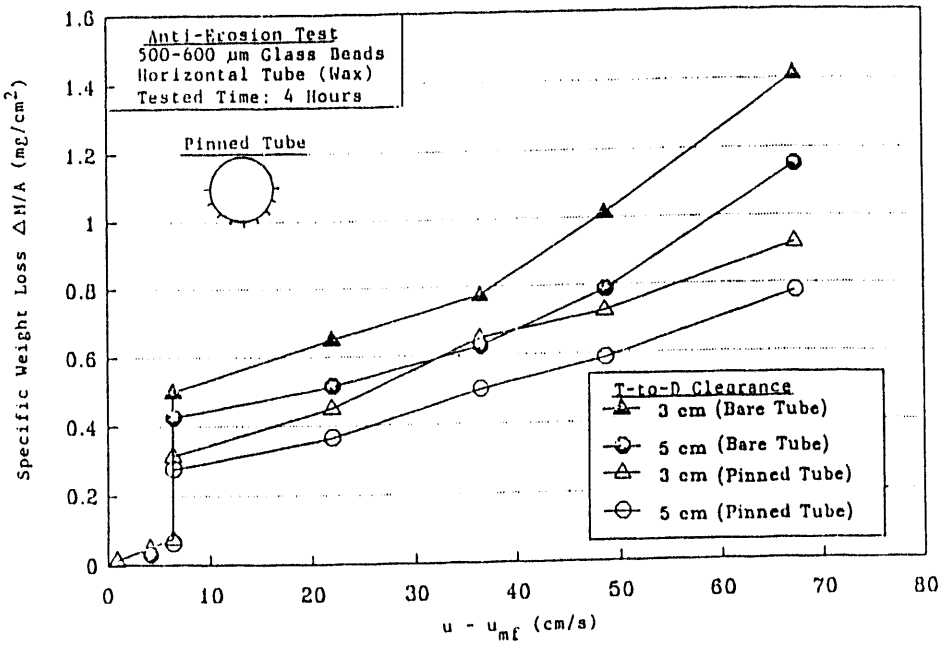

FIGURE 5.6.1 Effect of Anti-Erosion Device on In-Bed Tube Erosion at Different Fluidization Velocities(5.6.1)

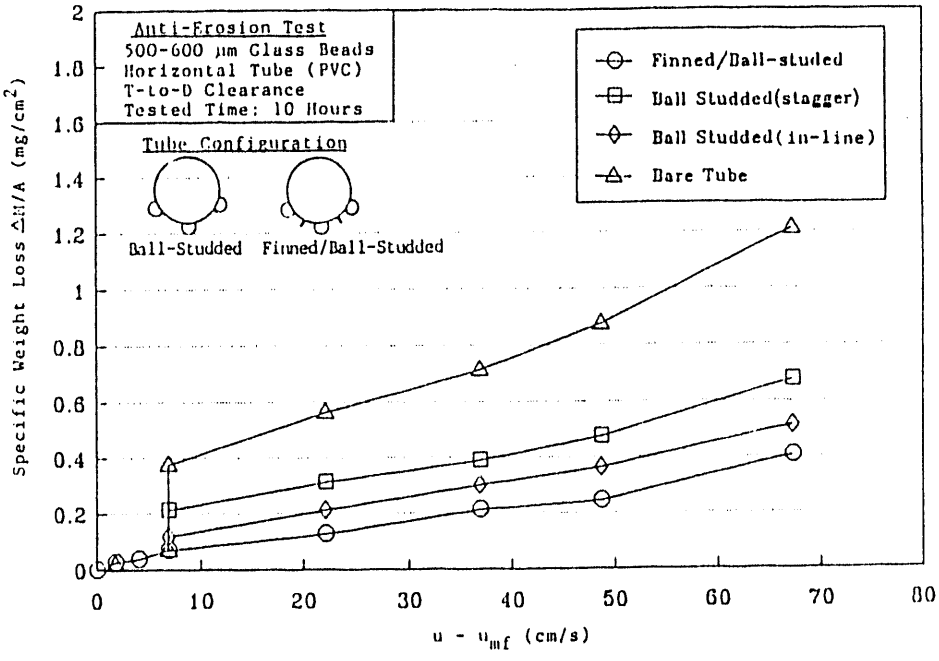

FIGURE 5.6.2 Effect of Anti-Erosion Device Configuration on In-Bed Tube Erosion(5.6.1)

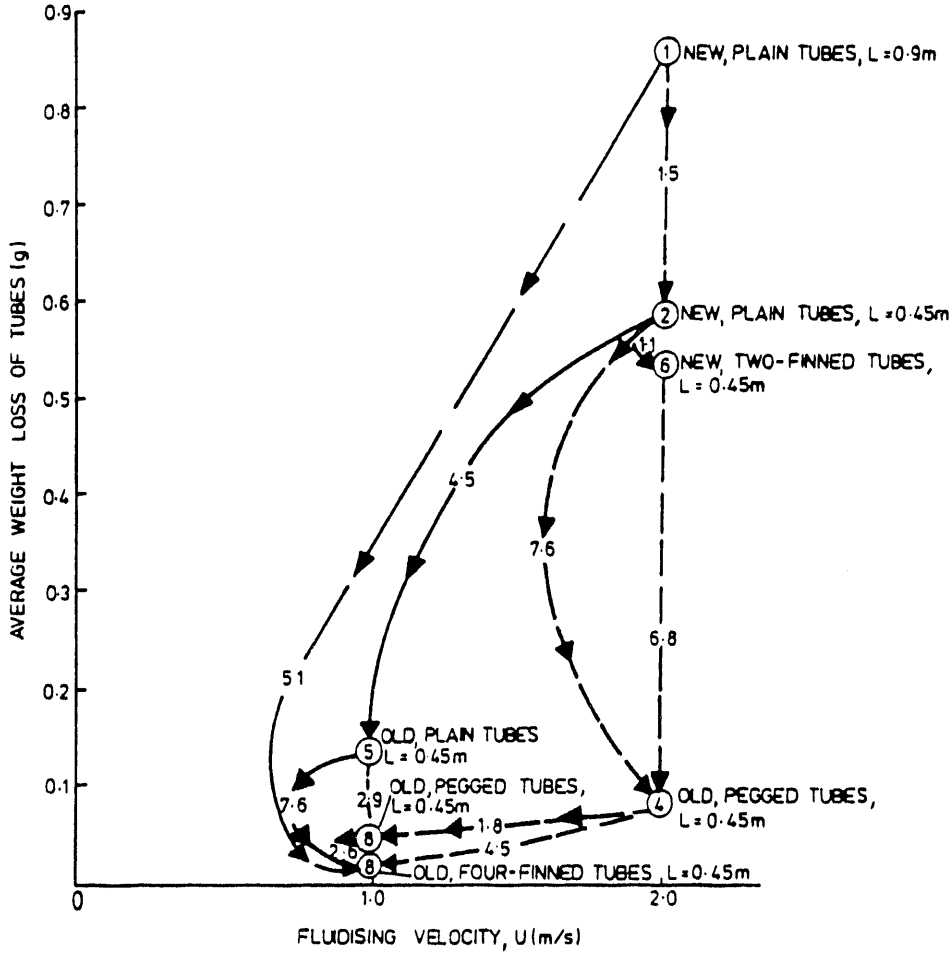

NOTES:

1. THE NUMBERS SHOWN IN THE CIRCLES ARE THE TEST RUN NUMBERS (SEE TABLE 1) THE NUMBERS SHOWN ON THE LINES JOINING THE CIRCLES ARE THE FACTORS BY WHICH EROSION IS REDUCED BY THE CHANGE DENOTED BY THE ENDPOINTS OF THE LINES.
2. THE WEIGHT LOSSES SHOWN FOR RUN 8 (150 HOUR TEST) HAVE BEEN NORMALISED TO 48 HOURS TO MATCH THE DURATION OF THE OTHER TESTS.

FIGURE 5.6.3 General Summary of Test Results for Horizontal Tubes[5.6.3]

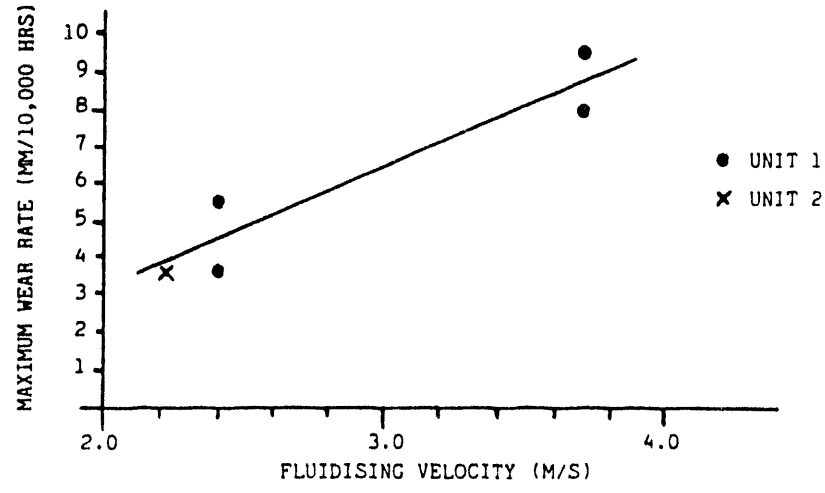

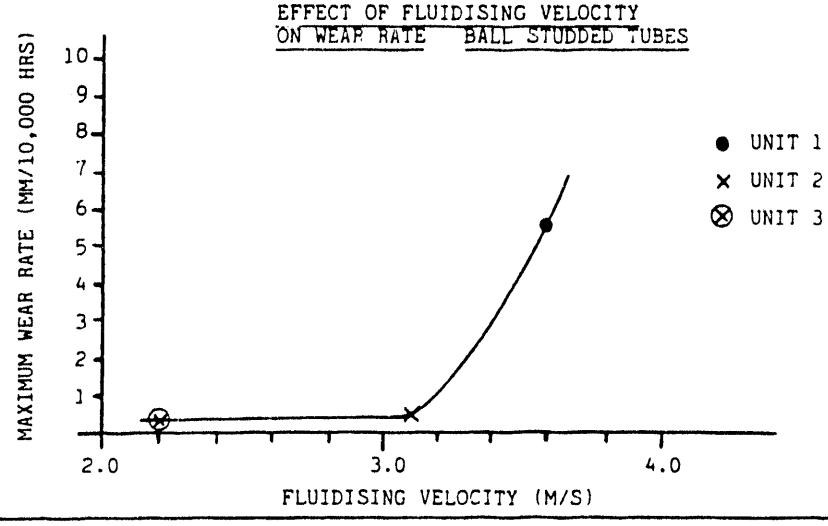

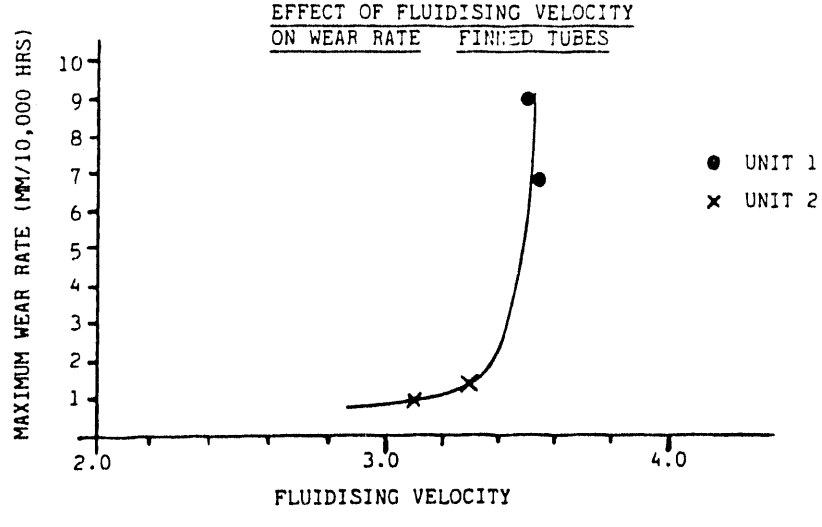

FIGURE 5.6.4 Effect of Fluidizing Velocity on Wear Rate for Plain, Ball-Studded, and Finned Tubes(5.6.4)

5.7 Distributor Design

5.7.1 Discussion

Zhu[5.7.1] conducted two tests at room temperature with the same operating conditions in their circulating fluidized-bed combustion unit. These tests provided some indication of the effect of different distributor designs. The conditions were nearly the same as the base conditions in the main column used in this work, but the particle size was 0.92 mm. The air distributor of the combustor consisted of three tuyeres, each with six orifices sloping downwards at an angle of 30° to the horizontal. The combustor had a cross-sectional area of 152 × 152 mm.

The results are shown in Figure 5.7.1, which were obtained by conducting the experiments at essentially the same conditions, except that a multi-orifice distributor was used in the low-temperature three-dimensional column. The results for Runs 52 and 59 were corrected for particle size by using Eq. 4.2.4. The comparison shows that erosion rates changed by a factor of up to 2.3 for some materials, with the multi-orifice distributor leading to much more severe erosion than the tuyere distributor. This dramatic change in erosion rate must have resulted from a change of gas and particle flow conditions in the vicinity of the tube. The tuyeres in the combustor discharged air nearly horizontally. This may have reduced the initial bubble rise velocity and bubble coalescence, hence reducing the bubble size and, therefore, the bubble or particle velocity at the level of the tube. Also, more of the bubble gas may have been distributed to the wall region, resulting in fewer bubbles in the center of the column.

5.7.2 Recommended Design Guidelines and Procedures

On the basis of the work of Zhu,[5.7.1] tuyeres or tees (such as those used in the FWDC ash bed experiment, Sec. 5.1.1.5) would be preferred over a multi-orifice distributor. Brain and Michner[5.7.2] warned that non-uniform air flows through the combustor will cause localized wear and need to be avoided. Factors that cause preferential air flows include poor plenum design, use of air distributors with too low a pressure drop, and accumulations of oversize ash or sintered material in parts of the bed.

References

5.7.1 Zhu, J., *Tube Erosion in Fluidized Beds,* Ph.D. Thesis, Department of Chemical Engineering, The University of British Columbian (May 1988).

5.7.2 Brain, S., and A. Michner, *Minimization of Wastage in Bubbling Atmospheric Fluidized Bed Boilers,* Proceedings on Corrosion-Erosion-Wear of Materials at Elevated Temperatures, Berkeley, Calif., Jan. 31-Feb. 2, 1990, A.V. Levy, ed., pp. 40.1 to 40.16, National Association of Corrosion Engineers, Houston, Texas (1991).

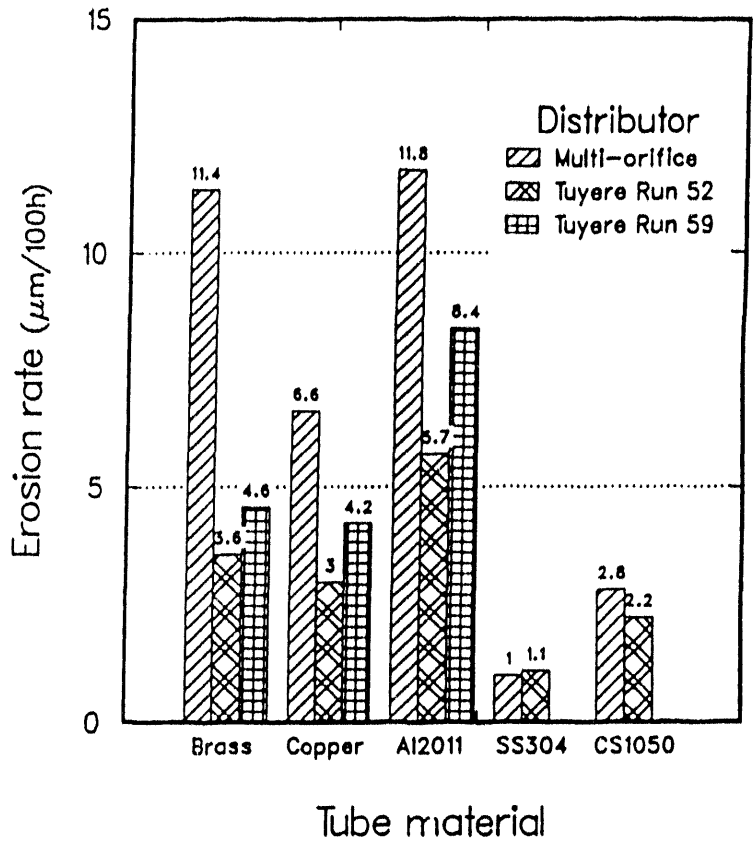

Operating conditions:

Particles: 1.0 mm silica sand
Particle sphericity: 0.89
Excess air velocity: 1.31 m/s
Tube: 32 mm single tube
Duration: 40 – 100 h

FIGURE 5.7.1 Effect of Distributor on Erosion Rate(5.7.1)

6 Scaling and Relationships between Dependent Variables and Metal Wastage

The simplified MED erosion model given by Eq. 3.1 or 3.4 shows clearly the relationship between the dependent variables and erosion, in particular, the porosity and the solids velocity. The solids velocity in the vicinity of the tubes is approximately the superficial velocity; alternatively, it may be estimated from Eq. 4.2.5 or from the balance between drag and buoyancy by using Ergun's equation. Depending upon how one estimates the parameters in the simplified MED erosion model, the bubble velocity also enters as a parameter (see Example 4, Sec. 4.1.1). These dependent variables can be expressed in terms of the independent operating variables.

By analogy to the energy dissipation in the simplified MED erosion model, Yates[6.1] proposed a simple erosion model that is expressed in terms of the bubble velocity and the mass of particles in the wake of the bubbles. He obtained a simple relationship for metal wastage given by

$$E_{wp} = 0.13(1-\varepsilon)\, f_w\, \rho_p\, g\, d_e^4/(1-f_w) \tag{6.1}$$

where

E_{wp} = kinetic energy of the wake particles, J;
ε = wave voidage;
f_w = fraction of bubbles occupied by wakes;
ρ_p = particle density, kg/m^3;
g = acceleration due to gravity m/s^2; and
d_e = equivalent sphere bubble diameter, m.

For 500-μm-diameter particles, f_w~0.2 and ε ~0.4, Eq. 6.1 becomes

$$E_{wp} = 480\, d_e^4. \tag{6.2}$$

The equivalent sphere diameter, d_e, may be estimated from:[6.2]

$$d_e = \frac{0.54(U-U_{mf})^{0.4}(H + 4\sqrt{A_o})^{0.8}}{g^{0.2}} \tag{6.3}$$

where

U = fluidizing velocity, m/s;
U_{mf} = minimum fluidizing velocity, m/s;
H = bed height, m; and
A_o = area of the distributor per orifice, m^2.

In order to link erosion to well-known dimensionless scaling parameters, the simplified MED erosion model given by Eq. 3.4 may be written in terms of the Archimedes, A_r, and Froude, F_r, numbers as

$$\frac{\dot{E}_{EDCF}}{\dot{E}_o} = f(\varepsilon)\left[1 + 0.01167(ArFr)^{1/2}\right] \tag{6.4}$$

since

$$Re = (ArFr)^{1/2} = \phi_s d_p \rho_g U/\mu_g \tag{6.4a}$$

where

$$A_r = d_p^3 \rho_g(\rho_s-\rho_g)g/\mu_g^2 \tag{6.4b}$$

and

$$F_r = v_g^2/\left[g\phi_s\, d_p(\rho_s - \rho_g)/\rho_g\right]. \tag{6.4c}$$

$\dot{E}_o$ and $f(\varepsilon)$ are given by Eqs. (3.2) and (3.5), respectively.

Hence, for proper scaleup, the porosity, Archimedes, and Froude numbers must be equal. Alternatively, the simplified MED erosion model may be expressed in terms of the Archimedes number alone using Ergun's equation as[6.3]

$$\frac{\dot{E}_{EDCF}}{\dot{E}_o} = f(\varepsilon)\left[1-C_1 + \left(C_1^2 + C_2 Ar\right)^{1/2}\right]. \tag{6.5}$$

The constants C_1 and C_2 are from Ergun's equation and are given by $C_1 = 33.637$ and $C_2 = 0.04081$.[6.3] The dimensionless erosion rate expressed in the form of Equation 6.5 shows that the simplified MED erosion model is proportional to $d_p^{1.5}$ and constitutes a mechanistic basis for the purely empirical correlations presented in Secs. 4.1 and 4.2. The dimensional erosion rate, $\dot{E}_{EDCF}$, is proportional to $d_p^{0.5}$ to $d_p^{1.0}$. In addition, Equation 6.5 predicts a maximum in the erosion rate, a phenomenon missed in the correlations, as discussed in Sec. 4.1. Equations 3.4, 3.5, 6.4, and 6.5 are the first, to the authors' knowledge, that express the dimensionless erosion rate in terms of fundamental dimensionless scaling parameters. The definition of $\dot{E}_o$ is given by Eq. 3.2 in Sec. 3.1.

The semi-empirical master equation of Zhu et al.[6.4] may be used as an alternative. Like the simplified MED erosion model, it relies upon the use of the particle's kinetic energy. Unlike others, and based upon their own analyses, the work done on the target is taken to be proportional to the Young's modulus. The final form is implicit in the target material properties and resulted in the following master equation:

$$\dot{E} = C f_v \rho_p d_p^m u_v^n (b - \phi_s) \tag{6.6}$$

where

$\dot{E}$ = erosion rate, μm/100 h;
f_v = void frequency, Hz;
ρ_p = particle density, kg/m^3;
d_p = particle diameter, mm;
u_v = void (bubble or slug) velocity ~ U, m/s;

U = fluidizing velocity, m/s; and

ϕ_s = particle sphericity.

The values of n, m, and b are given in Tables 4.1.1 (Sec. 4.1), 4.2.2 (Sec. 4.2, m=n), and 4.3.1 (Sec. 4.3, b=C_4), respectively, and were refit using multiple linear regression to give b = 1.1. The exponents n and m are given in Table 6.1 and are quite close to those given in Tables 4.1.1 and 4.2.2. The recommended final form of Eq. 6.6 is given by:

$$\dot{E} = C f_v d_p^{1.2} u_v^{2.1} (1.04 - \phi_s) . \qquad (6.7)$$

It is important to note that the group $(1.04 - \phi_s)$ plays a role similar to $(1 - e^2)$ where e is the coefficient of restitution, as discussed in Sec. 4.3. As ϕ_s decreases, ε would decrease, causing the erosion rate to increase because less energy is transmitted to the target surface. The recommended values of C in Eq. 6.7 for silica sand particles and their corresponding standard deviations are given in Table 6.2. C should be a function solely of the mechanical properties of both the particulate and tube materials. The Young's modulus of the tube material is implicit in C and is varies appreciably. The void frequency may be estimated as discussed by Zhu et al. but is in the range of 1-3 Hz.

Zhu et al.[6.4] successfully analyzed the Woodford and Wood[6.5] erosion data taken for 0.93- and 1.0-mm silica sand particles and 10 tube materials by assuming a shape factor, ϕ_s, of 0.89, a void rise velocity, u_v, of 2 m/s, and a void frequency, f_v, of 2.2 Hz. The results of this analysis are given in Table 6.3.

The U.K. shallow bed studies developed an empirical master equation of the form:[6.6]

$$\dot{E} = 1.873 \times 10^{-9} U^2 D^{0.6} L_s^{1.33} (1 + 0.1 P) \qquad (6.8)$$

where

$\dot{E}$ = erosion rate, mm/h;
U = fluidizing velocity, m/s;
L_S = bed depth before fluidization (static bed height), mm;
D = tube diameter, mm; and
P = tube inclination, deg.

The BCC concluded that comparison between the correlation given by Eq. 6.8 and observed metal loss for eleven boilers, considering the variety of boiler designs from six manufactures, was most encouraging. Remarkably, Eq. 6.7 predicts erosion rates on the same order as Eq. 6.8, 1 μm/100 h, over the same range of parameters for steel tube materials, as indicated in Fig. 4.1.11.

The parameters typical for FBCs are d_p = 1 mm, U~ 1 m/s, $\rho \sim 2 \times 10^3$ kg/m^3, $\phi_s \sim 1$, and $L_S \sim$ 500 mm (0.5 m). It should be noted that Eq. 6.8 predicts no explicit particle size dependence, but does predict erosion rates to increase with bed height and tube inclination. With P = 90°, a ten-fold increase in erosion is predicted for vertical tube banks over horizontal tube banks, in agreement with the BCC in-kind report studies discussed in Sec. 5.5.

References

6.1 Yates, J.G., *On the Erosion of Metal Tubes in Fluidized Beds*, Chem. Eng. Science, *42*(2):379-380 (1987).

6.2 Darton, R.C., R.D. Lanauze, J.F. Davidson, and D. Harrison, *Bubble Growth due to Coalescence in Fluidized Beds*, Trans. Inst. Chem. Eng., *55*:274 (1977).

6.3 Yang, W.-C., D.C. Chitester, R.M. Karnosky, and D.L. Keairns, *A Generalized Methodology for Estimating Minimum Fluidization at Elevated Pressure and Temperature*, AIChE Journal, *31*(7):1086-1092 (July 1985).

6.4 Zhu, J., C.J. Lim, J.R. Grace, and J.A. Land, *Tube Wear in Gas Fluidized Beds—II. Low Velocity Impact Erosion and Semi-Empircial Model for Bubbling and Slugging Fluidized Beds*, Chem. Eng. Sci., *46*(4):1151-1156 (1991).

6.5 Woodford, A.A. and R.T. Wood, *Effect of Particle Size and Hardness on Material Erosion in Fluidized Beds*, Proc. 7th Int. Conf. Erosion by Liquid and Solid Impact, *56*:1-10(1983).

6.6 British Coal Corporation, Coal Research Establishment, *Minimizing Erosion in Coal-Fired Boilers*, Commission of the European Communities Report EUR 12360EN, Contract No. 7220-ED/808, Final Report, Directorate-General, Telecommunications, Information Industries and Innovation, Luxembourg (1989).

TABLE 6.1 Fitted Least-Squares Experiments for Eq. 6.6[6.4]

Material	Experimental m	Experimental n
Brass	1.4	2.3
Aluminum 2011	1.1	2.1
Copper	1.1	2.1
Stainless steel 304	1.2	1.8
Carbon steel 1050	1.1	2.0
Overall	1.2	2.1

TABLE 6.2 Fitted Least-Squares Values of C for Eq. 6.7 for Silica Sand Particles[6.4]

Material	C	Standard deviation
Brass	0.115	0.0022
Aluminum 201	0.119	0.0046
Copper	0.0683	0.0029
SS 316	0.0097	0.0016
CS 1050	0.0199	0.0010
SS 304	0.0101	0.0001
CS 1020	0.0257	0.0009
Iron	0.0239	0.0008
Pure aluminum	0.237	0.033
Keewatin Steel 1	0.0146	0.0004
Keewatin Steel 2	0.0110	0.0005
Keewatin Steel 3	0.0105	0.0002
Keewatin Steel 4	0.0103	0.0001

The units of C and the standard deviation are $(\mu m \cdot s^{3.1})/(kg \cdot h \cdot m^{0.3})$.

TABLE 6.3 Comparison of Woodford and Wood[6.5] Measured Erosion Rates and Predictions from Eq. 6.7 with C Values from Table 6.2[6.4]

Tube material	Particle diameter (mm)	Erosion rate (μm/100 h)	
		Measured	Predicted
Copper	1.9	17	19
SS 316	1.9	3.0	2.8
Copper	0.93	6.7	8.2
SS 316	0.93	1.8	1.2

7 Parameters That Have Uncertain Effects upon Metal Wastage

Parameters that have unclear, uncertain, or speculative effects on metal wastage are briefly described in this section.

7.1 Tube Vibration

During the course of research at CRE in support of IEA Grimethorpe, vibrating plastic tubes were found to wear faster than nonvibrating tubes.[7.1] However, studies at CURL,[7.2] also in support of Grimethorpe, showed that PVC bars and PVC tubes stiffened with steel inserts produced higher erosion rates by a factor of 1.57 and 1.7, respectively. Oscillating tubes have been observed to produce bubble chains, which disappear immediately when the oscillations cease.[7.3]

7.2 Collisional Frequency

To identify the effect of particle impacts on tube erosion, a series of measurements was conducted by Nieh et al.[7.4] to determine the peripheral distribution of the collision frequencies using surface mounted electrostatic impact probes, as well as weight losses around an immersed tube. An instrumented tube having the same dimensions as the wax cylinders (17 mm) was placed horizontally at 5 cm above the distributor. Measurements of collision frequencies at different circumferential locations were made by rotating the instrumented tube each experimental run, with results shown in Fig. 7.1(b). These data were averaged values taken over 50 s of measurements with 0.55-mm glass beads at 67 cm/s fluidizing velocity. It can be seen in Fig. 7.1(b) that more particles impacted the lower half of tube (particularly in the 4 o'clock to 8 o'clock region) than the upper half of the tube. The highest frequency of particle impacts (90 counts/s) was found from the 5 o'clock to the 7 o'clock positions The maximum collision frequency was about three times higher than the minimum collision frequency at the tube top (12 o'clock).

Weight loss measurements were also made on an immersed tube under the same conditions. As illustrated in Fig. 7.1(b), the greatest tube erosion appeared at the bottom portion of the target tube (6 o'clock). The point of maximum erosion on the tube experienced a weight loss (2.4 mg/cm^2) about five times the minimum erosion at 12 o'clock. Comparing Figs. 7.1(a) and (b), a general correlation between particle-tube collision frequency and tube weight loss exists. These results indicate that the bottom tube surface had the largest weight loss as a result of frequent particle impacts, while the top tube surface had the smallest weight loss as a result of fewer collisions. Nieh et al. speculated that the mass removal process of an immersed tube is directly affected by the number of particle impacts per unit time and the particle impact velocity (or momentum). The difference between the distributions in Figs. 7.1(a) and (b) was attributed to the particle velocity profile around the tube, which was higher on the lower half of the tube. The electrostatic impact probe may be useful for identifying erosion details, such as maximum erosion points, and proper bundle arrangement for minimal erosion.

7.3 Bubble Coalescence

Levy and Bayat[7.5] studied the effect of bubble coalescence on tube erosion. A single tube was placed in a 0.759-m by 0.759-m bed. The bed was at minimum fluidization, and bubbles were injected just above the uniform distributor. The erosion rates were determined for single and

coalescing bubbles as a function of tube elevation. Figure 7.2 taken from Ref. 7.5 clearly shows that the erosion rate is approximately doubled when bubbles coalesce near the tube surface. The higher erosion rate is probably caused by higher forces (not measured) exerted on the tube surface during the coalescence process.

7.4 Pressure Fluctuations

In view of the qualitative observations on the quality of fluidization, determined by pressure oscillations, one might expect some correlation between pressure variance and erosion. Parkinson[7.6] et al. attempted to correlate pressure fluctuation with metal wastage but were unsuccessful, probably because fluctuations of a global nature (in the plenum chamber, between the tube bank, and immediately above the tube bank) were measured rather than *local* pressure fluctuations.

The FLUFIX/MOD2 and EROSION/MOD1 simulations of the generic few (3) tube model of the CRE cold model experiments were used to develop a preliminary correlation between the *local* pressure variance and erosion rates.[7.7]

Figure 7.3 shows an example of the results of comparing the MED erosion rate with the variance of pressure, $\overline{\sigma_p^2}$, as a function of fluidizing velocity at two positions for the shallow five-tube FLUFIX/MOD2 simulation discussed in Sec. 5.1.1.6. Good correlations of erosion increasing with the variance exist at these positions. The functional relation at each position is expected to be different, but trends would hopefully be unique and reproducible.

7.5 Tube Diameter

Zhu[7.8] studied the effect of diameter dependence upon erosion for a single tube located at 308 mm above the distributor. The bed material was 1.0-mm silica sand and the fluidizing velocity was 1.88 m/s.

The results are plotted in Figure 7.8. For tube sizes of 20, 25, and 32 mm, the erosion rate increased slightly as the tube size became smaller. For a tube size of 15 mm, the erosion rate increased dramatically for brass and A12011, while the erosion rate for the other three materials remained relatively constant. Zhu explained the results as follows.

The erosion of a tube is proportional to the mass flow rate of impacting particles. For bubbling or slugging, this mass flow rate is expected to depend on the wake volume. However, the wake is somewhat thicker near the axis of the bubble than at the outside. Because bubbles are more likely to swerve to avoid larger tubes than smaller ones,[7.9] the impact particle mass flow rate per unit area tends to be somewhat higher for smaller tubes than for larger tubes. As the tube size decreases, the volume of the de-fluidized cap appearing from time to time on top of the tube[7.10] decreases relative to the tube size (since the angle of repose for the particles is the same), while the tube surface becomes more curved. This provides more chance for particles to impact on the top part of the tube, hence increasing the average erosion rate there. When the tube diameter was smaller, particles impacting the tube surface were able to leave the tube more quickly, providing less protection against the next batch of impacting particles.

Zhu concluded that the above arguments may explain the small increase of erosion rate for a change in tube diameter from 32 to 20 mm, but not the sharp increase for the 15-mm brass and A12011 tubes. A possibility for the outstandingly high erosion rate for the 15-mm tubes offered

was that the 15-mm tubes tended to vibrate slightly, which may have enhanced the erosion rate (see Sec. 7.1). Zhu noted that Hosny,[7.11] Hosny, and Grace,[7.12] and Grace and Hosny[7.13] found that the rms (root mean square) forces for a given column were proportional to tube diameter for tube diameters of 15, 25, and 32 mm when $U-U_{mf}$ was larger than about 0.3-0.5 m/s. The full explanation of tube diameter dependence was not fully resolved and remained unclear.

Parkinson et al.[7.14] measured changes in tube wall thickness for tubes of 20, 33, and 60 mm in diameter. For all of these tests, the mean particle size of the sand was 1.3 mm and the bed was fluidized at a superficial velocity of 2 m/s. The total loss of material from the tubes increased with tube diameter. The measured weight change of the 60-mm-diameter tube was about twice that of the 20-mm tube. If these total losses were simply averaged over the surface of the different tubes, the mean change in tube thickness would decrease as the tube diameter was increased, as shown in Figure 7.5. This in the same trend as observed by Zhu.[7.8] However, inspection of the data shown in Figure 7.5 indicates that the highest losses (close to the bottom of the tubes) do not vary by as much as the overall weight change for the different diameter tubes. The large differences in tube weight change occur principally as a result of losses from the sides and tops of the tubes (i.e., the 0°, 90°, and 270° positions).

The in-kind data obtained from British Coal Corporation[7.15] indicate that while maintaining approximately the same heat transfer area in the tube bank, tube wastage appeared to reduce when tube radius was increased from 33.4 to 50.8 mm. Increasing the tube diameter from 50.8 mm to 75.2 mm showed no significant change in peak wear ratge. There was a slight tendency for reduced wear on the diagonal dimension and increased wear on the horizontal dimension. Increasing the tube diameter affected the distribution of wear around the tubes.

Earlier tests showed that there was a positive benefit of 30% in the vertical diameter and 48% in the diagonal diameter in using 50.8-mm- as opposed to 33.4-mm-diameter tubes, even though the tube packing density must be diminished to maintain constant area.[7.16] Brain and Michner[7.16] recommend that the smallest practicable diameter of tube commensurate with good circulation should be used.

Studies by the BCC for the UK shallow beds showed that single tubes showed a 100% in wear as tube size was increased from 50 mm to 114 mm in diameter.[7.18] However, the work with multiple tube arrays, 50-mm and 75-mm tubes, suggests that wear may be less on the 75-mm tubes. This anomaly has not been resolved, and therefore the influence of tube diameter on wear is unclear.

References

7.1 Wheeldon, J., Electric Power Research Institute, telephone conversation (Dec. 1, 1989).

7.2 Sparham, G.A., *Tube Wastage Investigations — Support Work of CURL*, in Reports Commissioned by the Project from Outside Consultants and Others, Vol. 2, NCB (IEA Grimethorpe) Ltd., Barnsley, S. Yorkshire, U.K. (Sept. 1984).

7.3 Rowe, P.N., and D.J. Everett, *Fluidised Bed Bubbles Viewed by X-rays, Part I— Experimental Details and the Interaction of Bubbles with Solids Surfaces*, Trans. Institution Chem. Engineers, *50*:42-48 (1972).

7.4 Nieh, S., S.Y. Lin, S.W. Lee, and T.T. Fu, *Measurements of In-Bed Tube Bundle Erosion and Particle-Tube Frequency in a Gas Fluidized Bed*, Particulate Science and Technology, *6*:269-283 (1988).

7.5 Levy, E.K., and F. Bayat, *The Bubble Coalescence Mechanism of Tube Erosion in Fluidized Beds*, in Fluidization VI, J.R. Grace, LW. Shemilt, and M.A. Bergougnou, eds., pp. 603-611, Engineering Foundation, New York (1989).

7.6 Parkinson, M.J., J.F.G. Grainger, A.W. Jury, and T.J. Kempton, *Tube Erosion at IAEA Grimethorpe: Cold Model Studies at CRE*, in Reports Commissioned by the Project from Outside Consultants and Others, Vol. 2, NCB (IEA Grimethorpe) Ltd., Barnsley, S. Yorkshire, U.K. (Sept. 1984).

7.7 Bouillard, J.X., D. Gidaspow, and R.W. Lyczkowski, *Hydrodynamics of Fluidization: Fast Bubble Simulations in a Two-Dimensional Fluidized Bed*, *66*:107-118 (1991).

7.8 Zhu, J., *Tube Erosion in Fluidized Beds*, Ph.D. Thesis, Department of Chemical Engineering, The University of British Columbia (May 1988).

7.9 Harrison, D., and J.R. Grace, *Fluidized Beds with Internal Baffles*, in Fluidization, J.F. Davidson & D. Harrison, eds., Academic Press, London and New York, pp. 599-626 (1971).

7.10 Glass, D.H., and D. Harrison, *Flow Patterns Near a Solid Obstacle in a Fluidized Bed*, Chem. Eng. Sci., *19*:1001-1002 (1964).

7.11 Hosny, N., *Forces on Tubes Immersed in a Fluidized Bed*, Ph.D. Dissertation, University of British Columbia (August 1982).

7.12 Hosny, N., and J.R. Grace, *Forces on Tubes Immersed within a Fluidized Bed*, in Fluidization IV, D. Kunii and R. Toei, eds., Engineering Foundation, New York, 111-120 (1983).

7.13 Grace, J.R., and N. Hosny, *Forces on Horizontal Tubes in Gas Fluidized Beds*, Chem. Eng. Research and Design, *63*:191-198 (1985).

7.14 Parkinson, M.J., A.W. Jury, B.A. Napier, T.J. Kempton, and J.C. Holder, *Cold Model Erosion Studies in Support of Pressurized Fluidized Bed Combustion*, Electric Power Research Institute Draft Final Report for Project 1337-2 (April 1986).

7.15 British Coal Corporation, Coal Research Establishment, *Grimethorpe Cold Model Tests 11 to 16: Evaluation of the Tube Bank "E" Final Design and Assessment of the Benefit of Further Tube Diameter Increases,* PFBC/MOA/P29, Stoke Orchard, Cheltenham, U.K. (April 28, 1988).

7.16 British Coal Corporation, Coal Research Establishment, *Results of the First Ten Cold Model Tests at Grimethorpe Leading to the Design of Combustor Tube Bank "E",* PFBC/MOA/P21, Stoke Orchard, Cheltenham, U.K. (Nov. 6, 1987).

7.17 Brain, S., and A. Michner, *Minimization of Wastage in Bubbling Atmospheric Fluidized Bed Boilers,* Proceedings on Corrosion-Erosion-Wear of Materials at Elevated Temperatures, Berkeley, Calif., Jan. 31-Feb. 2, 1990, A.V. Levy, ed., pp. 40.1 to 40.16, National Association of Corrosion Engineers, Houston, Texas (1991).

7.18 British Coal Corporation, Coal Research Establishment, *Minimizing Erosion in Coal-Fired Boilers,* Commission of the European Communities Report EUR/12360EN, Contract No. 7220-ED/808, Final Report, Directorate-General, Telecommunications, Information Industries and Innovation, Luxembourg (1989).

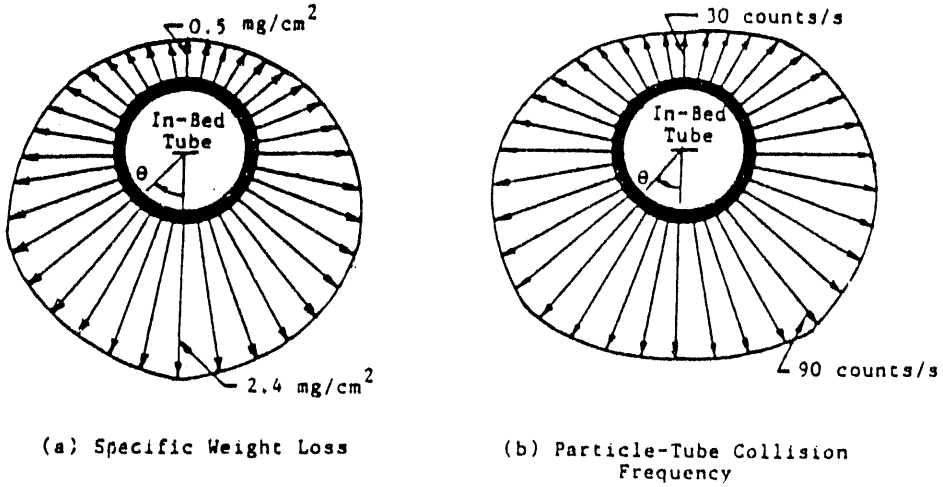

FIGURE 7.1 Time-Averaged Peripheral Distributions of Weight Loss and Collision Frequency of a Horizontal Tube Immersed in 500- 600-mm Glass Beads at a Superficial Velocity of 67 cm/s[7.4]

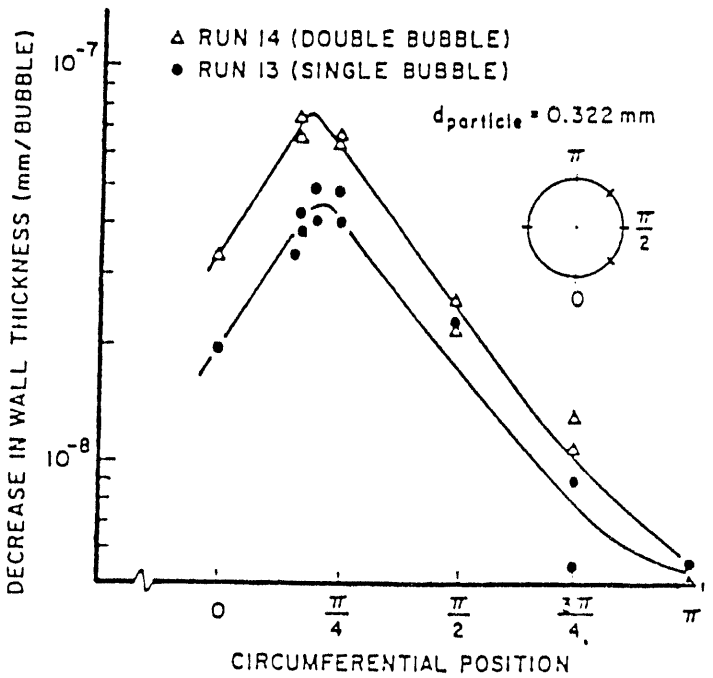

FIGURE 7.2 Circumferential Variation of Wastage Rate for Single Bubble and Coalescing Bubble Pair (double bubble)[7.5]

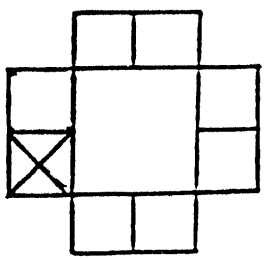

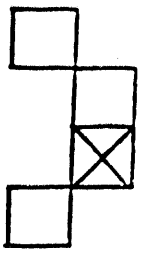

U/U_{mf}	$\dot{E}_{MED}$ mm/1000 hr	$\overline{\sigma_p^2}$ kPa
1.12	0.2	0.23
1.7	0.6	0.28
2.3	0.8	0.54

U/U_{mf}	$\dot{E}_{MED}$ mm/1000 hr	$\overline{\sigma_p^2}$ kPa
1.12	0.1	0.21
1.7	0.5	0.33
2.3	0.6	0.50

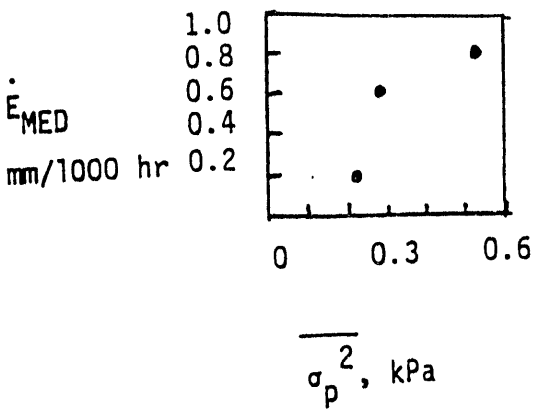

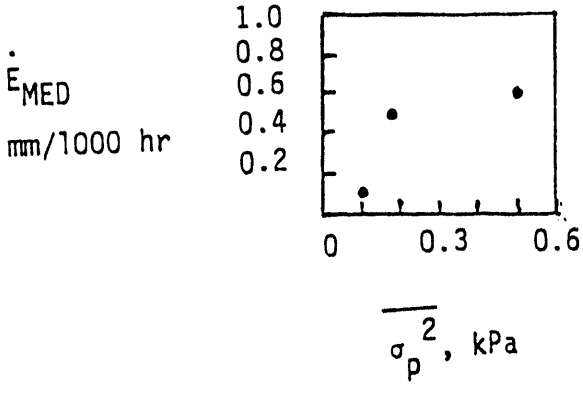

FIGURE 7.3 MED Erosion Rates as a Function of Pressure Variance

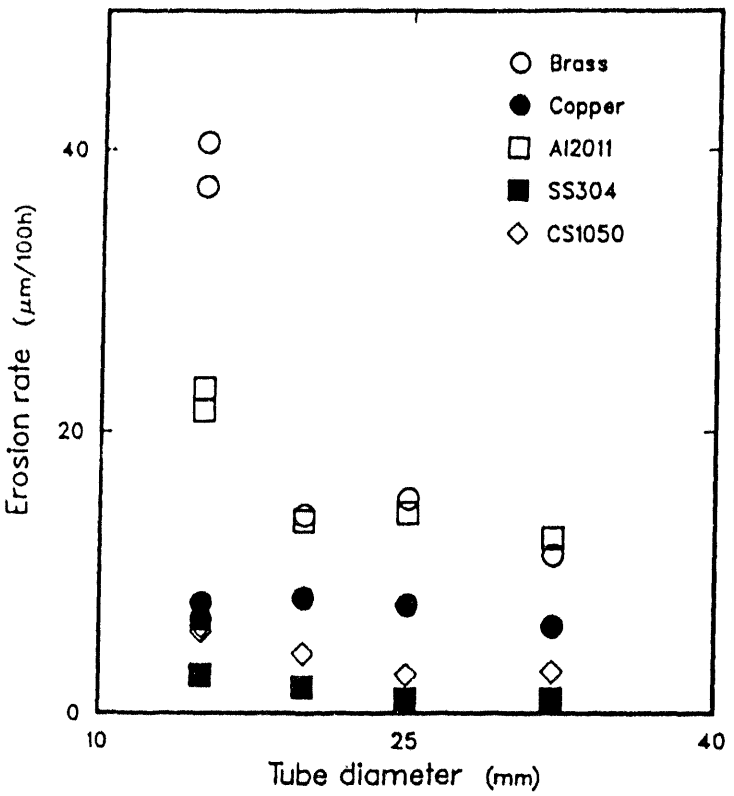

Operating conditions:

Particles: 1.0 mm silica sand
Particle sphericity: 0.89
Excess air velocity: 1.31 m/s
Duration: 46 – 65 h

FIGURE 7.4 Erosion Rate versus Tube Diameter[7.8]

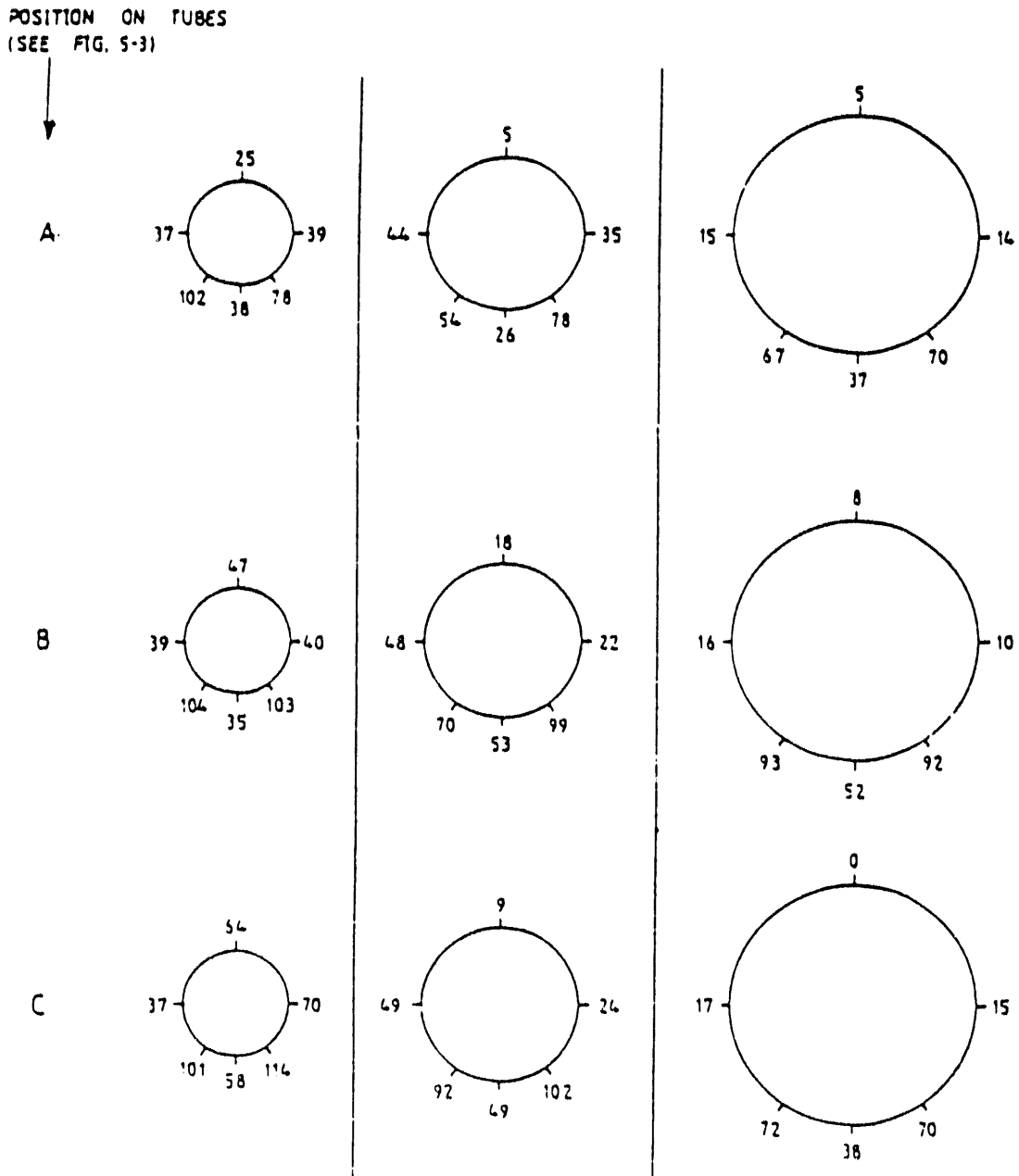

TUBE DIAMETER (mm)	20	33	50
ΔW_W (g)	0·99	1·63	2·59
ΔW_T (g)	1·42	1·72	2·25

(CHANGES IN TUBE THICKNESS IN μm)

FIGURE 7.5 Losses From Tubes of Different Diameter[7.14]

8 Conclusions and Recommendations

The most sensitive parameters affecting metal wastage have been found to be the superficial fluidizing velocity, particle diameter, and particle sphericity. Other parameters have secondary or uncertain effects upon erosion, but they cannot be ignored because they all compound and could result in unacceptable metal wastage rates.

Consistencies between disparate data sources using different techniques were found when the erosion rates are compared on the same basis using the concept of renormalization. The simplified mechanistic models and correlations, when validated, can be used to renormalize any experimental data so they can be compared on a consistent basis using a master equation.

For bed geometries and operating conditions that have not been reported in the literature, it is strongly recommended that the FLUFIX/MOD2,[8.1] FORCE2,[8.2] and EROSION/MOD1[8.3] software packages be used to assess fluidized-bed hydrodynamics and erosion rate dependencies upon design and operating parameters. Of course, one cannot depend entirely upon mere computer model predictions. Hence, together with computer model predictions, a supportive experimental plan should be carried out concurrently to validate the computer predictions. It is only in this perspective that fluidized-bed designs having minimal erosion can be achieved in a cost-effective manner.

An attempt has been made to relate the design guidelines to field data in a meaningful manner. This implies that erosion scaling procedures are needed. The simplified MED erosion model offers a simple-to-use method to accomplish this. Several examples demonstrated increased confidence in this model. The correlative approach and use of the FLUFIX/MOD2[8.1] and the MED erosion model in EROSION/MOD1[8.3] are alternatives. All produce about the same erosion rates, with the simplified MED erosion model being conservative.

What is needed is a regime map (similar to the map shown in Fig. 8.1) that relates the independent and dependent operating variables to erosion to determine bubble regimes.[8.4] This map would relate the independent parameters to the dependent parameters and/or directly to the various erosion regimes. The map should be in dimensionless form for universality.

References

8.1 Lyczkowski, R.W., J.X. Bouillard, and S.M. Folga, *Users Manual for FLUFIX/MOD2: A Computer Program for Fluid-Solids Hydrodynamics*, Argonne National Laboratory Report, Argonne, IL (April 1992).

8.2 Burge, S.W., *FORCE2: A Multidimensional Flow Program for Gas-Solids Flow, Theory Guide and User's Guide*, Babcock & Wilcox, Alliance, OH (May 1991).

8.3 Lyczkowski, R.W., J.X. Bouillard, S.M. Folga, and S.-L. Chang, *User's Manual for EROS/MOD2: A Computer Program for Fluid-Solids Erosion*, Argonne National Laboratory Report, Argonne, IL (September 1991).

8.4 Fitzgerald, T.J., *Fundamentals of Fluidized Bed Hydrodynamics as Applied to FBC System Design*, in Proceedings: DOE/WVU Conference on Fluidized-Bed Combustion Systems Design and Operation, pp. 8-57, CONF-8010187 (1980).

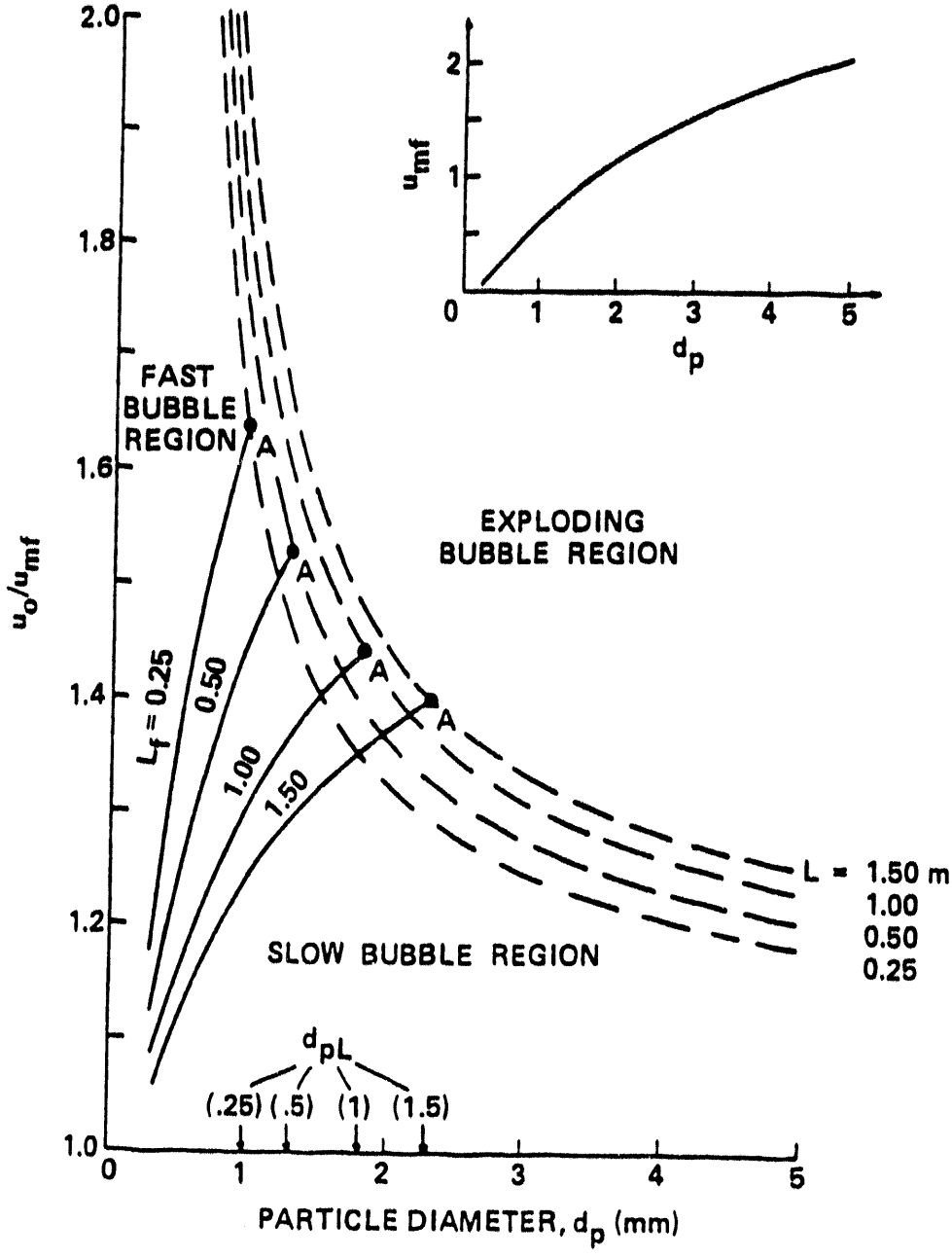

FIGURE 8.1 A Graphical Criterion for Determining Bubble Regimes in Large-Particle Beds of Limestone (Dolomite) at Room Temperature and Atmospheric Pressure, in Terms of U/U_{mf}[8.4]

Appendix A:

Some Conversion Factors Useful in Erosion Calculations

Density

$1\ g/cm^3 = 10^3\ kg/m^3$
Air at 1 atm and 20°C = $1.205\ kg/m^3$

Particle Diameter

$1000\ \mu m = 10^{-3}\ m = 0.1\ cm = 1.0\ mm$

Energy (power)

$10^7\ erg/s = J/s = W$

Energy Dissipation

$$\rho_s \varepsilon_s \vec{v}_S^2 = kg/s^3 = J/\left(s \cdot m^2\right) = W/m^2$$

$$dKE_s/dt = \dot{m}_s \frac{d\vec{v}_s}{dt^s} = kg/\left(m \cdot s^3\right) = J/\left(s \cdot m^3\right) = W/m^3$$

Erosion rate

$1\ mm/1000\ h = 1\ \mu m/h = 2.77 \times 10^{-10}\ m/s = 2.77\ nm/s$

$10\ \mu m/100\ h = 0.1\ mm/1000\ h = 100\ nm/h = 4\ mil/1000\ h$

$1\ \mu m/100\ h = 0.01\ mm/1000\ h = 10\ nm/n = 0.4\ mil/100\ h$

$= 0.0877\ mm/h = 3.51\ mil/yr$

Power

$$J = N \cdot m = kg \cdot m^2/s^2$$

Pressure (hardness)

$10\ dyne/cm^2 = Pa$

$9.8 \times 10^6\ kgf/mm^2 = Pa$

$$Pa = J/m^3 = kg/\left(m \cdot s^2\right)$$

Viscosity

Air at 1 atm and 20° C = 1.82×10^{-5} Pa· s

1 Poise = 0.1 Pa·s

Appendix B

Useful Design Information

In this appendix, we present some useful design information that aids in estimating erosion rates in fluidized beds. The chart shown in Fig. B.1 quickly provides the minimum fluidization velocity for air-solids and water-solids as a function of particle diameter and particle density at one atmosphere pressure and 293K.[B.1] For other pressures, densities, and temperatures, Ho and Park's[B.2] software package has proven extremely useful and user friendly.

Tables B-1 through B-3 list the hardnesses of several tube materials obtained by Wood and Woodford[B.3], quoted by Usimaru et al.[B.4] and Zhu et al.[B.5] Variations of ±50% exist for a given material, e.g. aluminum, 18.5-35 kgf/mm^2 (181 - 343 MPa). Such variability explains wide scatter in predicting erosion rates. The situation is even worse for PVC plastic tube materials, commonly used in accelerated erosion testing, which can have a spread of a factor of five or more in hardness values, depending on the type of plasticizers used.[B.6,B.7]

This document has made extensive use of References B.1 through B.7.

References

B.1 Grace, J.R., *Fluidized-Bed Hydrodynamics*, Chapter 8.1 in Handbook of Multiphase Systems, G. Hetsroni, ed., Hemisphere Publ. Corp., Washington, D.C. (1982).

B.2 Ho, T-C., and S.-C. Park, *FBCAD Fluidized Bed Computer Aided Design*, Version 1.0. Available from T.-C. Ho, Department of Chemical Engineering, Lamar University, Beaumont, Texas 77710 (Dec. 1988).

B.3 Wood, R.T., and Woodford, D.A., *Tube Erosion in Fluidized-Beds*, ERDA Report 81-12 911/ET-FUC/79), prepared for New York State Energy Research and Development Authority by General Electric Co., Schenectady, N.Y. (Dec. 1980).

B.4 Ushimaru, K., C.T. Growe, and S. Bernstein, *Design and Applications of the Novel Slurry Jet Pump*, Report No. E184-108, Technical Report, Energy International, Inc. (October 1984).

B.5 Zhu, J., J.R. Grace, and C.J. Lim, *Tube Wear in Gas Fluidized Beds—I. Experimental Findings*, Chemical Engineering Science, *45*(4):1003-1015 (1990).

B.6 Schmitz, J.V., *Testing of Polymers*, Vol. 2, Interscience Publishing, New York (1966).

B.7 Roff, W.J., J.R. Scott, and J. Pacitti, *Fibers, Films, Plastics, and Rubbers*, Butterworths, London (1971).

TABLE B.1 Hardness of Materials Tested by Wood and Woodford[B.3]

Material	Hardness (kgf/mm^2)
Aluminum	18.5
Copper	104
Nickel	131
Iron	90
Cobalt	210
SA213-T11	177
SS316	171
Stellite 6B	377
A286	393
High-speed steel	1010
Limestone	134
Silica sand	766
Alundum (Al_2O_3)	1890

[a]0.5-kg load

TABLE B.2 Typical Values of Material Hardness[(B.4)]

Material	Hardness (kgf/mm^2)
Lead	5
Aluminum	22-25
Copper	42-120
Brass	42-180
Nickel	115-350
Hardened steel	900

TABLE B.3 Mechanical Properties of the Materials Used by Zhu, et al[B.5]

Material	Elastic modulus (GPa)	Strength		Hardness		Density	Source[2]
		Yield (MPa)	Tensile (MPa)	Vickers (kg/mm^2)	Other[1]	(kg/mm^3)	
SS316	189	547	648	327			Measured
	190	760			HRC 35-45		Handbook
	190	276	621		HRb-85	7840	Manufacturer
SS304				276			Measured
	190	262	586		HRB-80	7840	Manufacturer
CS1020	180	508	646	230	HRA-53		Measured
	210	538	607		HB-177		Handbook
		327	441		HB-126	7840	Manufacturer
CS1050	203	627	692	230	HRA-52		Measured
	210	586	655		HB-179		Handbook
		531	628		HB-179	7840	Manufacturer
Brass (C36000)	63.2	327	402	155	HRA-41	8410	Measured
	97	310	400		HRB-78	8500	Handbook
		297	414			8490	Manufacturer
Copper (C14500)	115	346	348	98.0	HRA-30	8990	Measured
	115	305	330		HRB-48	8940	Handbook
		310	324			8910	Manufacturer
A12011-T3	67.0	353	420	132	HRA-40	2880	Measured
	70.0	296	379		HB-95	2820	Handbook
	71.0	296	379		HB-95	2820	Manufacturer
Pure aluminum	60.1	29.6	43.6	23	HRA-24	2670	Measured
	62	20	40			2700	Handbook
Armco iron		162	327	123	HRA-30	7780	Measured
	208						Handbook
Keewatin tool steel (1)	200	1132	1166	327	HRC-33	7790	Measured
	210						Handbook
						7780	Manufacturer
Keewatin tool steel (2)	202	1524	1580	448	HRC-44	7790	Measured
	210						Handbook
						7780	Manufacturer
Keewatin tool steel (3)	212			551	HRC-50	7790	Measured
	210						Handbook
						7780	Manufacturer

TABLE B.3 (Continued)

Material	Elastic modulus (GPa)	Strength		Hardness		Density (kg/mm^3)	Source[2]
		Yield (MPa)	Tensile (MPa)	Vickers (kg/mm^2)	Other[1]		
Keewatin tool steel (4)	204 210			836	HRC-63	7790 7780	Measured Handbook Manufacturer

*U.S. GOVERNMENT PRINTING OFFICE

[1]HRA, HRB, and HRC = Rockwell hardness, A, B, C scale; HB = Brinell hardness number.

[2]Measured = measured at U.B.C., handbook = from Bardes and Baker (1983), manufacturer = data provided by manufacturer or supplier.

DATE FILMED

3/7/94

END